CHAPTER THREE

Basins due to lithospheric stretching

Summary

Cratonic basins (intracontinental sags), continental rim basins, rifts, failed rifts, proto-oceanic troughs and passive continental margins fall within an evolutionary suite of basins unified by the process of lithospheric stretching. Rifts are a clear manifestation of lithospheric stretching, demonstrated by the shallow depth to the Moho, high surface heat flows, volcanic activity, seismic activity with predominantly extensional focal mechanism solutions, negative Bouguer gravity anomalies and commonly elevated rift margin topography.

Cratonic basins show little evidence of crustal stretching but subside over very long periods of time, probably due to cooling of relatively thick continental lithosphere. Continental rim basins are similar in overlying essentially unstretched crust, but are coeval with the drift phase of adjacent continental margins. Discrete, localised continental rifts appear to form on normal thickness crust and extend slowly over long periods of time. Rift zones evolve as linked fault arrays that control sediment dispersal during the syn-rift phase. At higher strain rates, localised rifts may evolve into passive margins. Wide extended domains with supra-detachment basins occur on previously thickened crust that extends quickly over a short period of time. Local anomalies in the ductile lower crust may be amplified to produce core complexes within these wide extended terranes.

At high levels of stretching the continental lithosphere attenuates sufficiently to allow the creation of new marine basins (proto-oceanic troughs) floored with oceanic crust. Passive continental margins evolve principally by slow cooling following break-up. They are in general seismically inactive, and their tectonics is dominated by gravity-driven collapse, salt movement and growth faulting. Heat flows are near normal in mature examples. Passive continental margins can be categorised according to their magmatic activity, their nourishment with or starvation of sediment, and the importance of salt and gravitational tectonics. There may be considerable asymmetry between conjugate margins, especially in the ductile lower crust.

Early investigations suggested that rifting fell into two end-member idealisations. *Active rifting* involves the stretching of the continental lithosphere in response to an active thermal process in the asthenosphere, such as the impingement of a hot mantle plume on the base of the lithosphere. *Passive rifting*, on the other hand, involves the mechanical stretching of the continental lithosphere from unspecified distant extensional forces, with passive upwelling of asthenosphere. Subsidence in rifts is an isostatic response to the stretching of the continental lithosphere. The post-rift stage of failed rifts and the drift stage of passive continental margins are due to thermal contraction during cooling of the stretched lithosphere and upwelled asthenosphere. The sediment loads are supported flexurally during this long phase of cooling. Dynamical extensional models of the lithosphere incorporate a rheologically layered lithosphere. These numerical models make predictions of strain rate evolution as a function of the changing temperature field and viscosity within this layered lithosphere.

The simplest formulation of continental extension is the 'reference' uniform stretching model and its derivatives. It involves uniform stretching with depth, instantaneous extension, one-dimensional heat transport by conduction, no magmatic activity, no internal radiogenic heat sources and the operation of Airy isostasy throughout. The reference uniform stretching model makes important first-order predictions. Initial fault-controlled subsidence is dependent on the initial crustal to lithospheric thickness ratio and on the stretch factor β. The subsequent thermal subsidence has the form of a negative exponential, and depends on the stretch factor β alone. The uniform stretching model serves as a useful approximation for subsidence and paleotemperature in rifted basins such as the North Sea, and in sediment-starved passive margins such as the Bay of Biscay and Galicia margin of the eastern central Atlantic. However, sediment-nourished passive margins require the post-rift subsidence to be modelled with flexural rather than Airy isostatic support. Volcanic margins require the effects of melt segregation, igneous underplating and transient dynamic uplift to be accounted for.

Subsequent modifications to the reference uniform stretching model have investigated: (i) the effects of a protracted period of stretching at low strain rate; (ii) depth-dependent stretching; (iii) extension by simple shear along trans-crustal detachments; (iv) elevated asthenospheric temperatures; (v) magmatic activity; (vi) secondary small-scale convection; (vii) radiogenic heat sources; (viii) greater depths of lithospheric necking; (ix) flexural support; and (x) phase changes. These modifications affect the predictions of syn-rift and post-rift subsidence, and in particular predict elevated syn-rift topography in the form of topographic swells or rift margin uplifts.

Dynamical approaches to lithospheric extension involve plane stress or plane strain models with various boundary conditions and initial conditions. Dynamical models are especially instructive in explaining why rifts remain narrow, with small bulk extensional strains, or develop into oceanic spreading centres. One set of dynamical models indicates that at moderate to low initial strain rates, extension is limited by an

Basin Analysis: Principles and Application to Petroleum Play Assessment, Third Edition. Philip A. Allen and John R. Allen.

increase in viscosity in the mantle lithosphere below the Moho. In contrast, at high initial strain rates, complete rifting results from the concentration of the extensional force on a progressively thinner high-strength layer within the lithosphere. The strength profile, extent of decoupling or coupling between upper and lower strong layers of the lithosphere, and the effects of strain softening in accelerating thinning are all important facets of numerical models of continental extension. Analogue models are able to replicate the narrow, localised rifts and extensive tilted fault block terranes observed in passive margins as a function of strain rate. Analogue models also show that gravity spreading of weak, previously thickened crust leads to wide extended terrains and exhumed ductile lower crust in core complexes.

The amount of extension (stretch factor β) and the strain rate history can be estimated by a number of techniques. The thermal subsidence history of stratigraphy penetrated in boreholes allows the amount of lithospheric stretching and strain rate history to be estimated. Crustal stretching can be calculated from imagery of the depth to the Moho using gravity and seismic data. Stretch factors can also be estimated from forward sequential tectonostratigraphic modelling using well-constrained crustal and basin profiles derived from deep seismic reflection and refraction data.

3.1 Introduction

3.1.1 Basins of the rift–drift suite

Continental sags (cratonic basins), rifts, failed rifts, continental rim basins, proto-oceanic troughs and passive margins form part of an evolutionary sequence of basins unified by the processes of lithospheric extension (Dietz 1963; Dewey & Bird 1970; Falvey 1974; Kinsman 1975; Veevers 1981). Two linked mechanisms explain the majority of observations in these basins: (i) brittle extension of the crust, causing extensional fault arrays and fault-controlled subsidence; and (ii) cooling following ductile extension of the lithosphere or negative dynamic topography sustained by downwelling mantle flow, leading to regional sag-type subsidence.

Basins of the rift–drift suite occur in an evolutionary sequence leading eventually to the formation of new ocean basins. They can be visualised as falling in an existence field with axes of the bulk strain due to stretching (stretch factor) and the extensional strain rate (Fig. 3.1):

- *Cratonic basins* (*syn.* intracratonic sags) lack evidence for widespread extensional faulting but experience long-lived sag-type subsidence; both bulk strain and strain rate are low.
- *Continental rim basins* are located on essentially unstretched continental lithosphere and experience slow sag-type subsidence coeval with the late syn-rift and drift phases of the adjacent passive margin.
- *Rifts* are characterised by well-developed extensional faulting. Tensile deviatoric stresses are sufficient to overcome rock strength. Bulk strain and strain rate vary widely from narrow-slow, localised rifts, to wide-fast, diffuse extensional provinces and *supradetachment basins*.
- *Failed rifts* occur where the brittle stretching stops before reaching a critical value necessary for the formation of an ocean basin, and subsequent subsidence takes place due to cooling.
- *Proto-oceanic troughs* occur where the stretching has rapidly attenuated the lithosphere to allow a new ocean basin to form; bulk strain and strain rate are both very high.
- *Passive margins* are dominated by broad regional subsidence due to cooling following complete attenuation of the continental lithosphere. The passage from rift to passive continental margin takes place at the *rift–drift transition*.

Some rifts are at high angles to associated plate boundaries (Burke 1976, 1977). Some of these rifts appear to be linked to arms of triple junctions associated with the early stages of ocean opening – these failed rifts are termed *aulacogens*. Others are aligned at high angles to associated collision zones and are termed *impactogens* or *collision grabens*. Whereas aulacogens are formed contemporaneously with the ocean opening phase, impactogens clearly post-date this period, being related temporally with collision. The Western European Rift System, containing the Rhine Graben, has been cited as an example of an impactogen (Sengör *et al.* 1978), and collision in the Grenville orogeny has also been invoked as a cause of the Keweenawan Rift in North America (Gordon & Hempton 1986).

In this chapter, the mechanisms of lithospheric extension are focused upon as a means of explaining the rift–drift suite of sedimentary basins. This suite is characterised by a distinctive set of geological, geophysical and geomorphological observations that collectively include elevated heat flows, volcanicity, extensional faulting, thinned crust and regional sag-type subsidence. Embedded within the overarching theme of lithospheric extension are complexities caused by the total amount of stretching, the strain rate and the thermal and mechanical properties of the continental lithosphere undergoing extension.

3.1.2 Models of continental extension

Early investigations of lithospheric extension suggested that rifting fell into two end-member classes (Sengör & Burke 1978; Turcotte 1983; Morgan & Baker 1983; Keen 1985; Bott 1992): active and passive (Fig. 3.2).

In *active rifting* deformation is associated with the impingement on the base of the lithosphere of a thermal plume or sheet. Conductive heating from the mantle plume, heat transfer from magma generation or convective heating may cause the lithosphere to thin. If heat fluxes out of the asthenosphere are large enough, relatively rapid thinning of the continental lithosphere causes isostatic uplift. Tensional stresses generated by the uplift may then promote rifting.

In *passive rifting* unspecified tensional stresses in the continental lithosphere cause it to fail, allowing hot mantle rocks to penetrate the lithosphere. Crustal doming and volcanic activity are only secondary processes. McKenzie's (1978a) widely cited model for the origin of sedimentary basins belongs to this class of passive rifting. If passive rifting is occurring, rifting takes place first and doming may follow but not precede it. Rifting is therefore a passive response to a regional stress field. It is not easy to determine whether a given rift is either active or passive, since for small mantle heat flows the amount of uplift may be minimal. In addition, it should be understood that active and passive models are idealised abstractions that represent 'end members'. Real-world cases may exhibit aspects of each (Khain

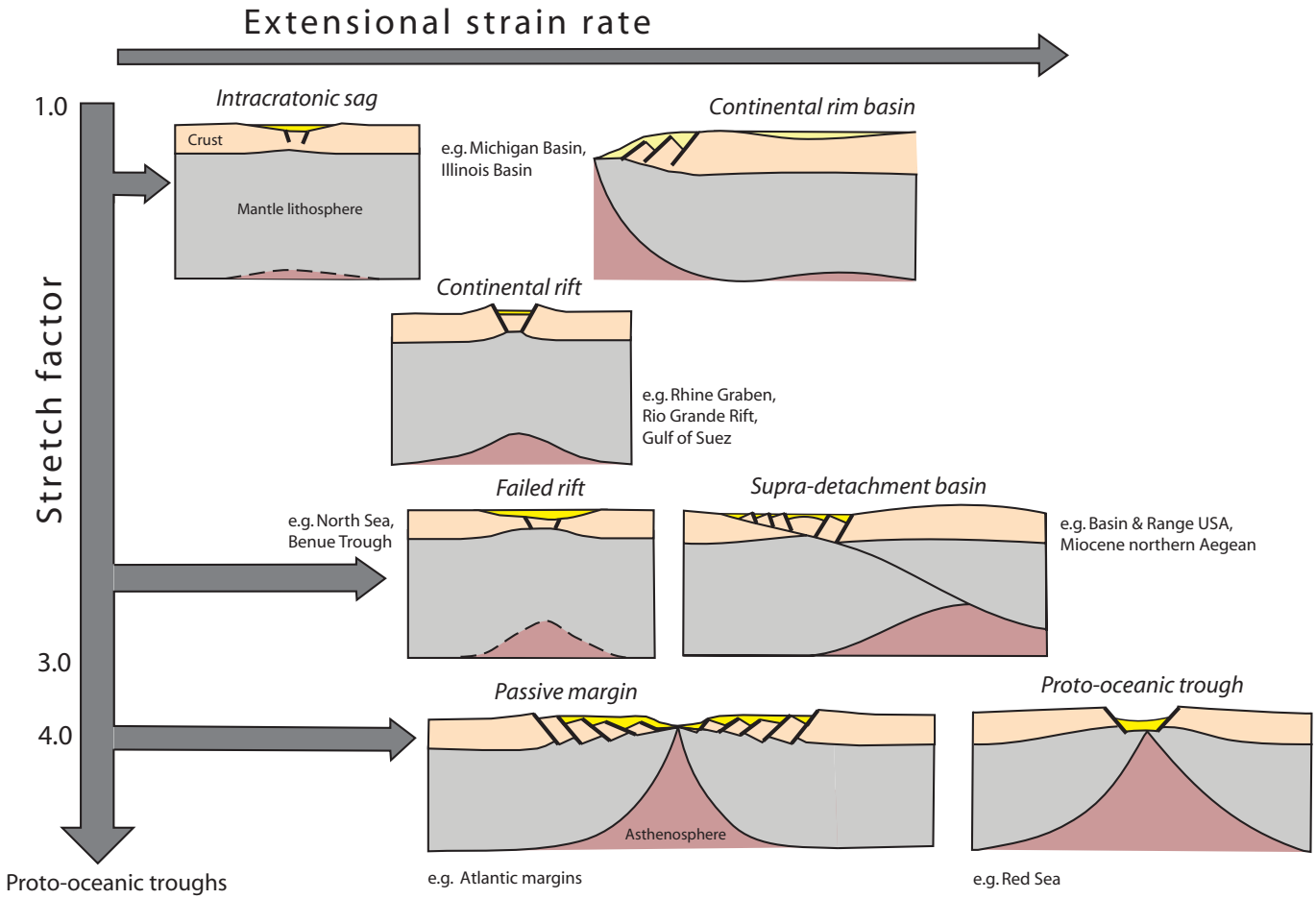

Fig. 3.1 Basins of the rift–drift suite in terms of increasing stretch factor and extensional strain rate.

1992). The East African and Ethiopian rifts (Fig. 3.3) are good candidates for active rifting whereas the wide Basin and Range province of southwestern USA (Fig. 3.4) is a candidate for passive rifting.

The syn-rift subsidence during stretching of the lithosphere is caused by brittle extension of the crust. Several mechanisms have been postulated as influences on the subsidence characterising the post-rift (or syn-drift) phase of passive margin development (§3.3.2). It is universally agreed that the main mechanism for post-rift subsidence is cooling following lithospheric thinning: the upwelling of asthenosphere (McKenzie 1978a) is followed by thermal contraction (for detailed treatment see Appendices 17 and 19). Lithospheric stretching, however, may be accompanied by important magmatism, producing dyke swarms, plutons and extensive basaltic sheets (Royden *et al.* 1980; White & McKenzie 1989). Emplacement of large volumes of basaltic melt into the crust (or along its base) should produce transient uplift, followed by subsidence as the extruded, intruded and underplated material cools. The result, long after emplacement, is determined by the density and thickness of the igneous additions to the lithosphere (Appendix 27). Commonly, these igneous additions have a higher density than the crust but lower density than the mantle. Assuming that the bulk of the igneous accretion replaces lithospheric mantle, passive margins with large amounts of magmatic activity should remain relatively elevated compared to non-magmatic margins.

It has also been postulated that subsidence may result from phase changes in lower crustal or mantle lithosphere rocks (Podladchikov *et al.* 1994; Kaus *et al.* 2005). Mineral phase changes may cause a rapid increase or decrease in the density of the lithosphere. The change from gabbro to eclogite may cause basin subsidence due to a density increase (Ahern & Dikeou 1989; Stel *et al.* 1993), whereas a density decrease, causing uplift, may result from the change from garnet to plagioclase-lherzolite. Phase changes are most likely to be important where the stretching is rapid (Armitage & Allen 2010).

The growing sediment prism acts as a load on the lithospheric substrate and is supported isostatically. This may be by lithospheric flexure (Watts *et al.* 1982; Beaumont *et al.* 1982), as long as the wavelength of the load is sufficiently short. Historically, there was much debate as to whether flexural support involved an elastic plate or a viscoelastic (Maxwell) plate (§2.3) overlying a weak substratum (Watts *et al.* 1982). Since active faulting and high heat flows accompany the early stages of rifting it has been assumed that an Airy isostatic model is most applicable during this period, although a small but finite flexural strength (Chapter 4) has been inferred for the active rifting phase in East Africa (Ebinger *et al.* 1989, 1991).

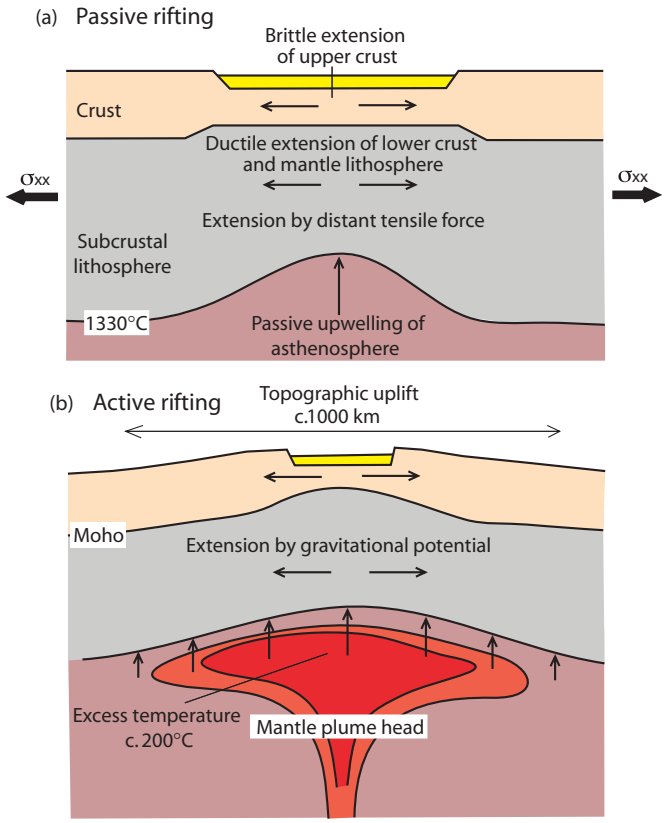

Fig. 3.2 Active and passive rifting end-member idealisations. (a) Passive rifting driven by a distant tensile deviatoric force σ_{xx} causing thinning of the lithosphere and passive upwelling of hot asthenosphere. (b) Impingement on the base of the lithosphere of a mantle plume causes long-wavelength topographic doming and gravitationally driven extension of the lithosphere.

Post-rift sediments, however, are gently dipping and of wide extent, suggesting that flexure takes over at some stage after the end of rifting. Watts *et al.* (1982) believed that the characteristic pattern of stratigraphic onlap on the eastern Atlantic and other continental margins suggested an increasing rigidity of the lithosphere with time – the expected result of an elastic lithosphere heated during the rifting stage and subsequently cooling.

In the last decade or two, emphasis has shifted away from active and passive rifting models and towards an understanding of the dynamics of stretching a piece of continental lithosphere with a particular strength and viscosity structure (§3.5) (Houseman & England 1986; Sonder & England 1989; Newman & White 1999; Huismans & Beaumont 2002, 2008). Increasingly, numerical model predictions are examined alongside high-resolution 3D seismic reflection data sets. The fundamental infrastructure of these numerical models is the description of the rheology of the continental lithosphere (Fernandez & Ranalli 1997).

The *strength of the lithosphere* can be judged from laboratory experiments (e.g. Kohlstedt *et al.* 1995), though there is the problem of 'scaling-up' laboratory experiments to the strain rates experienced by rocks in the lithosphere. The concept of the *strength envelope* (Goetze & Evans 1979; Ranalli 1995), which is the profile of lithospheric strength as a function of depth, underpins the rheological modelling of lithospheric extension (see §2.3.4).

The *rheology of the lithosphere* and its response to extensional deformation is most strongly controlled by its temperature and its mineralogy, and is strongly affected by the presence of volatiles such as water. A material can only maintain stresses over geological time if the ratio of actual temperature to its melting temperature (known as the *homologous temperature*) is less than about 0.4. This implies that only the upper parts of the crust and upper mantle are capable of supporting elastic stresses over long periods of time. Most dynamical models of lithospheric extension use laboratory data for the dominant mineral comprising crust and mantle – that is, quartz + feldspar for the crust, and olivine for the mantle. On a graph of stress at which failure takes place ($\sigma_1 - \sigma_3$) versus depth in the continental lithosphere, two brittle–ductile transitions and two stress-supporting regions are commonly predicted, one in the upper-mid crust, and the other in the upper mantle lithosphere (Fig. 2.38). Since the quartz + feldspar rheology of the continental lithosphere is weak at high temperatures, zones of orogenic thickening are prone to collapse by extension – an idea originally proposed by Tapponnier and Molnar (1976).

We examine the results of numerical models of lithospheric extension in §3.5. One of the major results of numerical modelling is that the changing temperature field of lithospheric particles during extension results in a changing viscosity of the mantle lithosphere over time. Consequently, dependent on the initial strain rate, the lithosphere may extend rapidly into a run-away state, or may stop extending (Newman & White 1999). This may explain dynamically the strain rate and bulk strain history of narrow rifts, wide rifts and passive margins (Fig. 3.5). The compilation in Fig. 3.5 shows a clustering of examples as relatively narrow, localised rifts (<100 km), but with extensional strain rates varying over two orders of magnitude (from $<10^{-16}\,s^{-1}$ to $10^{-14}\,s^{-1}$).

3.2 Geological and geophysical observations in regions of continental extension

3.2.1 Cratonic basins

'Intracratonic basins', 'cratonic basins', 'interior cratonic basins' and 'intracontinental sags' are circular- to oval-shaped crustal sags, located on stable continental lithosphere (Sloss & Speed 1974; Sloss 1988, 1990). We restrict the use of the term 'cratonic basin' to those basins located some distance from stretched or convergent continental margins, distinct from rifts where a history of continental extension is unequivocal, but located on a variety of crustal substrates, irrespective of whether they are crystalline shields *sensu stricto*, accreted terranes, or ancient foldbelts and rift complexes (Holt *et al.* 2010; Allen & Armitage 2012). Many cratonic basins overlie thick continental lithosphere (Hartley & Allen 1994; Downey & Gurnis 2009; Crosby *et al.* 2010).

Cratonic basins are characterised by predominantly shallow-water and terrestrial sedimentation. Their subsidence history is prolonged, occasionally marked by an initial stage of relatively fast subsidence, followed by a period of decreasing subsidence rate (Nunn & Sleep 1984; Stel *et al.* 1993; Xie & Heller 2009; Armitage & Allen 2010), somewhat similar to that of ocean basins (Sleep 1971). Cratonic basins generally lack well-developed initial rift phases, though this

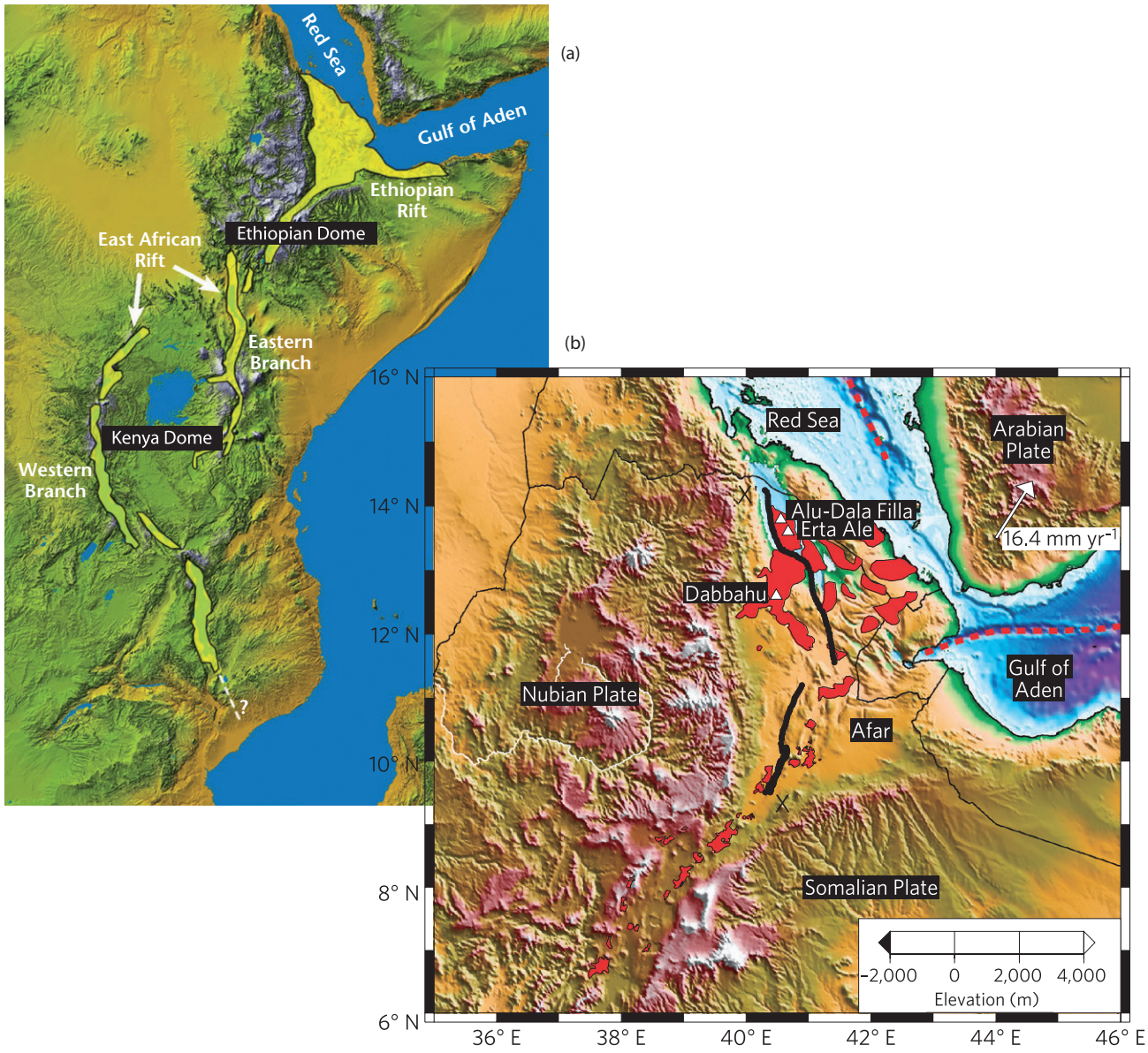

Fig. 3.3 (a) Topographic swells of east and northeast Africa, with location of main rift zones. (b) Topography of the Ethiopia-Afar region with magmatism in red. Reproduced from Bastow & Keir (2011), with permission of Nature Publishing Group.

may be due in part to the poor seismic imaging of the base of cratonic basins preserved on land. In some cases, cratonic basins are connected by a rift or failed rift zone to the ocean, as in the Neoproterozoic Centralian Superbasin of Australia (Walter *et al.* 1995; Lindsay 2002), the Lower Paleozoic Illinois and Oklahoma basins of USA (Braile *et al.* 1986; Kolata & Nelson 1990; Leighton *et al.* 1990) and the Mesozoic phase of the Chad Basin of north-central Africa (Burke 1976). This geometry suggests that many cratonic basins lie at the tips of failed rifts extending into the continental plate at a high angle from the extensional plate margin, which may be the site of former triple junctions (Burke & Dewey 1973). The association of cratonic basins with continental stretching is supported by the local occurrence of rifts below the sag-type basin-fill. Stretch factors are, however, very low beneath the cratonic basin, for example 1.05 to 1.2 in the Hudson Bay (Hanne *et al.* 2004) (Fig. 3.6) and <1.6 in the West Siberian Basin (Saunders *et al.* 2005).

Cratonic basins are large, with surface areas ranging from the relatively small Anglo-Paris Basin (10^5 km^2), through to the large Hudson Bay (1.2×10^6 km^2), Congo (1.4×10^6 km^2) and Paraná basins (1.4×10^6 km^2) to the giant Centralian Superbasin (2×10^6 km^2) and West Siberian Basin (3.5×10^6 km^2) (Sanford 1987; Leighton & Kolata 1990, p. 730; Walter *et al.* 1995, p. 173; Vyssotski *et al.* 2006; Crosby *et al.* 2010). In cross section, they are commonly simple saucers, with sediment thicknesses typically less than 5 km, and rarely <6–7 km (as in the West Siberian (Fig. 3.7), Illinois and Paraná basins). However, in some cases, the circular planform shape is a result of later compartmentalisation of a previously more extensive platform or ramp, as in the cratonic basins of North Africa, such as

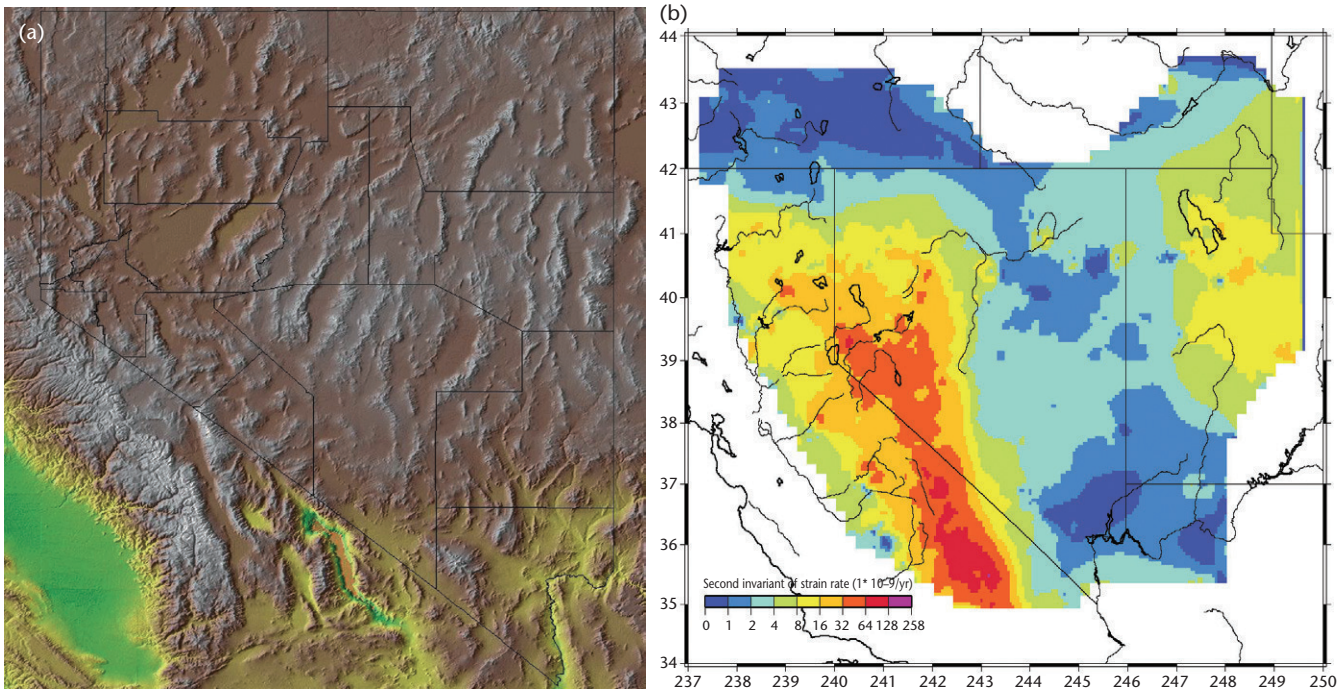

Fig. 3.4 (a) Topography of the Basin and Range province, southwestern USA, showing a large number of extensional fault blocks and basins over an extensive area of approximately 1000 km × 1000 km. Digital elevation model from National Geophysical Data Center, National Oceanic and Atmospheric Administration (NOAA), http://www.ngdc.noaa.gov/. (b) Map of crustal strain rate along the plate boundary between the Pacific and North American plates, derived from GPS measurements of horizontal station velocities (arrows). Strain rate is contoured in units of $10^{-9}\,yr^{-1}$. The range of values shown is from 0 to 3600 × $10^{-9}\,yr^{-1}$, equivalent to 0 to 11 × $10^{-14}\,s^{-1}$. A value of 72 × $10^{-9}\,yr^{-1}$ (yellow tone) corresponds to 23 × $10^{-16}\,s^{-1}$. Note the very high rates of deformation along the plate boundary zone and the lower strain rates in the Basin and Range province responsible for the N–S extensional fault blocks seen in part (a). From Map 178, Nevada Bureau of Mines and Geology, A geodetic strain rate model for the Pacific-North American plate boundary, western United States, by Kreemer, C., Hammond, W.C., Blewitt, G., Holland, A.A. & Bennett, R.A.

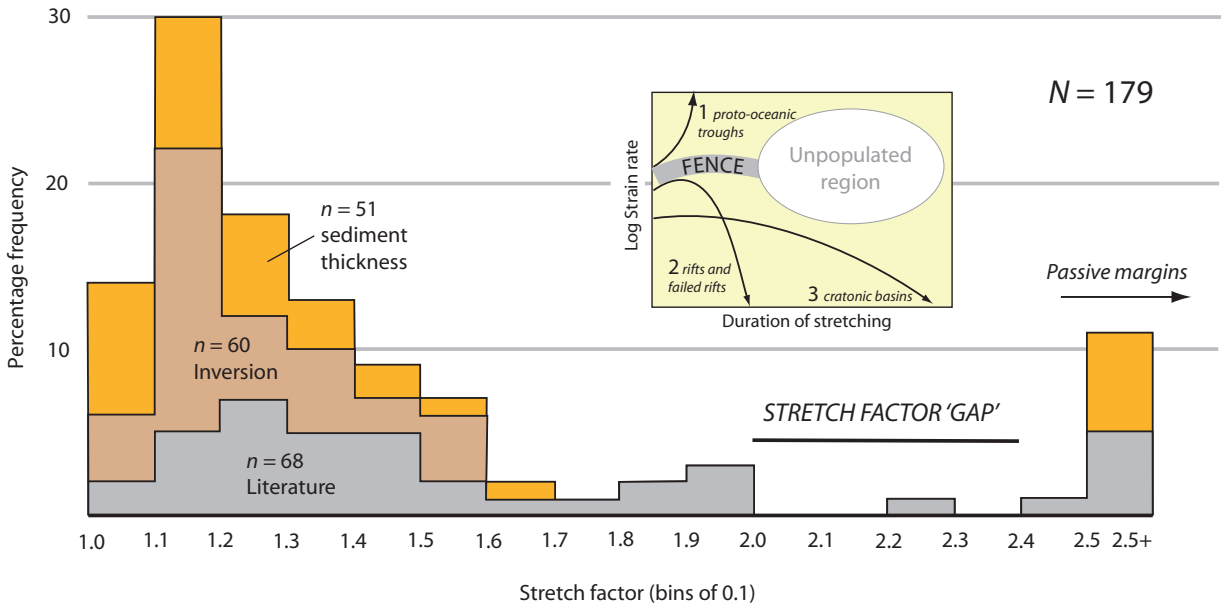

Fig. 3.5 Rift basins plotted in an existence field of stretch factor and strain rate. Literature-based data (grey) were obtained by MSc Petroleum Geoscience students at Imperial College London in 2010 and 2011.Other estimates were obtained from sediment thickness information (particularly ICONS database) and from inversion of thermal subsidence data (Wooler *et al*. 1992; White 1994). There is a scarcity of rift basins with stretch factors in the range 2.0 to 2.5.

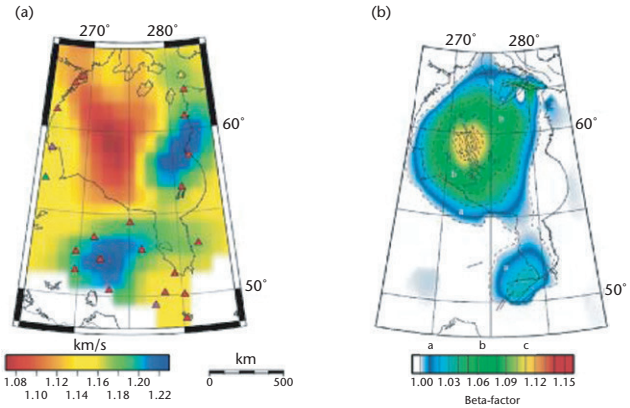

Fig. 3.6 Hudson Bay Basin, Canada. (a) Seismic velocity anomalies based on tomographic reconstructions (Pawlak *et al*. 2011), representative of the mid-crust, showing a slowing in the region beneath the main sedimentary depocentre; and (b) calculated stretch factors based on modelling of sediment thickness (from Hanne *et al*. 2004).

Al Khufra, Murzuk and Ghadames (Selley 1972, 1997; Boote *et al*. 1998) and the latest Proterozoic–Early Ordovician 'Sauk' sequence of east-central North America (Sloss 1963, 1988). They experience a long duration of subsidence, measured in hundreds of millions of years, implying slow sediment accumulation rates. The cratonic basins of North America, for instance, accumulated sediment at rates of 20 to 30 m Myr^{-1} (Sloss 1988), which is extremely slow compared to rifts, failed rifts, young passive margins, foreland basins and strike-slip basins (Allen & Allen 2005), but relatively fast compared to the adjacent platforms. Laterally equivalent platformal areas, such as the Transcontinental Arch of USA, accumulated c.1 km of sediment between Cambrian and Permian, at a rate of 3–4 m Myr^{-1} (Sloss 1988).

Although cratonic basins are very long-lived, it is important to recognise that the basin-fill is commonly composed of a number of different megasequences (or *sequences* of Sloss 1963), some of which may be associated with entirely different mechanisms of formation, such as strike-slip deformation, flexure and unequivocal stretching. Consequently, it is important, wherever possible, to extract the cratonic basin megasequence from the polyhistory basin-fill (Kingston *et al*. 1983a) for analysis. In other cases, basins have remained as

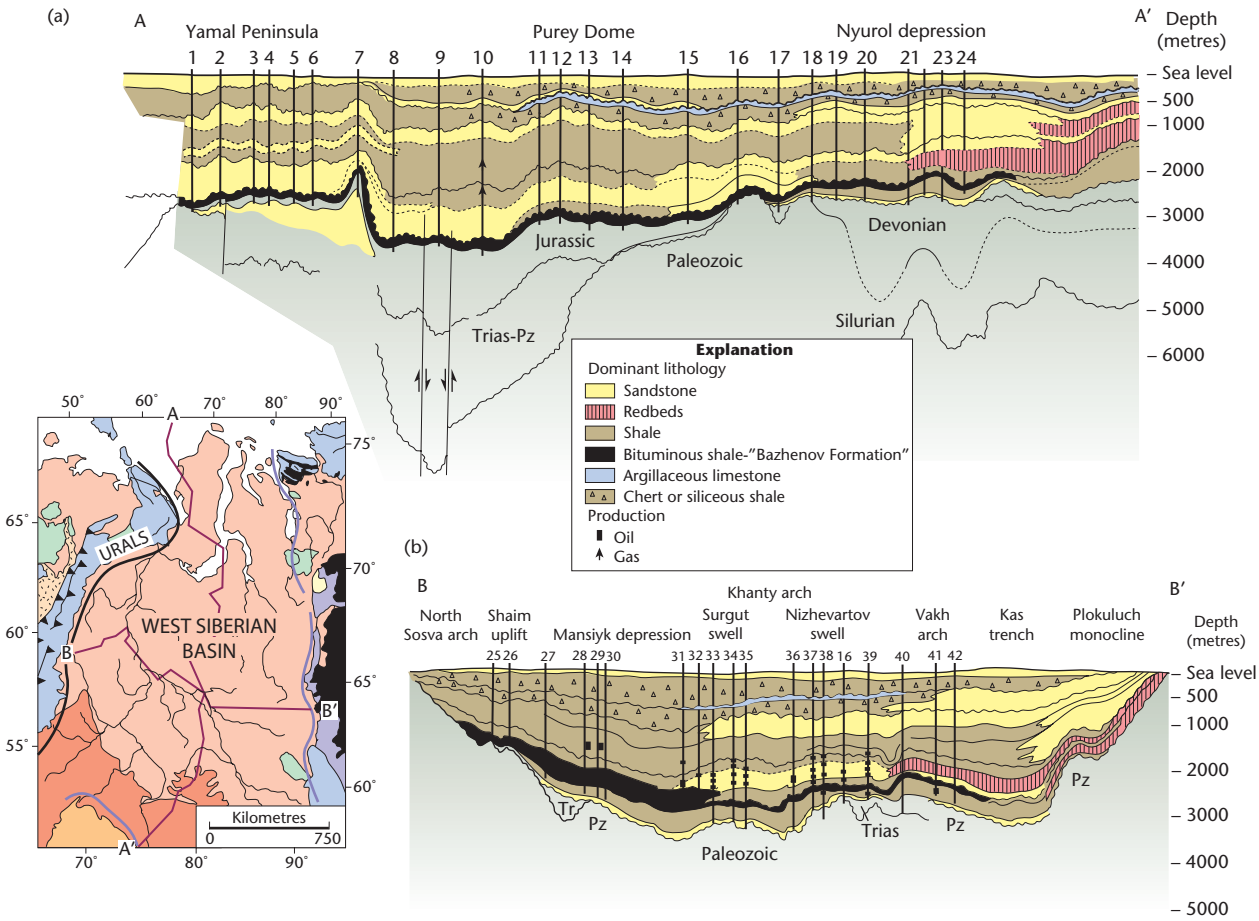

Fig. 3.7 Cross-sections of West Siberian Basin, A-A′ and B-B′, along transects shown in the inset geological map. From Vyssotski *et al*. (2006) and Saunders *et al*. (2005).

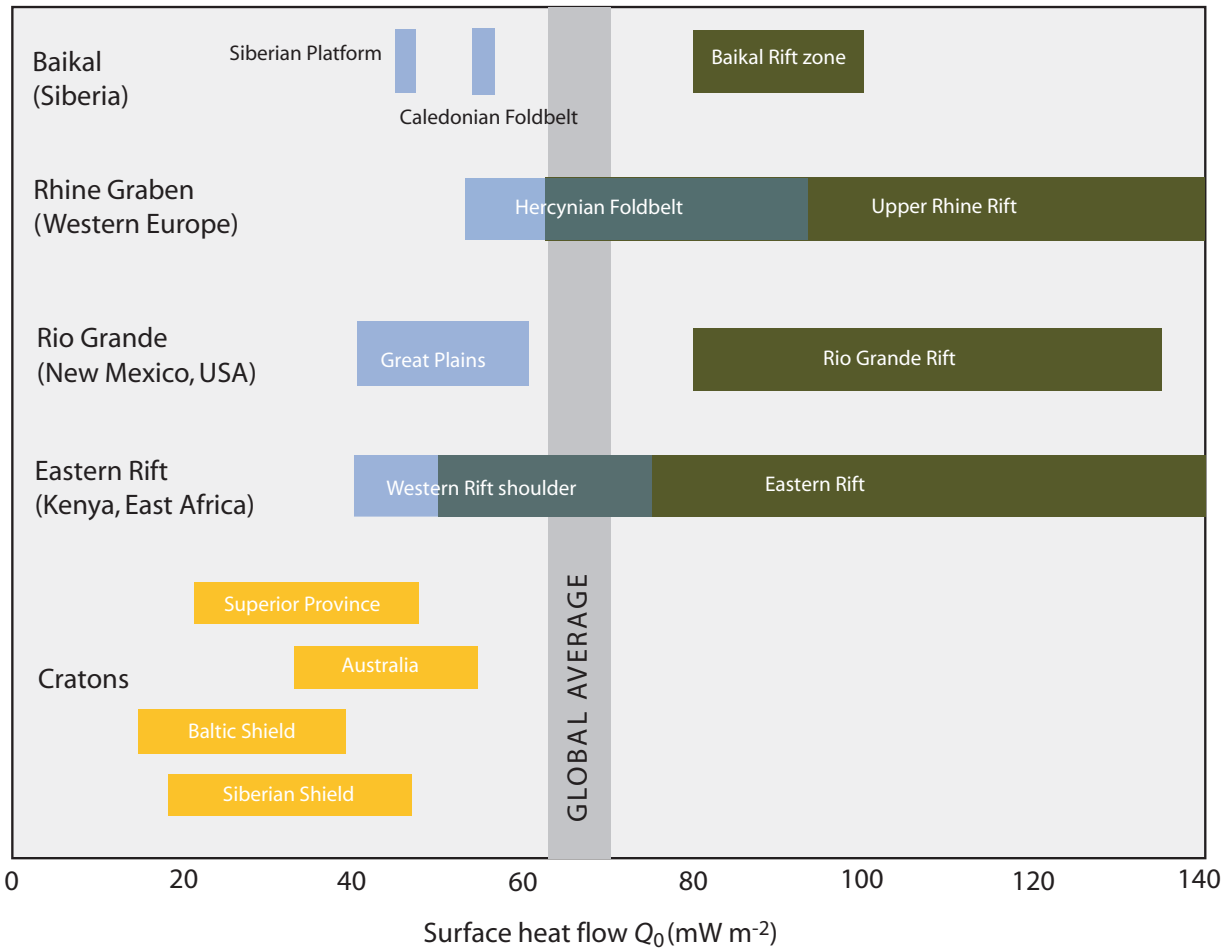

Fig. 3.8 Surface heat flows in some continental rifts and surrounding regions, compared with some cratonic basins and the global continental surface heat flow average.

cratonic basins throughout their history but have existed long enough to have been strongly affected by several tectonic mechanisms of subsidence and uplift. Consequently, there may be a primary mechanism for basin formation, and different secondary mechanisms for later modification (Allen & Armitage 2012).

3.2.2 Rifts

Rifts (classified as 'interior fracture basins' by Kingston *et al.* 1983a, b) are areas of crustal extension, and seismic studies show them to overlie thinned crust. Regions of rifting at the present day are characterised by negative Bouguer gravity anomalies, high surface heat flow and volcanic activity, all of which suggest that in addition to crustal extension, a thermal anomaly exists at depth. The essential observations in zones of continental extension are summarised here in terms of heat flow, seismicity, crustal thickness, gravity data, faults, surface topography, bulk strain and strain rates.

The presence of active volcanoes and elevated heat flows in rift zones demonstrates active thermal processes. However, the measured values of heat flow are often difficult to interpret, owing to complications caused by shallow magmatic intrusions, groundwater convection and spatial/temporal variability of conductive sediments and rocks. In general, rift zones have surface heat flows of 90–110 mW m^{-2}. This is up to a factor of 2 higher than in surrounding unstretched terranes (Fig. 3.8). Values are higher in volcanic rifts such as the Eastern Rift, Kenya, and lower in non-volcanic rifts such as those of Malawi, Tanganyika and the Jordan–Dead Sea rift zone of the Middle East. Volcanic activity has a major influence on rift sedimentation, as exemplified by the Eastern Rift of Kenya (Ebinger & Scholz 2012) and the Rio Grande Rift of southwestern USA (Mack & Seager 1990).

Rifts are characterised by high levels of earthquake activity. In the continental lithosphere, earthquake epicentres commonly delineate active rift zones or reactivated orogenic belts. Focal mechanism solutions in general indicate normal dip-slip faulting with orientations roughly parallel to the long-axis orientation of the rift. In some continental rifts, such as the Rhine Graben, strike-slip focal mechanisms dominate dip-slip solutions by 3:1 (Illies 1977). Although earthquakes are common in regions of continental rifting, they typically have moment magnitudes of up to 5.0 (Rhine Graben) or 6.0 (East African Rift), with shallow focal depths of <30 km, indicating that the earthquakes are located in the brittle upper crust.

Seismic studies show that the Moho is elevated beneath rift zones. The southern Rhine Graben is an example (Fig. 3.9). The Moho reaches a depth of 24 km near the Kaiserstuhl volcano due west of Freiburg, Germany, directly beneath the centre of the graben. The Moho is dome-shaped, deepening to the north, NW and NE to about 30 km. Approximately 3 km of syn-rift sedimentary rocks are found in the graben, so the continental crust has been thinned from 30 km to 21 km, that is, by a factor of 1.4. In the North Sea failed rift, the crust (pre-Triassic) is greater than 31 km thick beneath the Shetland Platform and Scandinavian Shield, but is less than 16 km thick beneath the Viking Graben (Klemperer 1988). The continental crust has therefore been thinned by a factor of approximately 2 immediately beneath the deepest part of the Viking Graben (Fig. 3.10). An important observation, however, is that some regions of extensive, diffuse extension, such as the Basin and Range province of SW USA, are located on previously thickened crust. The Moho was therefore anomalously deep at the onset of extension, and extension/thinning has brought the Moho back to 'normal' depth. This is also the case for the Tibetan Plateau, which is undergoing active extension and overlies crust as much as 70 km thick.

Rift zones have characteristic gravity signatures – typically a long-wavelength Bouguer gravity low with sometimes a secondary high located in the centre of the rift zone. The conventional explanation is that rift zones have anomalously hot material in the mantle beneath the rift, producing a mass deficit and therefore a negative gravity anomaly. The mass deficit is commonly associated with slow shear wave velocities, as below the Rio Grande Rift of southern USA (Fig. 3.11). The subsidiary gravity high is thought to be due to the intrusion of dense magma bodies within the continental crust. Regions of widespread, diffuse extension, such as the Basin and Range province of SW USA, show a series of gravity highs corresponding to basement blocks, and c.20 km-wide gravity lows corresponding to sedimentary basins. The gravity lows most likely reflect the mass deficit of light basin sediments.

Rift zones are typified by normal dip-slip faults with a variable number of strike-slip faults depending on the orientation of the rift axis in relation to the bulk extension direction. Consequently, the central Death Valley Basin is close to orthogonal to the extension direction and is typified by dip-slip normal faults, whereas the northern Death Valley Basin is more oblique and has faults with important strike-slip motion (Burchfiel & Stewart 1966).

Faults in rifts are not infinite in extent: instead there is a displacement-length relationship, with most of the slip being taken up on a small number of interacting major fault segments. Fault displacement dies out towards the tips of fault segments. A single fault segment, whose length is commonly between 10 and 100 km, has a maximum cumulative displacement (*d*)-length (*L*) relationship (Schlische 1991; Dawers & Anders 1995)

$$d \approx kL \qquad [3.1]$$

where k is a constant of proportionality that varies between 0.01 and 0.05 for many fault systems (Fig. 3.12).

The growth of populations of interacting faults is affected by a stress feedback that promotes the growth of a small number of major through-going border faults at the expense of smaller displacement faults that become dormant (Schlische 1991; Dawers & Anders 1995; Cowie *et al.* 2000). The evolution of the fault array has a profound effect on the topography and river drainage of rifted regions (Gupta *et al.* 1999; Cowie *et al.* 2000, 2006) (Fig. 3.13), and therefore on the gross depositional environments and sediment thicknesses of the basin-fill (Gawthorpe & Leeder 2000). Relay ramps between fault segments along the basin edge are commonly the entry points of river systems into the hangingwall depocentres. Footwall evolution, however, controls the establishment of the main drainage divide and therefore the size and sediment discharge of river catchments draining into the rift (Cowie *et al.* 2006). The Jurassic Brent–Strathspey–Statfjord fault array system in the North Sea Basin (McLeod *et al.* 2000), the Neogene fault array of the Gulf of Suez in eastern Sinai (Sharp *et al.* 2000) and the modern fault array of the Lake Tanganyika Basin (Rosendahl *et al.* 1986) are all excellent examples. Studies of such evolving fault arrays during the Jurassic syn-rift phase of the North Sea Basin suggest that linkage takes place rapidly, perhaps over 3–4 Myr (McLeod *et al.* 2000). Most major border faults dip steeply inwards towards the basin centre and are planar as far as they can be imaged. However, some rift-bounding faults are low-angle and listric, taking up very large amounts of horizontal extension, as in the supra-detachment basins of SW USA. Metamorphic rocks may be unroofed from <25 km depth in footwall 'core complexes' (Wernicke 1985).

The stratigraphic patterns of rift basins reflect this underlying pattern of fault array evolution (Gawthorpe & Leeder 2000). The common evolution from small, disconnected faults to full linkage produces a stratigraphic theme of isolated continental, hydrologically closed basins with lakes evolving into open rifts connected to the ocean, containing shallow-marine or deep-marine sediments fringed by fan deltas. The Miocene evolution of the Gulf of Suez is a classically documented example of such a rift evolution (Garfunkel & Bartov 1977; Evans 1988; Sharp *et al.* 2000). The concept of fault linkage also underpins the interpretation of extensional fault basins recognised on seismic reflection profiles (Prosser 1993).

Currently or recently active rift zones typically have elevated rift flank topography bordering a depositional basin. There may be two length scales of surface uplift. The best examples of the large length scale (several hundred kilometres) are the >3 km-high topographic swells of Ethiopia and East Africa (Baker *et al.* 1972; King & Williams 1976) (Fig. 3.14). Other domal uplifts are found in northern Africa, such as those in the Tibesti and Hoggar regions. These swells are commonly associated with widespread volcanic activity. Whereas the large domes of eastern and northeastern Africa are currently undergoing rifting, the smaller domes of north-central Africa are not. At a smaller length scale (<100 km) are the linear rift flank uplifts associated with border fault arrays. The <1 km-high highlands bordering the Gulf of Suez are a good example. Border fault footwalls involve upward tectonic fluxes, leading to enhanced denudation. In the southern Rhine Graben, tectonically driven exhumation of the rift flank has resulted in 2 to 3 km of erosion, exposing Hercynian crystalline basement in the Vosges of Alsace (France) and the Black Forest

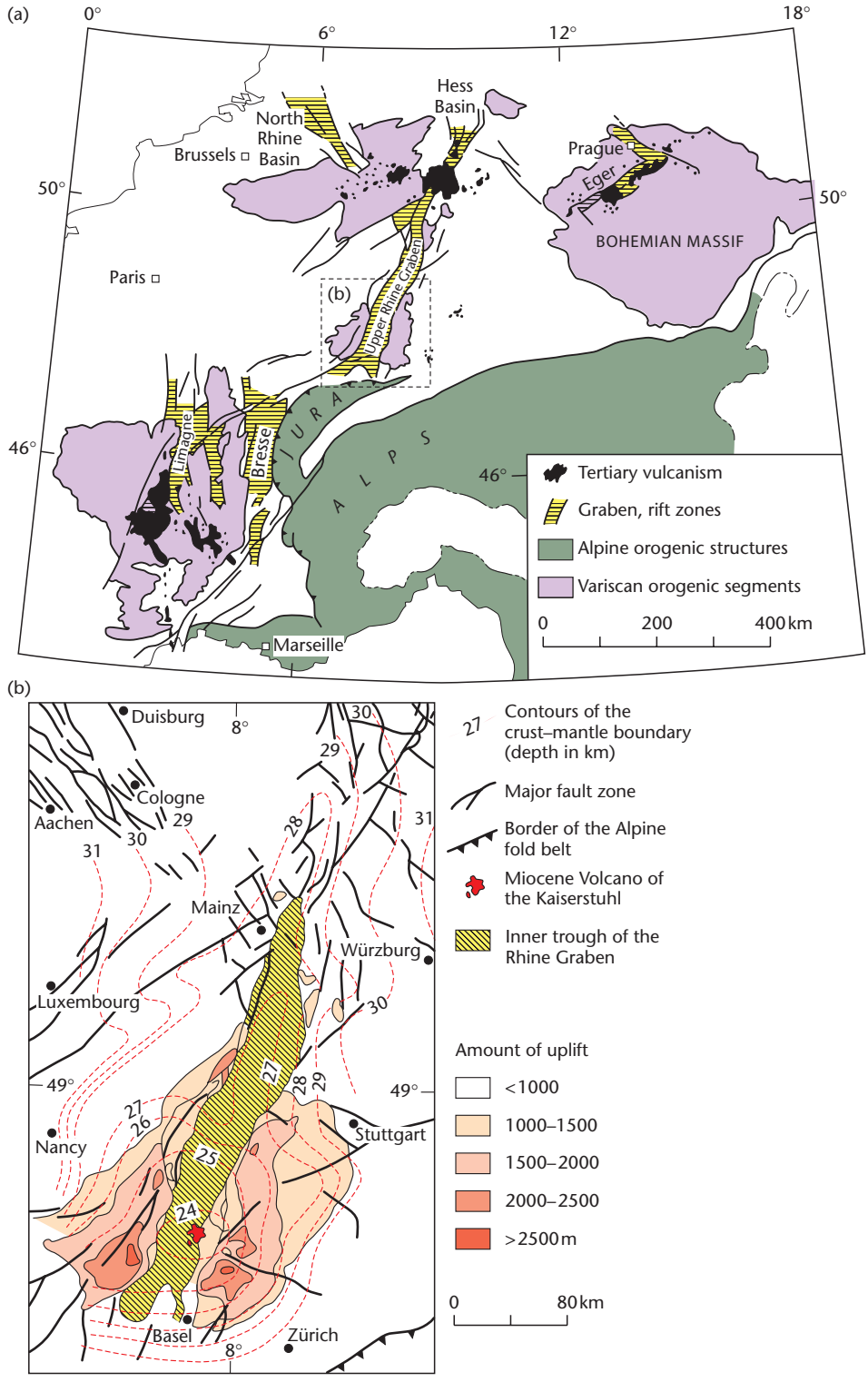

Fig. 3.9 (a) Location and main elements of the late Eocene–Recent Western European Rift System, with sites of Tertiary volcanicity. (b) Depth to the Moho below sea level (in km), showing a mantle bulge in the southern Rhine Graben centred on the Kaiserstühl volcano (Illies 1977). The largest amounts of denudation are found on the rift flanks above the shallow mantle.

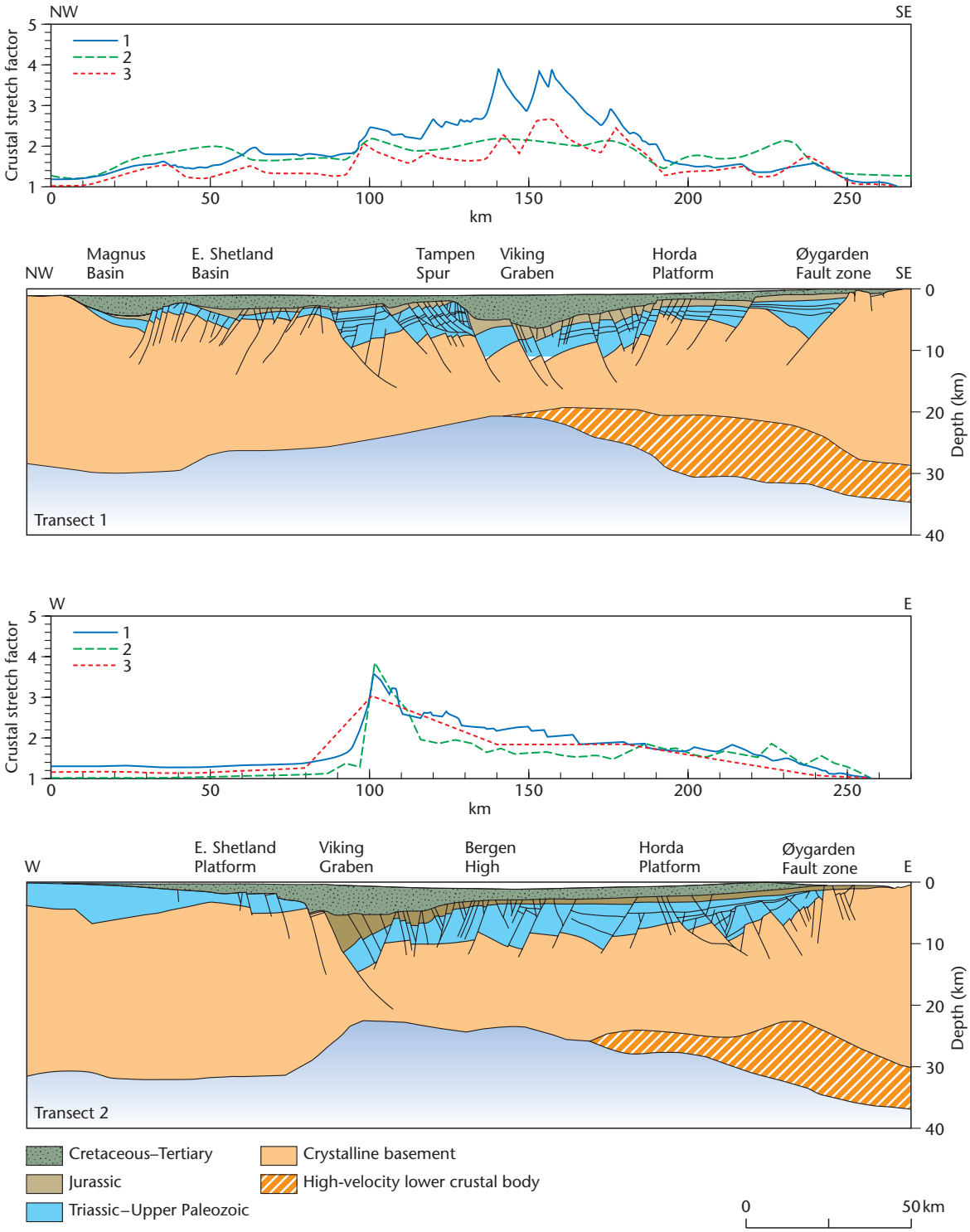

Fig. 3.10 Two crustal transects across the Viking Graben, northern North Sea (from Christiansson *et al*. 2000; Skogseid *et al*. 2000), based on the integration of all available geological and geophysical information, with estimates of crustal stretch factor, based on: (1) crustal thinning, assuming an initial crustal thickness of 36 km; (2) reverse modelling; and (3) forward tectonostratigraphic modelling.

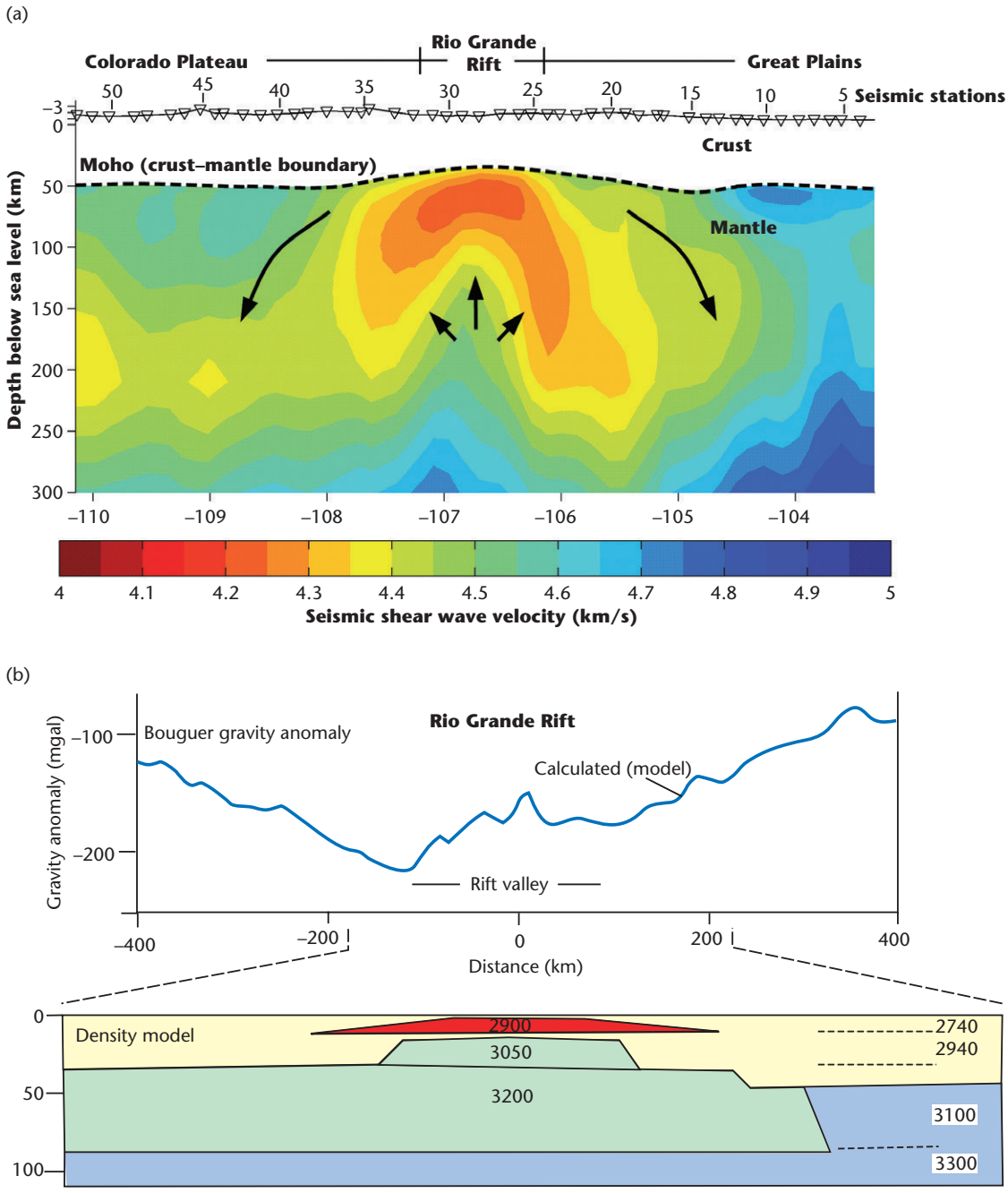

Fig. 3.11 (a) Seismic shear wave velocities ($km\,s^{-1}$) beneath the Rio Grande region, USA, indicating the existence of hot mantle, perhaps associated with a mantle upwelling. The mass deficit is responsible for a large-wavelength gravity low. Image from RISTRA programme, Wilson *et al.* (2005). (b) Gravity profile (c.33°N) and density model for the Rio Grande Rift of New Mexico, after Ramberg (1978). The secondary gravity high is thought to be due to the presence of dense igneous bodies beneath the rift. Densities shown in $kg\,m^{-3}$.

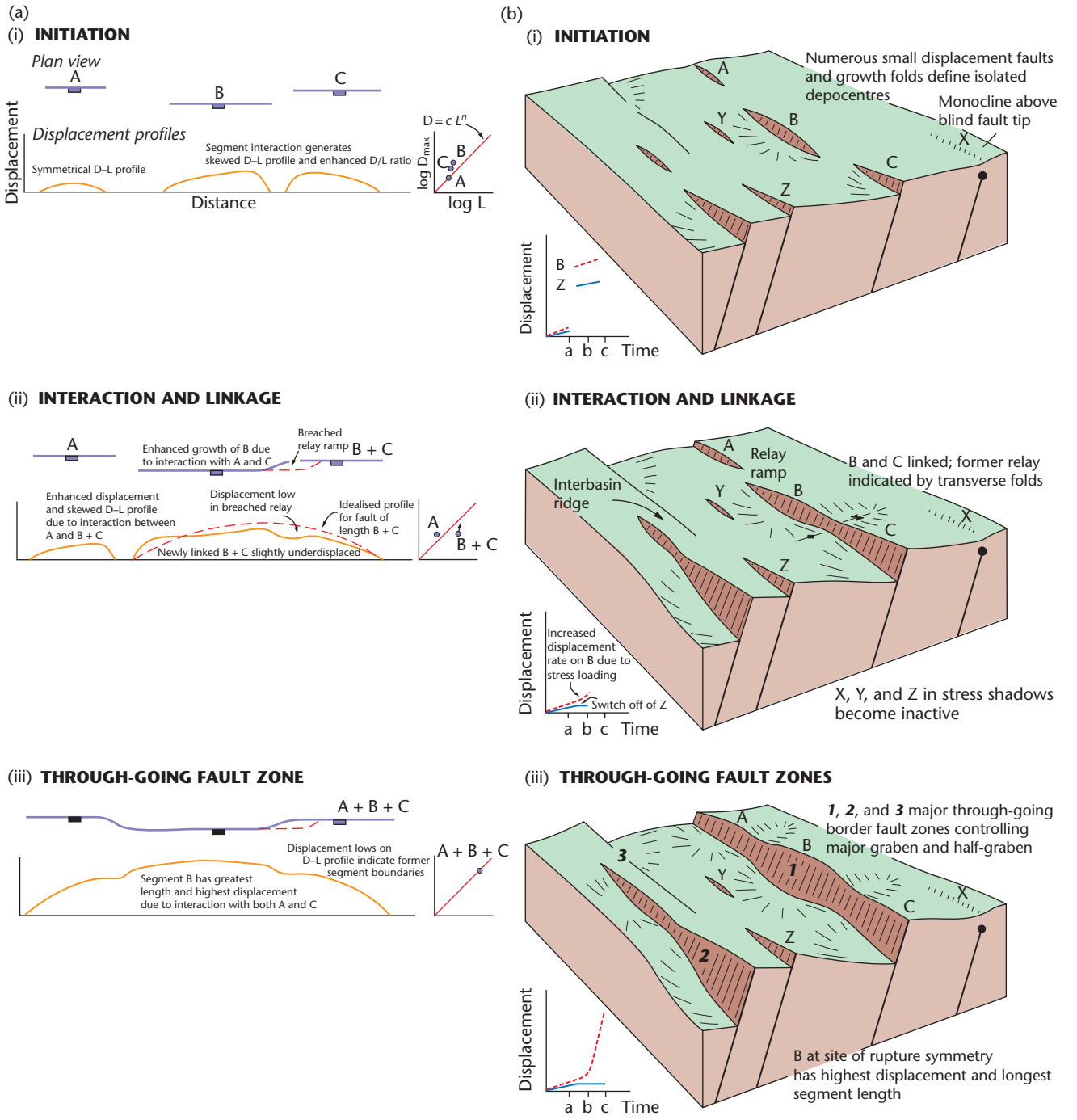

Fig. 3.12 (a) Displacement-length relationship of normal faults. Fault segments grow from an initiation stage (i) with individualised displacement-length relationships, to interaction and linkage (ii), and then to a through-going fault zone (iii), where there is one displacement-length profile that may contain remnant information of the original fault segments. (b) 3-D expression of fault interaction and growth from initiation, interaction and linkage, to a through-going fault zone. Reproduced from Gawthorpe & Leeder (2000), with permission of John Wiley & Sons, Ltd.

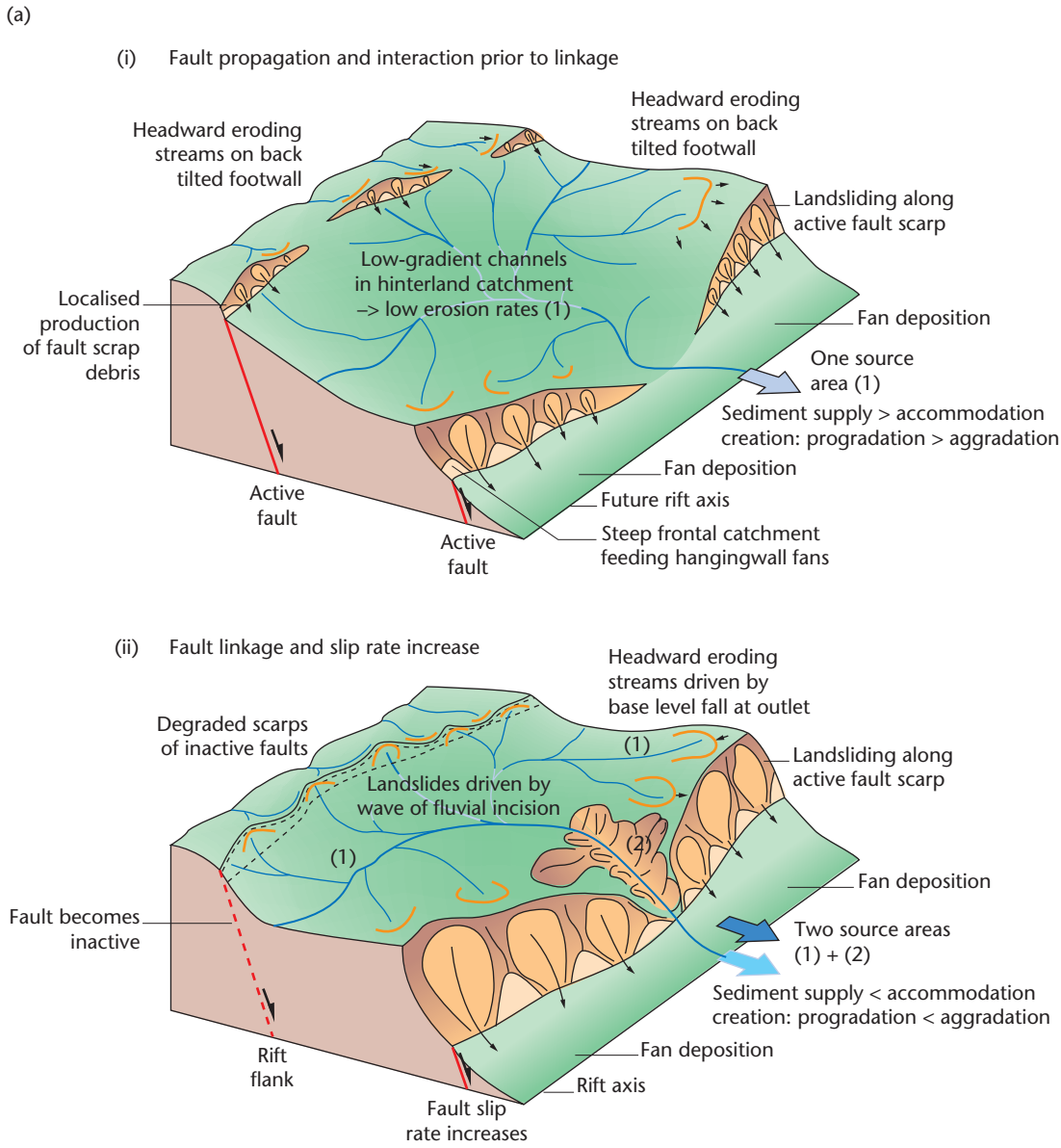

Fig. 3.13 (a) Schematic diagrams showing effects of fault linkage on surface topography and drainage in the fault propagation and interaction stage (i) and after fault linkage, which transfers extension to the main border fault (ii). (b) Numerical model results from fault linkage/surface processes model, showing evolution of erosional footwall. Reproduced from Cowie *et al*. (2006), with permission of John Wiley & Sons, Ltd.

of Germany. Regions of extensive, diffuse extension are associated with plateau-type topography, such as the Basin and Range, USA, and especially Tibet. In the first case, shallow subduction of relatively buoyant oceanic lithosphere beneath the North American plate, and in the second case, thickening of continental lithosphere during India-Asia collision, are the driving forces for extensive topographic uplift and extension.

Extensional basins vary greatly in their duration of subsidence, total extensional strain, and therefore in their strain rate (Fig. 3.5). Friedmann and Burbank (1995) recognised two distinct families of basins, which could be differentiated according to their strain rate, total extensional strain (or stretch factor β) and the dip of the master faults (Fig. 3.15):

- Discrete continental rifts located on normal thickness crust (such as the Rhine Graben, Baikal Rift, Rio Grande Rift) extend slowly (<1 mm yr^{-1}) over long periods of time (10–>30 Myr), with low total extensional strain (generally <10 km). Master fault angles are steep (45–70 degrees). Seismicity suggests that crustal extension takes place down to mid-crustal levels. At higher strain rates, narrow rifts may evolve through increased stretching into passive margins.

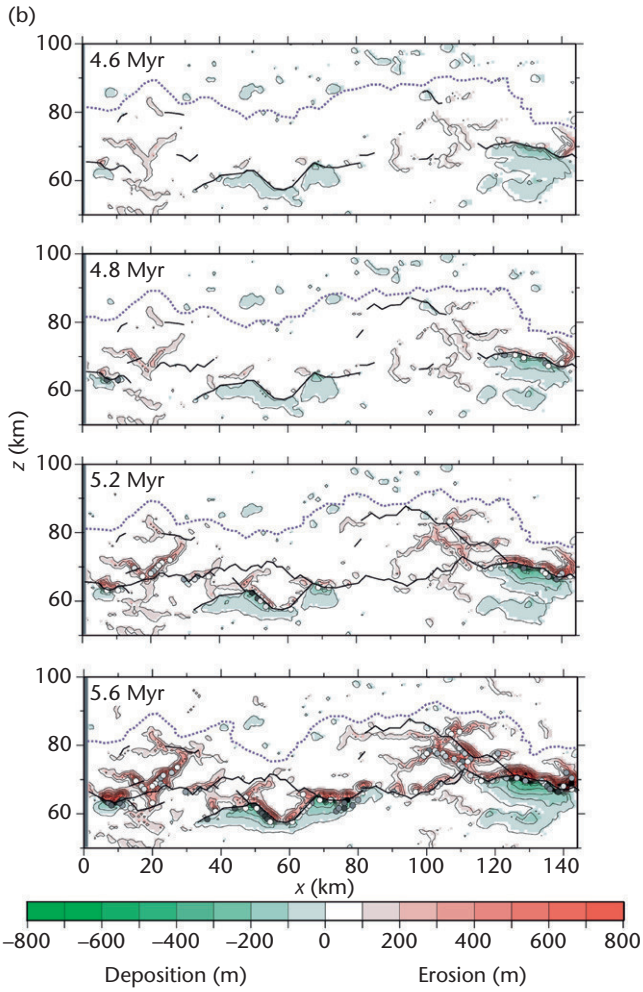

Fig. 3.13 *Continued*

- Supra-detachment basins occur within wide extended domains with previously thickened crust. They typically extend quickly (<20 mm yr^{-1}) over short periods of time (5–12 Myr) with a high amount of total extensional strain (10–80 km). Master faults (detachments) are shallow in dip (10 to 30 degrees), but may have originated at higher angles. Local anomalies in the ductile lower crust are amplified to produce core complexes (Wernicke 1985).

The location of continental rifts is commonly determined by the existence of old fundamental weaknesses in the lithosphere. A number of examples of this phenomenon are the opening of the modern Atlantic Ocean along the Paleozoic Iapetus suture (Wilson 1966), the Cretaceous separation of southeastern Africa from Antarctica along a Paleozoic failed rift (Natal Embayment) (Tankard *et al.* 1982) and Cenozoic rifting in the East African Rift system, which follows Precambrian structural trends (McConnell 1977, 1980).

3.2.3 Failed rifts

Failed rifts are those basins in which rifting has been aborted before the onset of seafloor spreading and passive margin development. Their rift phase is identical to that outlined in the previous paragraphs (§3.2.2). During cooling, failed rifts widen and post-rift sedimentary rocks onlap the previous rift shoulders, producing a *steer's head* geometry. A sedimentary evolution from non-marine to shallow-marine in the syn-rift phase and deeper-marine in the post-rift phase is typical.

The Benue Trough of central-western Africa and the North Sea are two excellent examples of aborted rifting. The Benue Trough is 1000 km long, 100 km wide, and is filled with <5 km of fluvial, deltaic and marine Cretaceous sedimentary rocks. At the southwestern end of the failed rift, the Tertiary Niger Delta has built a wedge of fluvial, deltaic and submarine fan deposits 12 km thick. A similar focusing of river drainage and delta growth along failed rift arms is found in the Lena Delta of the giant West Siberian Basin (Vyssotski *et al.* 2006) and the Brent Delta of the Viking Graben of the North Sea Basin (Morton *et al.* 1992).

In the northern North Sea a major period of rifting took place in the Middle Jurassic. At this time sediment was dispersed longitudinally along the graben. In the N–S oriented Viking Graben fluviatile deposits pass northwards into deltaic and shallow-marine deposits of the Brent Group (Morton *et al.* 1992). The Mid-Cretaceous saw the end of the rift phase and sediment onlapped the graben shoulders onto the East Shetland Platform in the west and the Norwegian Platform in the east. Thick deposits of Cretaceous chalks, Paleogene submarine fan sandstones and basinal shales, and Neogene mudstones typify this post-rift phase. In the southern part of the North Sea, the basin was filled by major sediment supplies from rivers draining the European mainland, producing mega-clinoforms due to westward delta progradation (Overeem *et al.* 2001; Huuse & Clausen 2001) (Fig. 3.16). The southern-central North Sea therefore shows the tendency for shallowing due to basin filling during the later stages of the thermal subsidence phase of failed rifts.

3.2.4 Continental rim basins

Continental rim basins or 'sag basins' (Huismans & Beaumont 2002) are thought to evolve over unstretched to slightly stretched continental lithosphere at the same time as passive margin development. They occur during the formation of new ocean basins where each continental margin subsides to produce a wide, shallow basin inboard of the ocean-facing margin (Veevers 1981, 2000; Favre & Stampfli 1992). The broad sag-type subsidence is suggested to be due to cooling following plume activity driving continental rifting (Fig. 3.17), but similar effects might be caused by thermal relaxation of upwelled asthenosphere relayed laterally from brittle upper crustal stretching associated with passive margin formation, or by cooling following convective thinning of the mantle lithosphere during continental attenuation (Huismans & Beaumont 2002). The hallmark of continental rim basins is that their centres are located in the order of 10^3 km inboard from the continental edge, their basin-fills are contemporaneous with the late syn-rift and drift phase of adjacent passive margins, their subsidence rates are low, their continental basement is typified by minimal amounts of brittle faulting, and magmatism is absent.

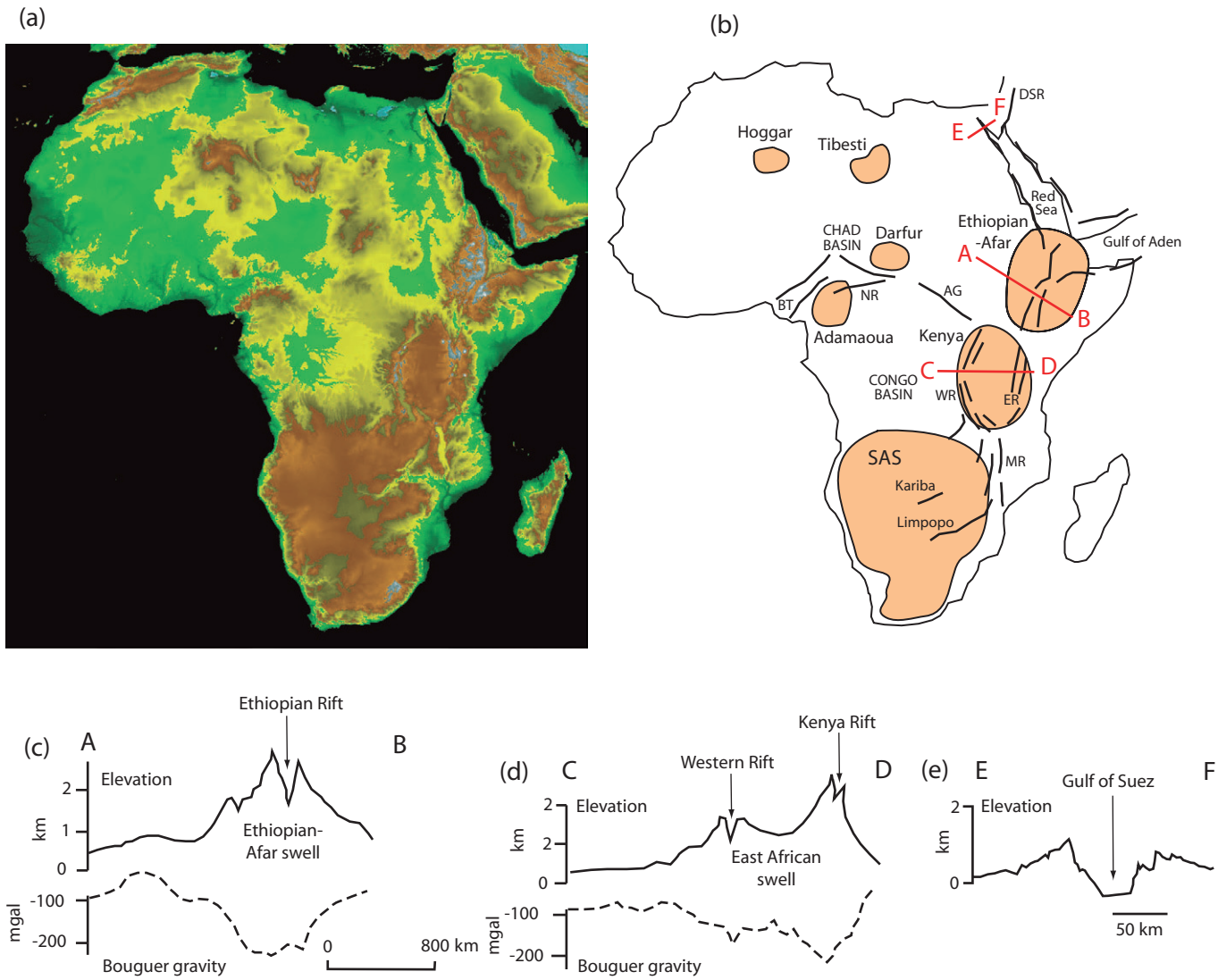

Fig. 3.14 (a) Topographic image of Africa (reproduced with the permission of NASA). (b) The major domal uplifts of Africa (Afar and East African domes) are due to uplift over hotspots in the mantle. SAS, Southern Africa swell. Also shown are the smaller topographic uplifts of central Africa and the main rift systems: AG, Abu Gabra Rift; BT, Benue Trough; DSR, Dead Sea Rift; MR, Malawi Rift; ER and WR, Eastern and Western Rifts; NR, Ngaoundere Rift. Topographic and Bouguer gravity profiles across the Afar (A–B) and East African (C–D) swells are shown in (c) and (d). (e) Topographic profile along E–F showing rift flank uplift across the Gulf of Suez (after Ebinger *et al.* 1989).

Sag-type subsidence commonly produces extensive, shallow-marine basins, which may accumulate widespread carbonate and organic-rich deposits, with a semi-restricted connection to the open ocean. Continental rim basins therefore have considerable economic importance (Hillgärtner *et al.* 2003).

3.2.5 Proto-oceanic troughs

At high amounts of stretching, continental rifts or backarc basins may evolve into new oceanic basins through a stage known as a proto-oceanic trough. Proto-oceanic troughs are characterised by young oceanic crust and very high surface heat flows. The transition from stretched continent to new ocean basin can be seen in north-eastern Africa and Arabia. The southern Red Sea contains young (<5 Ma) oceanic crust along its 50 km-wide axial zone, with flanking shelves underlain by stretched continental lithosphere. To the south the Red Sea undergoes a transition to the continental Afar Rift, and to the north into the continental Gulf of Suez Rift. The sedimentary evolution of the Red Sea area involves Oligo-Miocene syn-rift deposition of continental and shallow-marine sediments. As stretching continued through the Miocene, thick evaporites formed in the periodically isolated, proto-oceanic trough. During the Pliocene to Holocene, the Red Sea accumulated pelagic foraminiferal-pteropod oozes in deep water.

At the transition from rift basin to youthful ocean basin, subsidence commonly outpaces sediment supply, leading to the deposition

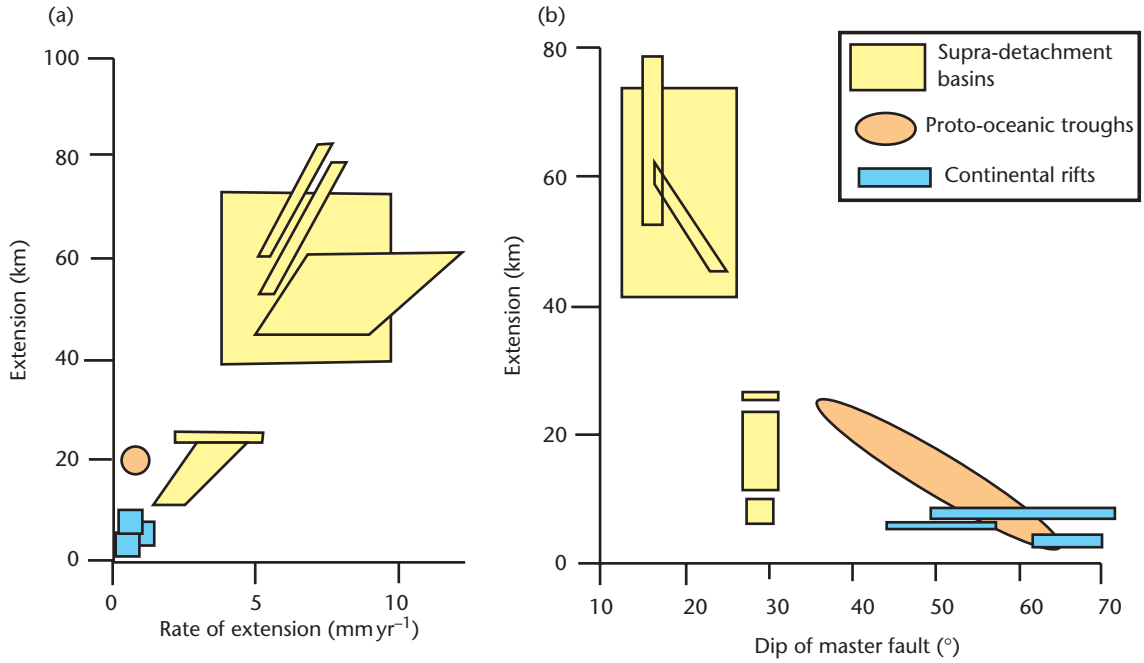

Fig. 3.15 Rifts, supra-detachment basins and proto-oceanic troughs in terms of their strain rate, total extensional strain, and dip of master faults. Based on Friedmann & Burbank (1995), reproduced with permission of John Wiley & Sons, Ltd.

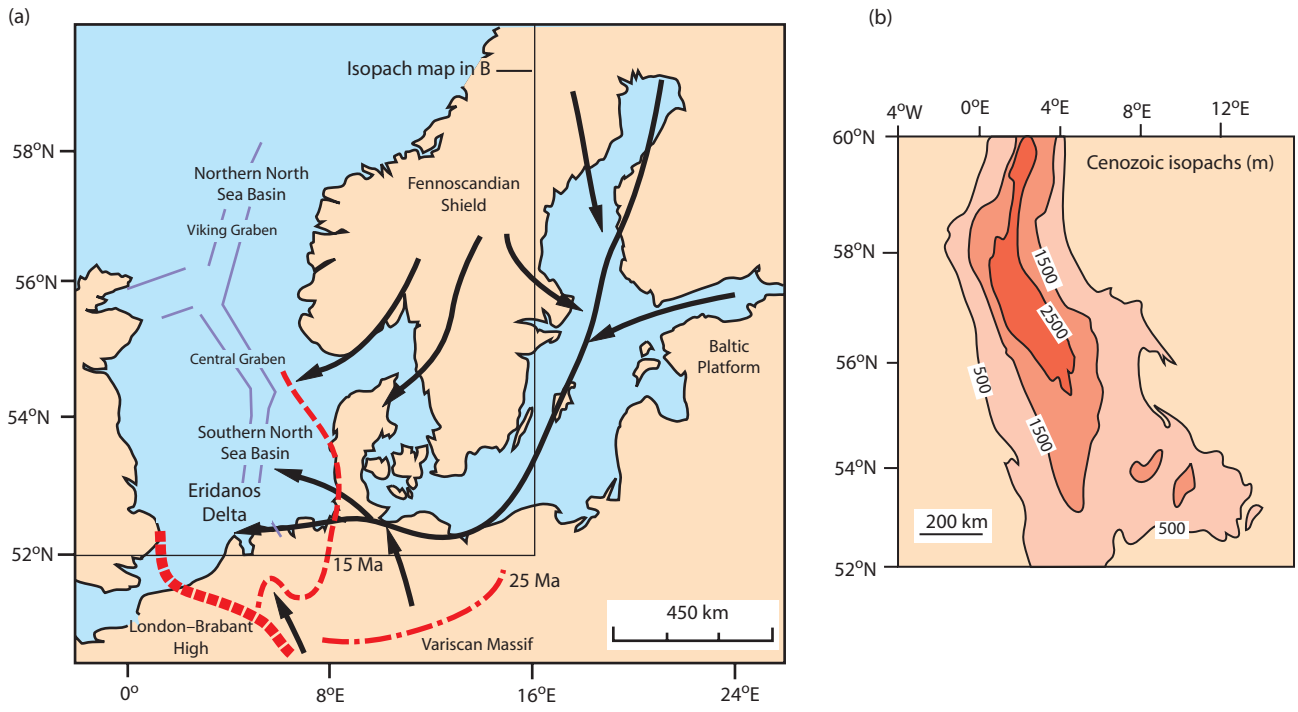

Fig. 3.16 Post-rift stratigraphy in the southern North Sea basin is dominated by megaclinoforms produced by delta progradation related to major river systems draining Europe, such as the Eridanos Delta. (a) Drainage system for the Eridanos Delta, with the shoreline shown at 25 Ma and 15 Ma (after Overeem *et al*. 2001; reproduced with permission of John Wiley & Sons, Ltd.); (b) Cenozoic isopachs (excluding Danian) in the North Sea (after Huuse & Clausen 2001; reproduced with permission of John Wiley & Sons, Ltd.).

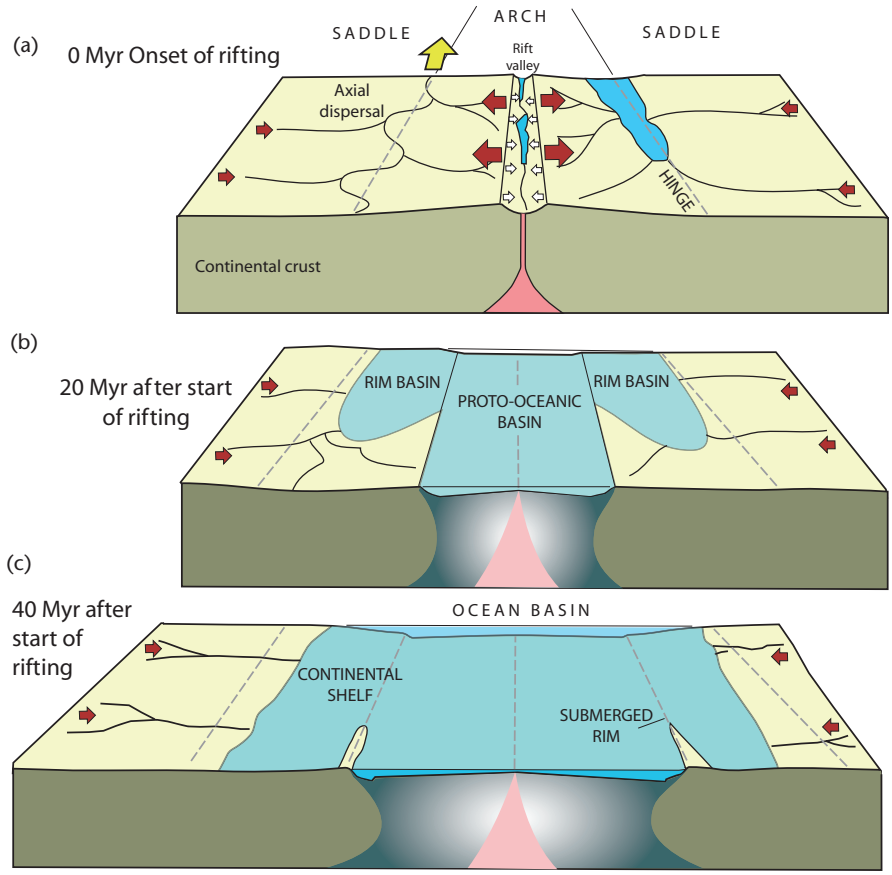

Fig. 3.17 Formation of continental rim basins (Veevers's model), as a component in the evolution of a continental margin and spreading centre. (a) Onset of rifting with rift valley and rift flank uplift, with small transverse river systems in rift axis, larger axial systems running down hinge line. (b) 20 Myr after the start of rifting, flooding of rim basins with restricted ocean circulation, adjacent to new ocean basin, with transverse continental drainage. (c) 40 Myr after the start of rifting, rim basins fully connected to ocean over flooded rift margin. From Veevers (1984), with permission of Oxford University Press.

of a triad of distinctive facies associations indicative of sediment starvation:

- *Evaporites.* The intermittent connection of developing rifts with the sea during the incipient stage provides ideal conditions for the formation of thick evaporites. Such evaporites occur along the margins of the Atlantic Ocean (Emery 1977; Rona 1982) and under the Red Sea (Lowell & Genik 1972).
- *Black organic-rich shales.* High organic productivity and restricted marine circulation may allow the preservation of organic-rich shales. Such conditions are likely to prevail where youthful ocean basins contain submarine sills restricting the throughput of water.
- *Pelagic carbonates.* In new ocean basins with little particulate sediment supply, deep-water pelagic carbonates may directly overlie the foundered pre-rift 'basement' or newly created seafloor. The faulted basement topography controls the type of deposit, with uplifted fault block edges and seamounts accumulating shallow-water carbonates, and intervening troughs being the sites of fine-grained oozes. This pattern of sedimentation related to fault block shoulders and troughs has been interpreted from the Triassic–Jurassic of the Tethyan realm of southern Europe (Bernoulli & Jenkyns 1974).

3.2.6 Passive continental margins

The formation of juvenile oceanic spreading centres, as in the 20 Myr-old Red Sea–Gulf of Aden, and then mature (>40 Myr) ocean basins is accompanied by the development of passive margins on the adjacent stretched continental lithosphere (review in Bond *et al.* 1995). Fully developed passive margins, such as those bordering the Atlantic Ocean, are characterised by extensional faulting, large-scale gravitational tectonics (slumps, slides, glide-sheets) and salt tectonics.

Passive continental margins involve strongly attenuated continental crust stretched over a region of 50–150 km, and exceptionally as much as 400–500 km (Keen *et al.* 1987), overlain by thin or thick sediment prisms. They are in general seismically inactive, and in mature examples heat flows are normal. Passive continental margins (also known as *Atlantic-type margins*) are characterised by seaward-thickening prisms of marine sediments overlying a faulted basement

Table 3.1 Conjugate margins of the Atlantic

Western margin	Eastern margin	Start of main rifting and duration
Southern Grand Banks	Iberia/Galicia	Valanginian (137 Ma) 15–25 Myr
Flemish Cap	Goban Spur	Barremian (127 Ma) 15–20 Myr
Labrador	SW Greenland	Barremian (127 Ma) 40–65 Myr

with syn-rift sedimentary sequences, often of continental origin. The post-rift seaward-thickening sediment prisms consist predominantly of shallow-marine deposits. Seismic reflection sections show some passive margins to be underlain by linked listric extensional fault systems that merge into low-angle sole faults. The post-rift or drifting phase, in contrast, is typically dominated by gravity-controlled deformation (salt tectonics, mud diapirism, slumps, slides, listric growth faults in soft sediments) (Rowan *et al.* 2004).

Passive margins overlie earlier rift systems that are generally subparallel to the ocean margins, or less commonly at high angles to the ocean margin (as in the case of failed arms of triple junctions such as the Benue Trough, Nigeria), or along transform fault zones (e.g. Grand Banks and Gulf of Guinea). The early syn-rift phase of sedimentation is commonly separated from a later drifting phase by an unconformity (the 'breakup' unconformity of Falvey 1974). Some passive margins exhibited considerable subaerial relief at the end of rifting (leading to major unconformities), as in the case of the Rockall Bank, northeastern Atlantic, whereas in others, the end of rifting may have occurred when the sediment surface was in deep water, as in the Bay of Biscay and Galicia margin of Iberia (Montadert *et al.* 1979; Pickup *et al.* 1996).

Since passive margins represent the rifted edges of a piece of continental lithosphere, now separated by an ocean basin, it is possible to identify the original matching margins on either side of the ocean. These are known as *conjugate margins*. They are particularly well developed on either side of the northern Atlantic (Table 3.1).

Comparison of conjugate margins is informative regarding the geometry of extension prior to ocean basin development. For example, deep seismic reflection profiles show some conjugate pairs of passive margin to be symmetric, with seaward-dipping rotated fault blocks, whereas other deep profiles suggest the presence of a flat-lying or landward-dipping detachment or shear zone, producing a markedly asymmetrical pattern (Fig. 3.18). The profiles across the Labrador and SW Greenland margins show that although the brittle upper crust has been extended symmetrically, the lower crustal extension is particularly asymmetrical. Some margins show thin sediment covering wide regions of highly faulted upper crust, commonly separated from underlying serpentinised upper mantle by a horizontal detachment (e.g. Iberia, Galicia and SW Greenland margins). Other margins with thick sediment prisms consist of one or two major tilted crustal blocks and lack a horizontal detachment (e.g. Labrador margin).

Passive margins can be categorised according to:

- the abundance of volcanic products;
- the thickness of sediments, from sediment nourished to sediment starved;
- the presence or absence of gravitationally driven and salt tectonics in the post-rift phase (§11.7.2).

Volcanically active margins (Fig. 3.19) are characterised by extrusive basalts, lower crustal igneous accretions, and significant uplift at the time of break-up. Continental extension and ocean spreading are thought to be intimately related to mantle plume activity (Fig. 3.20). Volcanic activity, generally tholeiitic, occurring at the time of break-up (White & McKenzie 1989), is commonly associated with subaerial emergence, as in the northern North Atlantic in the Early Tertiary (e.g. Skogseid *et al.* 2000). *Non-volcanic margins* lack evidence of high thermal activity at the time of break-up.

Sediment-starved margins have relatively thin 2–4 km-thick sediment veneers draping large arrays of rotated syn-rift fault blocks above a sub-horizontal detachment, as in the Bay of Biscay (Fig. 3.20b). *Sediment-nourished margins* comprise very thick (<15 km) post-rift sedimentary prisms overlying a small number of tilted upper crustal fault blocks and a wide region of mid-lower crustal extension, as in the Baltimore Canyon region of the Eastern Seaboard of North America (Fig. 3.20c), and the Labrador margin.

Extensional faulting dies out in the post-rift phase with only minor reactivation of older normal faults. Growth faults are common in areas of high sedimentation rate (e.g. off the Niger Delta, African coast). Gravitational mass movements, from small slumps to gigantic slides, are very important during the post-rift drifting phase (§11.7.2.2). The continental slope and rise off southwestern and southern Africa were subject to major slope instability during the Cretaceous and again in the Tertiary (Dingle 1980). The slide units are over 250 m thick and can be traced for 700 km along strike and for nearly 50 km down paleoslope. The recent 3500 km^3 Storegga slide (8150 yr BP) off the Norwegian margin (Bondevik *et al.* 1997) is a reminder of the ongoing gravitational instability of continental margins.

The sediment supply to the passive margin prism comes principally by rivers eroding the continental land surface, but significant quantities of sediment may be accreted to the lower continental slope by thermohaline current-driven drifts. Major river systems build out large embankments and submarine fans that may extend directly onto oceanic crust, as in the case of the Amazon fan.

Evaporites typify the first marine incursions during the incipient ocean phase of the proto-oceanic trough or young passive margin. When buried under an overburden of passive margin sediments these evaporites become mobile, producing sheets and diapirs (Fig. 3.21). The Brazilian continental margin and the western Grand Banks, Newfoundland, show examples of major diapiric activity. The movement of subsurface salt and its penetration of the seabed causes submarine bathymetry that is important in the guiding of gravity flows to perched basins and the deep sea. Basins perched on the gravitationally driven post-rift thrust wedge may be 'filled and spilled' in a cascading process of sediment filling. Structures such as salt diapirs, whose growth affects seabed topography, interact with the incisive power of submarine channelised currents (Mayall *et al.* 2010). Incisive currents flowing over slow-growing structures tend to cut through, whereas less powerful currents are deflected by fast-growing seabed structures. Clark and Cartwright (2009) referred to such channel-topography interaction as 'confinement' and 'diversion'.

The Atlantic margin shows great variety in the nature of the passive margin prograding wedge. The Senegal margin of western Africa contains a thick carbonate bank extending over the stretched continental crust. Further to the SE the Niger has built a thick deltaic clastic wedge, provoking growth faulting and mud diapirism.

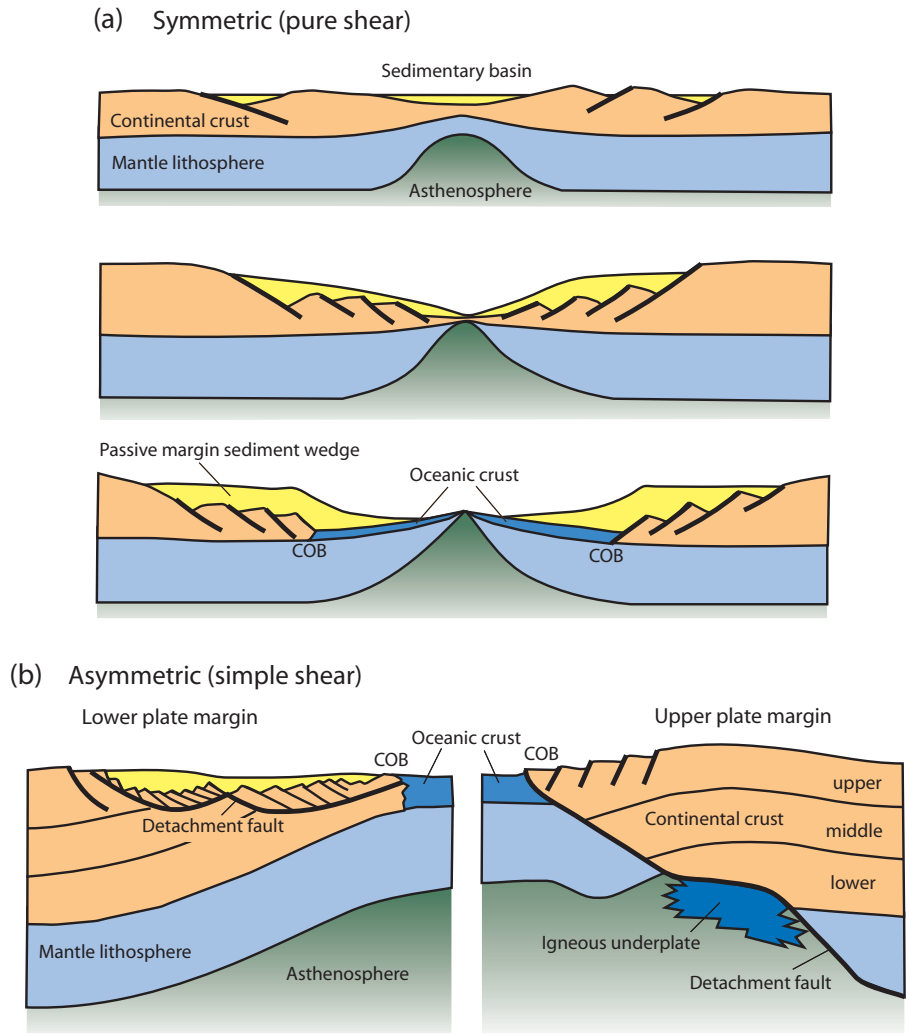

Fig. 3.18 Conjugate margins based on deep seismic information (after Lister *et al*. 1986; Louden & Chian 1999). (a) Symmetric margin (pure shear), and (b) asymmetric margin (simple shear) with a lithospheric detachment fault. COB is continent–ocean boundary.

Further south off Gabon and remote from the Niger Delta, oceanic muds overlie thick diapirs of evaporite. Off the coast of southwestern Africa a 'normal' siliciclastic margin exists with seaward-prograding clinoforms reaching far out into the basin and overlying the oceanic crust. This latter type is also common to the highly sediment-nourished North American Atlantic margin, where a well-developed coastal plain and continental shelf extend to 200 m water depth, with a continental slope descending to the abyssal plain of the Atlantic Ocean at water depths in excess of 4 km.

3.3 Uniform stretching of the continental lithosphere

3.3.1 The 'reference' uniform stretching model

Falvey (1974) proposed that the subsidence histories of various continental rift basins and continental margins could be explained qualitatively by extension in both crust and subcrustal lithosphere. The crust was assumed to fail by brittle fracture and the subcrustal lithosphere to flow plastically. The isostatic disequilibrium caused by the crustal extension leads to a compensating rise of the asthenosphere, and consequent regional uplift. Partial melting of upwelled asthenosphere leads to volcanism and further upward heat transfer. Eventually, after the continental lithosphere has been extended and thinned to crustal levels, new oceanic crust is generated as the rift evolves into a continental margin.

McKenzie (1978a) considered the quantitative implications of a passive rifting or mechanical stretching model, assuming the amount of crustal and lithospheric extension to be the same (*uniform stretching*). The stretching is symmetrical, no solid body rotation occurs, so this is the condition of *pure shear*. He considered the instantaneous and uniform extension of the lithosphere and crust with passive upwelling of hot asthenosphere to maintain isostatic equilibrium (Fig. 3.22). The initial surface of the continental lithosphere is taken to be at sea level, and since the lithosphere is isostatically compen-

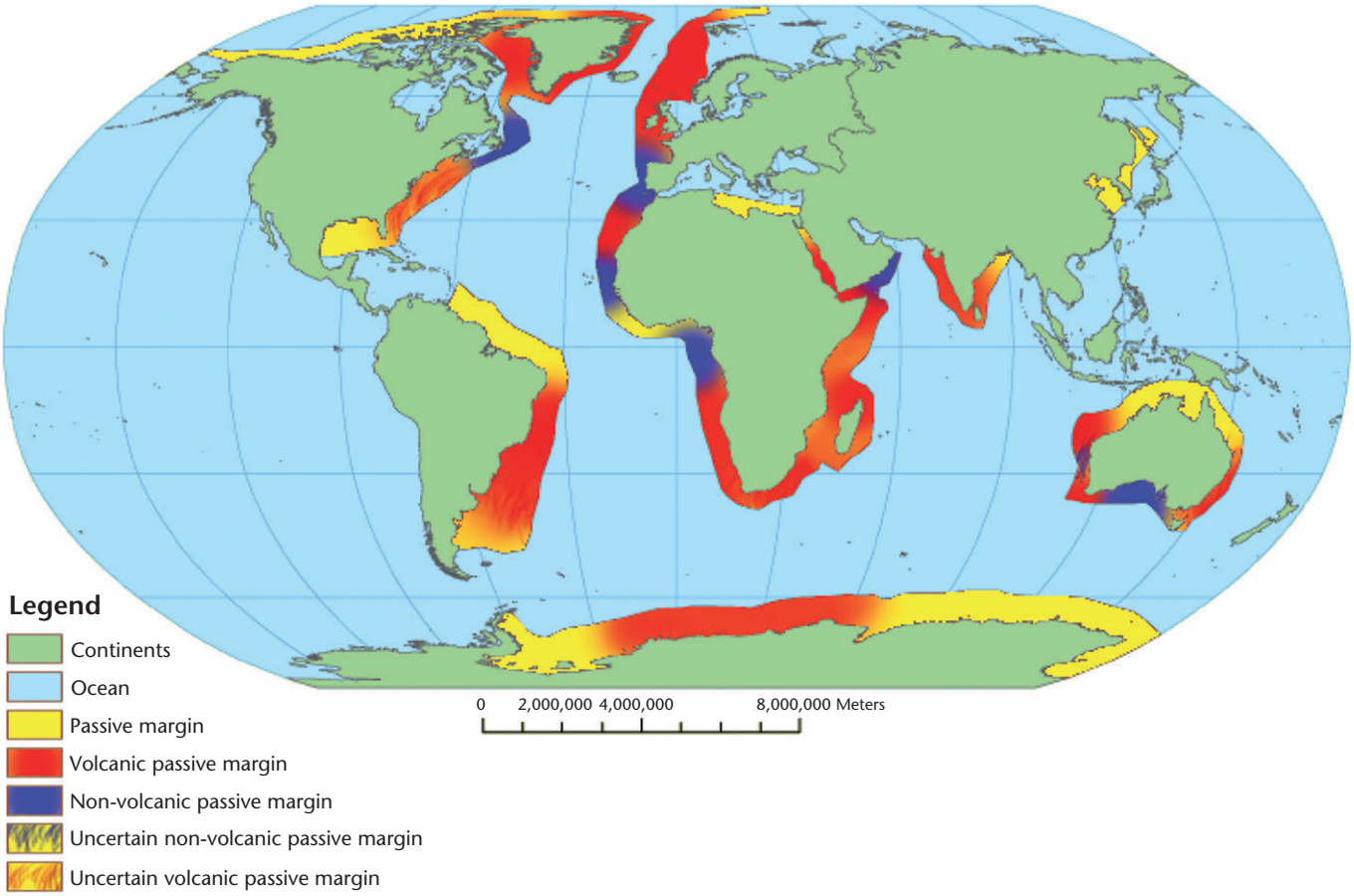

Fig. 3.19 Global distribution of passive margins, categorised as volcanic or non-volcanic, from http://en.wikipedia.org/wiki/File:Globald.png.

sated throughout (Airy model), the subsidence or uplift consequent upon mechanical stretching can be obtained (Appendices 19, 21).

A key component of the reference uniform stretching model is the assumption that the base of the plate remains at the same temperature during the stretching and subsequent cooling of the continental lithosphere. Consequently, the heat flow increases instantaneously (by a factor β) as a result of the mechanical stretching, since by Fourier's law it is proportional to the temperature gradient, and subsequently declines (Appendix 23). The steady-state geotherm before stretching is linear. Following stretching, the new, elevated geotherm relaxes as the stretched lithosphere cools and thickens, so that the post-rift subsidence is driven by a time-dependent transient cooling (Fig. 3.23). Much of the mathematics of the reference uniform stretching model is geared to calculating this transient component (Appendix 22).

The results of McKenzie's (1978a) quantitative model of uniform stretching can be summarised as follows:

- The total subsidence in an extensional basin is made up of two components: an initial *fault-controlled subsidence*, which is dependent on the initial thickness of the crust y_c compared to the initial thickness of the lithosphere y_L, and the amount of stretching β; and a subsequent *thermal subsidence* caused by relaxation of lithospheric isotherms to their pre-stretching position, which is dependent on the amount of stretching alone.
- Whereas the fault-controlled subsidence is modelled as instantaneous, the rate of thermal subsidence decreases exponentially with time. This is the result of a decrease in heat flow with time (Fig. 3.24a). The heat flow reaches 1/e of its original value after about 50 Myr for a 'standard' lithosphere, so at this point after the cessation of rifting, the dependency of the heat flow on β is insignificant.

The time scale of the thermal subsidence following stretching is determined by a diffusive thermal time constant of the lithosphere. For an initial lithosphere thickness of 125 km and a thermal diffusivity of lithospheric rocks of $10^{-6}\,m^2\,s^{-1}$, the time constant used by McKenzie (1980a) is $\tau = y_L^2 / \pi^2\kappa$, which is equal to 50 Myr. After two lithospheric time constants (c.100 Myr) thermal subsidence curves for all values of the stretch factor are similar (Fig. 3.24b).

The elevation change of the surface of the Earth at the time of the onset of stretching is a trade-off between the effect of crustal stretching (causing subsidence by faulting) and the effect of the stretching of the subcrustal lithosphere (causing uplift by thermal expansion).

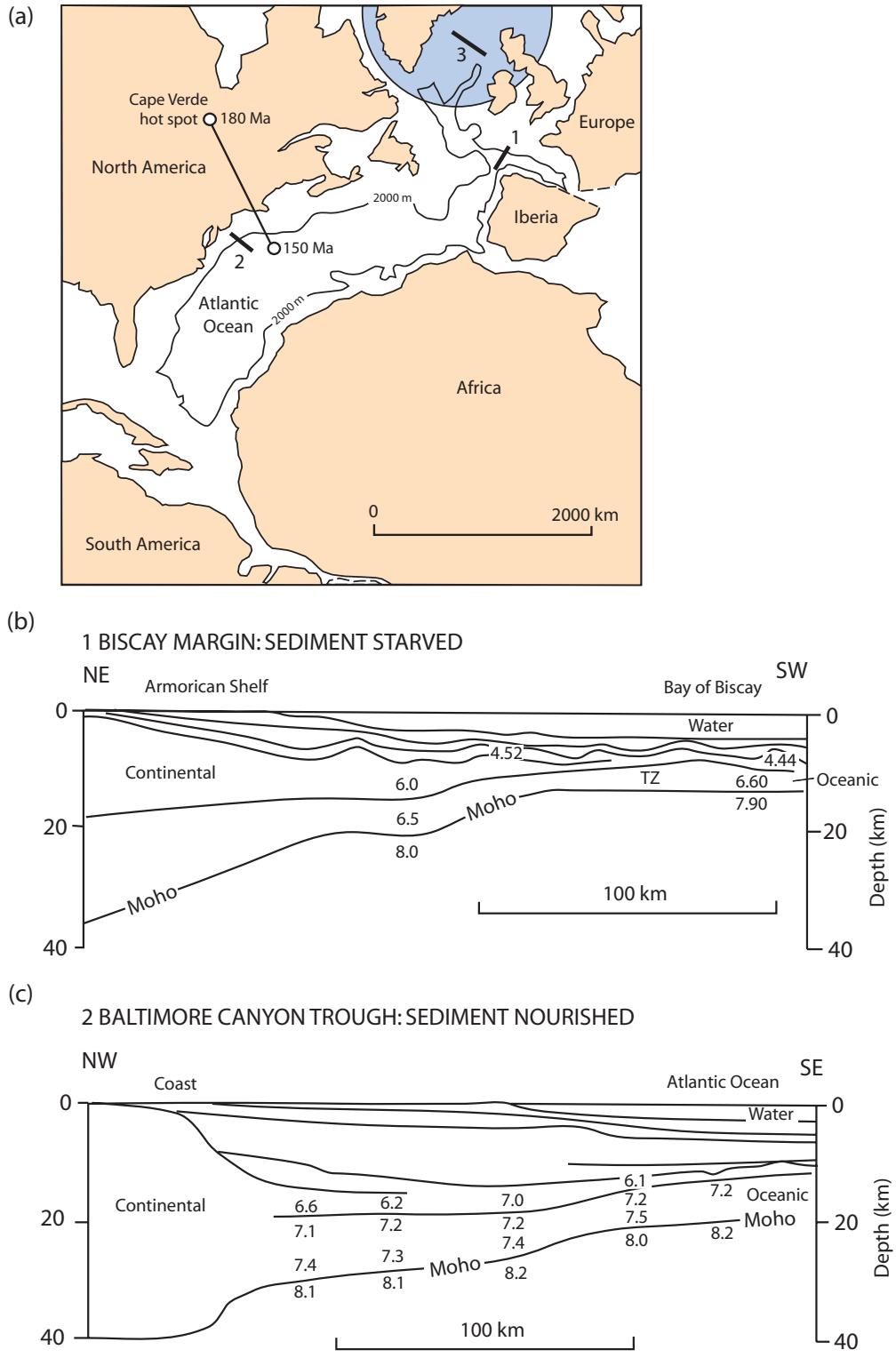

Fig. 3.20 (a) Location of margins in the central–north Atlantic region on a Middle Jurassic reconstruction (170 Ma), shortly after the onset of seafloor spreading. (b) Biscay margin, which is sediment starved. (c) Baltimore Canyon Trough margin, which is thickly sedimented. (d) Hatton bank margin, which is characterised by important magmatic activity. Shaded area shows extent of extrusive basalts. Moho is overdeepened due to the presence of an igneous underplate. TZ, ocean–continent transition zone; OC, ocean crust; numbers are seismic wave velocities in km s^{-1}. After White & McKenzie (1989), reproduced with permission of the American Geophysical Union.

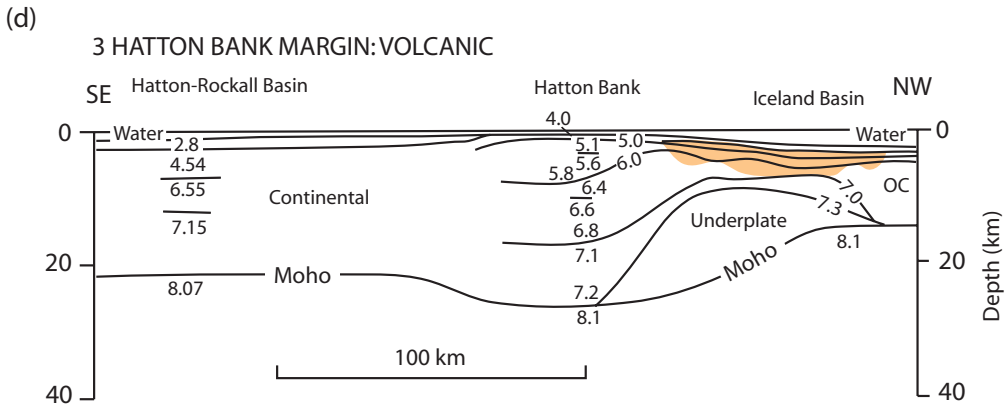

Fig. 3.20 *Continued*

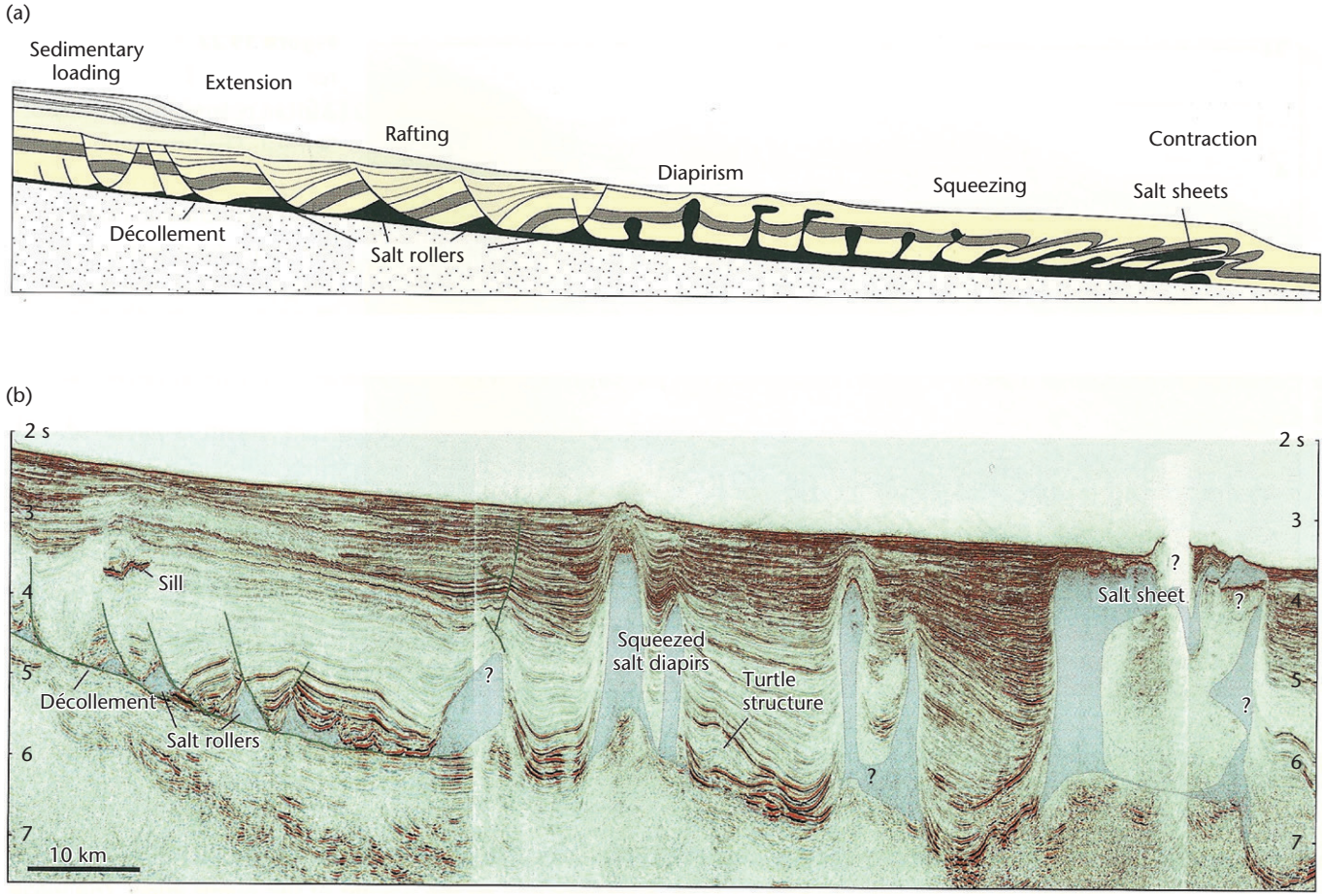

Fig. 3.21 (a) Structures commonly found on passive margins related to a salt detachment, dominated by sediment loading and extension at the rear, diapirism in the centre and fold-thrust deformation at the front (after Fossen 2010, p. 391). (b) Salt diapirs originating from a detachment level, Espirito Santo Basin, offshore Brazil (CGG Veritas, in Fossen 2010, p. 391). Haakon Fossen, 2010 © Cambridge University Press.

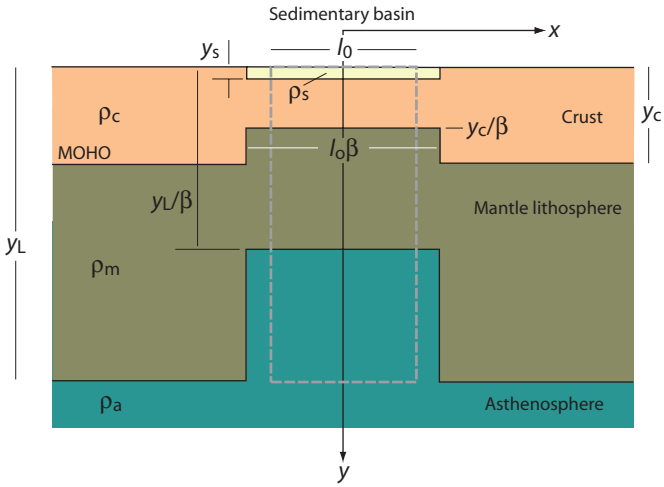

Fig. 3.22 Set-up for the reference uniform stretching model (McKenzie 1978a). The crust and subcrustal lithosphere stretch horizontally and thin vertically, uniformly with depth. Sediment, crustal, mantle lithosphere and asthenospheric densities are ρ_s, ρ_c, ρ_m and ρ_a. The crust and lithosphere have an initial thickness of y_c and y_L, and the zone of stretching has an initial width l_0. The crust and subcrustal (mantle) lithosphere stretch uniformly by a factor β.

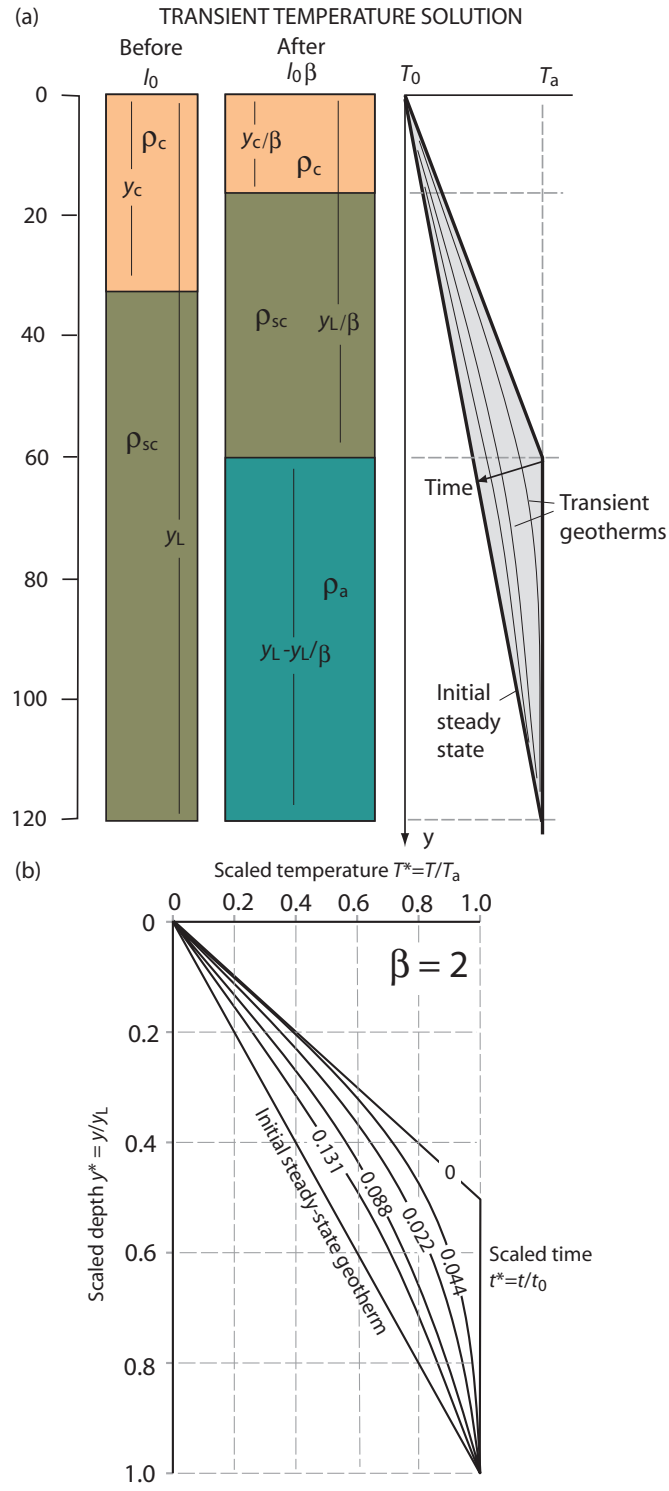

Fig. 3.23 (a) The initial steady-state geotherm is linear, due to conduction through a lithosphere of initial thickness y_L. The geotherm at time $t = 0$ immediately after stretching is linear from the surface to a new depth y_L/β. Shown for $\beta = 2$ are the transient geotherms at different times during the subsequent cooling. (b) Temperature versus depth for different times following stretching, for a stretch factor of $\beta = 2$. Temperature is scaled by the asthenospheric temperature T_a; depth is scaled by the initial lithospheric thickness y_L; time is scaled by a diffusive time constant of the lithosphere $t_0 = y_L^2/\kappa$, as in eqn. 2.29 (§2.2.7).

At a y_c/y_L ratio of 0.12, corresponding to a crustal thickness of 17 km and a lithosphere thickness of 125 km, there is no surface elevation change (Fig. 3.25). Consequently, regions with thick crusts should experience larger amounts of fault-controlled subsidence than those with thin crusts. Similarly, regions with thick subcrustal lithosphere should experience greater and more prolonged post-rift thermal subsidence than those with thin subcrustal lithospheres.

The assumptions, boundary conditions and development of the model are elaborated in Appendices 17 to 23.

Modifications of the boundary conditions and assumptions of the uniform stretching model are discussed in §3.4. For convenience, these assumptions and boundary conditions are listed below (some are implicit rather than stated):

- stretching is uniform with depth;
- stretching is instantaneous;
- stretching is by pure shear;
- the necking depth is zero;
- Airy isostasy is assumed to operate throughout;
- there is no radiogenic heat production;
- heat flow is in one dimension (vertically) by conduction;
- there is no magmatic activity;
- the asthenosphere has a uniform temperature at the base of the lithosphere.

3.3.2 Uniform stretching at passive continental margins

The uniform stretching model has been applied to the formation of passive margins (e.g. Le Pichon & Sibuet 1981). The assumptions are identical to those given above (§3.3.1): stretching of the whole lithosphere occurs instantaneously at time $t = 0$ (or within a period of 20 Myr, following Jarvis & McKenzie 1980; see also §3.4.1), heat

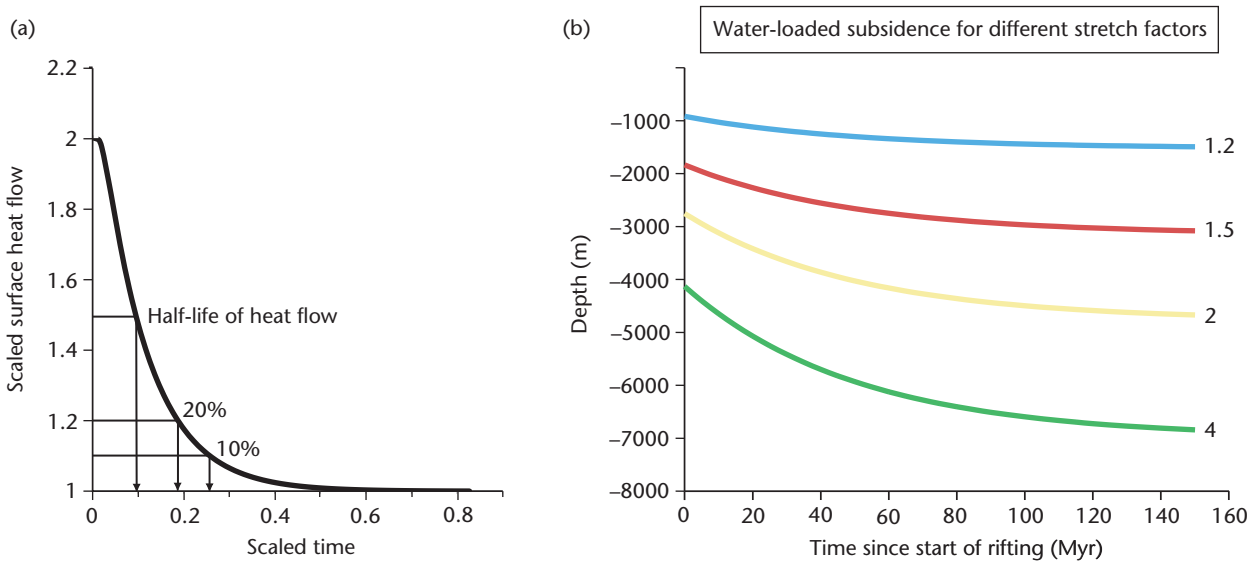

Fig. 3.24 (a) Surface heat flow, scaled by the surface heat flow prior to stretching, versus time scaled by the diffusive time constant of the lithosphere, for a stretch factor of 2. Note the exponential reduction in heat flow over time. The half-life for the surface heat flow is at 0.1 of the scaled time, that is, 0.1 t_0. (b) Water-loaded subsidence due to cooling, plotted against time since the start of rifting, as a function of the stretch factor, shown for β values of 1.2, 1.5, 2, and 4.

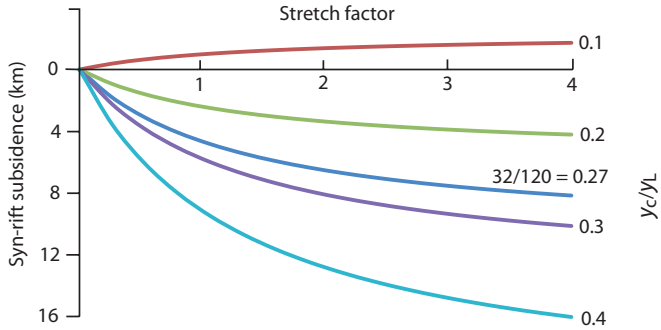

Fig. 3.25 Syn-rift subsidence as a function of the crustal/lithosphere thickness ratio y_c/y_L for stretch factors β up to 4, using the uniform stretching model. Crustal, mantle and sediment densities are 2700 kg m^{-3}, 3300 kg m^{-3} and 2000 kg m^{-3} respectively. At a crust/lithosphere thickness ratio of 0.12 (corresponding to a crust of 15 km in a lithosphere 125 km thick), there is neither uplift nor subsidence during rifting. For thinner crusts, uplift occurs, and for thicker crusts, subsidence occurs. Since crustal thicknesses are typically 30–35 km, the syn-rift phase should normally be characterised by subsidence.

production from radioactivity is ignored, local (Airy) isostatic compensation is maintained throughout, and the continental surface is initially at sea level. The initial fault-controlled subsidence (Appendix 21) is determined by the stretch factor and y_c/y_L ratio. However, in the case of passive margins, it is important to investigate the subsidence $S(\infty)$ at time $t = \infty$. Just as the initial subsidence S_i is a linear function of $(1 - 1/\beta)$, so $S(\infty)$ can also be expressed as a linear function of $(1 - 1/\beta)$. By introducing new parameters ρ'_L and ρ'_c as the average densities of the mantle part of the lithosphere and crust at time $t = \infty$, the final subsidence $S(\infty)$ can be expressed in terms of the average densities of the crust and lithosphere, the initial thicknesses of the crust and lithosphere and the stretch factor (Appendix 28).

The difference between the initial subsidence S_i and the final subsidence $S(\infty)$ is the subsidence caused by the progressive return to thermal equilibrium, i.e. that due to thermal contraction on cooling. The latter is termed thermal subsidence S_t and of course $S_t = S(\infty) - S_i$.

As an example of this kind of analysis, it is possible to examine seismic reflection profiles across the northern Bay of Biscay and Galicia continental margins (Montadert *et al.* 1979) (Fig. 3.20b) and to test whether the uniform stretching model accurately predicts the observed subsidence. Active extensional tectonics started in the Late Jurassic–Early Cretaceous (c.140 Ma). Extension extended outwards from a central region, creating new fault blocks that were progressively tilted. By the time oceanic crust was emplaced (120 Ma) the subsiding trough had reached a depth of about 2.4 km, and simultaneously active tectonics ceased, giving way to thermal subsidence. The Bay of Biscay is relatively starved of sediment, minimising the effects of sediment loading compared to, for example, the US Atlantic continental margin (Fig. 3.20c).

The following constants were chosen (Parsons & Sclater 1977) to fit the Biscay and Galicia data (Le Pichon & Sibuet 1981):

initial lithospheric and crustal thicknesses; $y_L = 125$ km and $y_c = 30$ km (from refraction data)
mantle density at 0 °C; $\rho^*_m = 3350$ kg m^{-3}
crustal density at 0 °C; $\rho^*_c = 2780$ kg m^{-3}
water density; $\rho_w = 1030$ kg m^{-3}
volumetric coefficient of thermal expansion; $\alpha_v = 3.28 \times 10^{-5}$ °C^{-1}
temperature at base of lithosphere; $T_m = 1333$ °C

Using these constants, the initial fault-controlled subsidence simplifies to $S_i = 3.61(1 - 1/\beta)$ km, the final subsidence becomes

$S(\infty) \sim 7.83(1 - 1/\beta)$ km, so the thermal subsidence is the difference between $S(\infty)$ and S_i, giving $S_t \sim 4.21(1 - 1/\beta)$ km.

However, since the Bay of Biscay margin is 120 Myr old rather than being infinitely old, S_{120} is somewhat smaller than $S(\infty)$. As a result, the total subsidence at 120 Myr is $S_{120} \sim 7.23(1 - 1/\beta)$ and the thermal subsidence at 120 Myr is $S_{t120} \sim 3.64\ (1 - 1/\beta)$.

Mid-ocean ridge crests are generally at about 2.5 km water depth, suggesting that zero-age oceanic lithosphere under 2.5 km of water is in equilibrium with a 'standard' continental lithospheric column. Therefore, during rifting, the asthenosphere should theoretically not be able to break through the thinned continental lithosphere as long as S_i is less than 2.5 km. Using the equation for the initial subsidence, the stretch factor required to produce 2.5 km of subsidence is 3.24; the crust by this time will be reduced in thickness to 9.25 km and will most likely be highly fractured – it is probable therefore that the asthenosphere would break through when this depth was reached. This represents the continent–ocean transition.

In the Bay of Biscay the estimated total subsidence at 120 Myr since rifting (S_{120}) for $\beta = 3.24$ is 5.2 km, and the final subsidence $S(\infty)$ for an infinitely large β is 7.8 km. One should therefore expect to find continental crust in the Bay of Biscay at water depths of 5.2 km or shallower in the absence of sedimentation. Oceanic crust should not be found at shallower water depths.

The extension estimated from fault block geometries in the upper crust is relatively high (approximately $\beta = 2.6$) based on migrated seismic reflection profiling, indicating that the crust is substantially thinned and close to the value at which the asthenosphere could break through. Along the seismic profile the depth to the surface of the continental block is 5.2 km, which shows that the model very satisfactorily explains the main features of the Biscay margin.

A regional synthesis suggests that water depth S_w varies linearly with the thinning of the continental crust, following a relation close to $S_w = 7.5(1 - 1/\beta)$, which is almost identical to the model prediction of $7.23(1 - 1/\beta)$.

It is perhaps surprising that the Biscay and Galicia data fit the simple uniform stretching model so well. This is probably because during phases of rapid stretching, and in the absence of large sediment loads, the lithosphere is compensated on a local scale rather than responding by flexure.

The eastern US and Canadian passive margin, however, is very thickly sedimented, with over 10 km along most of the margin (Fig. 3.26), and considerably more in areas such as the Baltimore Canyon, where a deep offshore well (COST B-2) was drilled in March 1976 (Poag 1980). The subsidence history of thickly sedimented margins such as this is profoundly affected by the *sediment load*. The sediment load is supported by the rigidity of the plate, and the borehole records (and seismic reflection profile data) need to be *backstripped* to obtain the tectonic subsidence (§9.4).

3.4 Modifications to the uniform stretching model

It is clear that there are a number of observations in regions of continental extension that suggest that the assumptions in the uniform stretching model should be re-examined. We firstly consider the effect of finite (protracted) periods of rifting, since rifts typically have syn-rift phases lasting 20–30 Myr or longer. We then briefly consider other possible modifications to the reference uniform stretching model. Modifications are dealt with under the following headings:

- *Protracted periods of stretching* cause slowly extending lithosphere to cool during the phase of stretching.
- *Non-uniform (depth-dependent) stretching*: the mantle lithosphere may stretch by a different amount to the crust.
- *Pure versus simple shear*: the lithosphere may extend along trans-crustal or trans-lithospheric detachments by simple shear.
- *Elevated asthenospheric temperatures*: the base of the lithosphere may be strongly variable in its temperature structure due to the presence of convection systems such as hot plumes.
- *Magmatic activity*: the intrusion of melts at high values of stretching modifies the heat flow history and thermal subsidence at volcanic rifts and some passive margins.
- *Induced mantle convection*: the stretching of the lithosphere may induce secondary small-scale convection in the asthenosphere.
- *Radiogenic heat production*: the granitic crust provides an additional important source of heat.
- *Depth of necking*: necking may be centred on strong layers deeper in the mid-crust or upper mantle lithosphere.
- *Flexural compensation*: the continental lithosphere has a finite elastic strength and flexural rigidity, particularly in the post-rift thermal subsidence phase.

3.4.1 Protracted periods of rifting

The reference model assumes instantaneous rifting of the lithosphere followed by thermal subsidence as the lithosphere re-equilibrates to its pre-extension thickness. This is an attractive assumption since it gives a simple, well-defined initial condition for the thermal calculations. Jarvis and McKenzie (1980) revised this one-dimensional model by allowing for protracted periods of stretching. If the duration of stretching is large compared with the diffusive time scale of the lithosphere ($\tau = y_L^2/\pi^2\kappa$), which is 50–60 Myr for a standard lithosphere, some of the heat diffuses away before the stretching is completed. In the general case, if the time taken to extend the continental lithosphere by a factor β is less than τ/β^2 Myr, the results are similar to those of the uniform stretching model with instantaneous stretching. However, the sensitivity of the results depends on the value of the stretch factor and whether total subsidence or heat flow is being considered:

- Considering total subsidence, if $\beta < 2$, the duration of extension must be less than τ/β^2 Myr for the instantaneous stretching model to be a reasonable representation. If $\beta > 2$, the duration of extension must be less than $\tau\,(1 - 1/\beta)^2$.
- Considering heat flow, if $\beta < 2$, the duration of extension must be less than τ Myr for the instantaneous stretching model to be a reasonable representation. If $\beta > 2$, the duration of extension must be less than $\tau\,(2/\beta)^2$.

Although stretching is known to be short-lived in some extensional provinces, such as the Pannonian Basin (<10 Myr to reach a stretch factor of 3) (Sclater *et al.* 1980b), many sedimentary basins appear to have undergone more protracted periods of rifting, considerably in excess of $60/\beta^2$ Myr. The Paris Basin, for instance, rifted in the Mid-Permian and sedimentation was restricted to elongate rift troughs until close to the end of the Triassic. The rift phase was therefore close to 60 Myr in duration. The Triassic (Carnian–Norian, 212–200 Ma) continental red beds and evaporites of the Atlantic margin of northeastern USA and Canada were deposited in fault-bounded rifts, but seafloor spreading did not commence until the

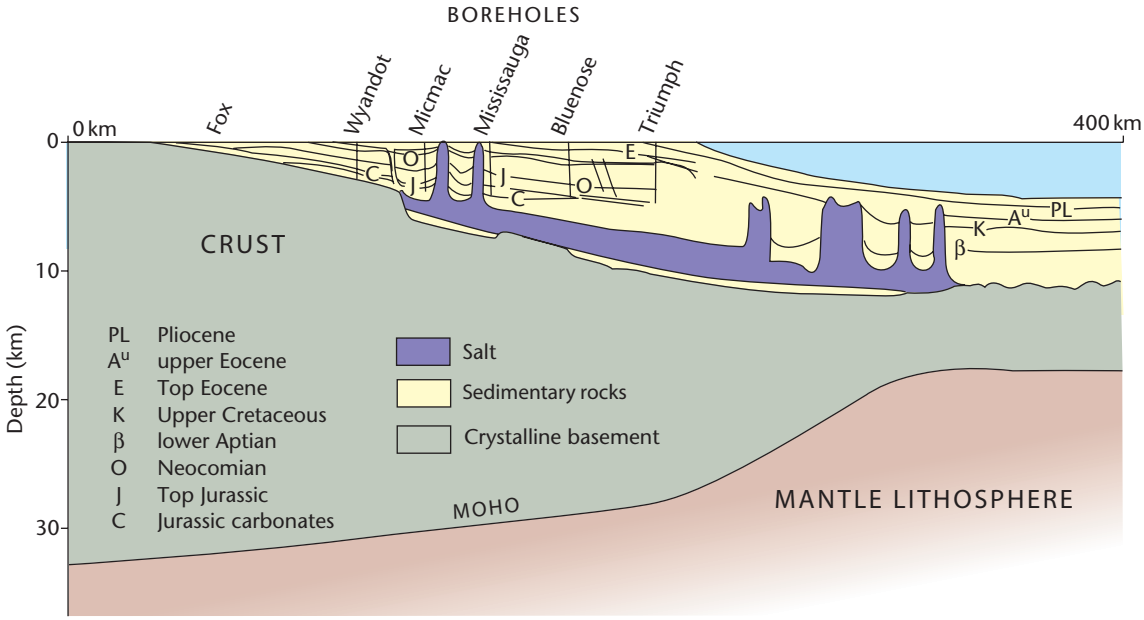

Fig. 3.26 Composite cross-section of the Scotian margin and basin. The sediment–basement interface is based on wells that penetrate it, in addition to seismic reflection and refraction observations (Jansa & Wade 1975). After Beaumont *et al*. (1982), reproduced with permission of John Wiley & Sons, Ltd.

Bajocian at about 170 Ma. The stretching in the Red Sea (Cochran 1983) appears to have occurred diffusely through a combination of extensional block faulting and dyke injection over an area of the order of 100 km wide. This phase of diffuse extension has lasted for 20 to 25 Myr in the northern Red Sea and is still occurring. A phase of rifting took place in the North Sea in the Permo-Triassic. There was another phase in the Jurassic that lasted until the Early Cretaceous. The duration of this major phase of extension was of the order of 50 Myr.

Taking the North Sea as an example, the stretch factor for the Jurassic extensional phase rarely exceeds 1.5, except along the axis of the Viking Graben. Using $\tau = 50$ Myr and $\beta = 1.5$, the critical duration of rifting from Jarvis and McKenzie (1980) is about 27 Myr. Consequently, on this basis, we should expect the protracted duration of extension during the Jurassic phase in the North Sea to have had significant effects on the heat flow and subsidence history. Despite this, the North Sea appears to be satisfactorily explained by the uniform stretching model (Sclater & Christie 1980; Wood & Barton 1983).

Although the concept of instantaneous extension is useful for modelling of sedimentary basins that form by extension at high strain rates ($>10^{-15}\,s^{-1}$), at lower strain rates the thinning lithosphere and asthenosphere cool during its slow upward advection (Jarvis & McKenzie 1980; Armitage & Allen 2010; Allen & Armitage 2012) (Fig. 3.27). During slow stretching, the lithosphere is subject to heat conduction, upward advection due to the lateral extension, and internal heating due to radioactive decay. The geotherm is then solved through time as the lithosphere extends and cools. The composition of the upwelled asthenosphere is assumed to be identical to that of the lithospheric mantle it replaces, so that there is no additional downward-acting load due to a change in chemical composition and therefore density (cf. Kaminski & Jaupart 2000).

At very low rates of extension (strain rates of $10^{-16}\,s^{-1}$) the heat loss by conduction and the upward advection of warm lithosphere are similar in value. In this case the lithosphere is less thermally buoyant to counter faulting in the crust, resulting in syn-rift subsidence that is more prolonged and greater than in the reference model. Subsequent thermal subsidence is less than in the faster strain rate reference model. The overall subsidence profile therefore has a more constant slope, with a slight elbow when the stretching ceases (Fig. 3.27).

In problems where there are competing effects of diffusion (heat conduction) and advection, it is conventional to use a Péclet number:

$$Pe = \frac{vy_L}{\kappa} \qquad [3.2]$$

where v is the mean upward velocity, y_L is the thickness of the lithosphere and κ is the thermal diffusion coefficient. Since the strain rate $\dot{\varepsilon}$ (in 1D) is $\delta v/\delta y$, eqn. [3.2] becomes

$$Pe = \frac{\dot{\varepsilon} y_L^2}{2\kappa} \qquad [3.3]$$

We assume that for $Pe > 10$, upward advection dominates, whereas if $Pe < 1$ then diffusion dominates. For a strain rate of $10^{-15}\,s^{-1}$ upward advection dominates as $Pe = 20$. If the strain rate is $10^{-17}\,s^{-1}$, $Pe = 0.2$ and thermal diffusion dominates, such that as the lithosphere is extended, it cools as material is slowly advected upwards (Figs 3.28, 3.29). For strain rates of the order of $10^{-16}\,s^{-1}$, $Pe = 2$, which means that the thermal diffusion and upward advection of material are comparable, and the assumption of instantaneous extension is no longer an accurate representation.

Returning to the Viking Graben example, we can calculate the Péclet number in order to assess the effects of protracted rifting.

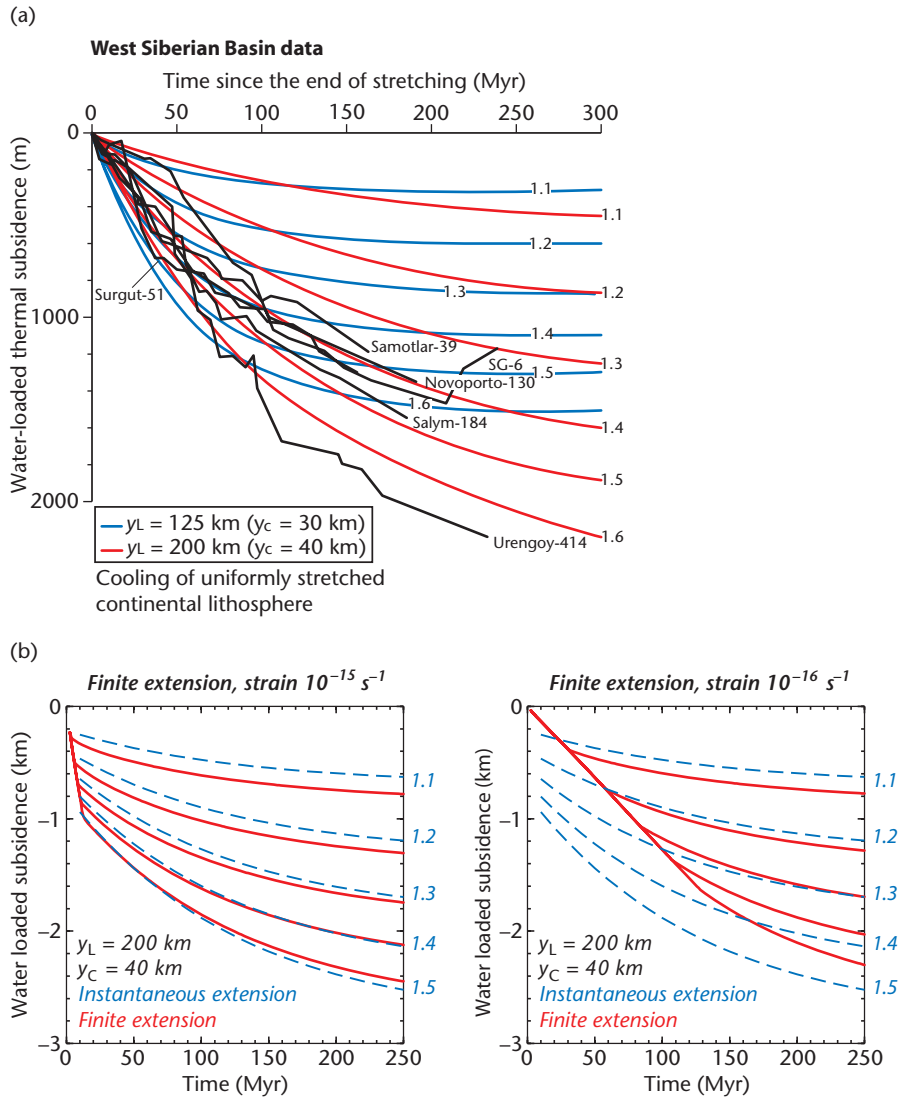

Fig. 3.27 (a) Water-loaded subsidence for a continental lithosphere with an initial thickness of 200 km, compared with the reference model for y_L = 125 km, with subsidence curves from the West Siberian Basin superimposed (red). Subsidence is calculated assuming that the lithosphere is isostatically compensated locally and that the initial configuration is at sea level. We assume that density remains constant within the crust at 2900 kg m^{-3}, and varies linearly due to thermal expansion within the lithosphere. The density at the base of the lithosphere is assumed to be 3400 kg m^{-3}, and the temperature is assumed to be 1330 °C. Simple instantaneous extension of a piece of 200 km-thick lithosphere produces subsidence due to thermal relaxation that continues for more than 250 Myr. (b) Effect on subsidence of finite times of rifting (Armitage & Allen 2012). Water-loaded subsidence for instantaneous extension is compared with subsidence for finite extension at strain rates of 10^{-15} and 10^{-16} s^{-1}. The base of the lithosphere is initially at 200 km, at a temperature of 1330 °C, and the crust is initially at 40 km thick. Slow upward advection of rock causes heat loss by conduction during the protracted rift phase.

If $\beta = 1.5$, the width of the stretched crust is 150 km (initial width 100 km), the lithospheric time constant $\tau = 50.2$ Myr ($y_L = 125$ km), $\kappa = 10^{-6}$ m^2 s^{-1}, and the duration of stretching is 50 Myr, the strain rate becomes 3.17×10^{-16} s^{-1}, and the Péclet number is 2.5. This indicates that the effects of protracted rifting should be significant.

3.4.2 Non-uniform (depth-dependent) stretching

Two families of models have been proposed to deal with the possibility of non-uniform stretching:

- *discontinuous* models, in which there is a discontinuity or decoupling between two layers with different values of the stretch factor β;
- *continuous* models, where there is a smooth transition in the stretching through the lithosphere.

The extent of coupling or decoupling of rheologically contrasting layers, such as the mid-upper crust and lower crust, is a fundamental factor in controlling the evolution of stretched continental lithosphere (Huismans & Beaumont 2002, 2008).

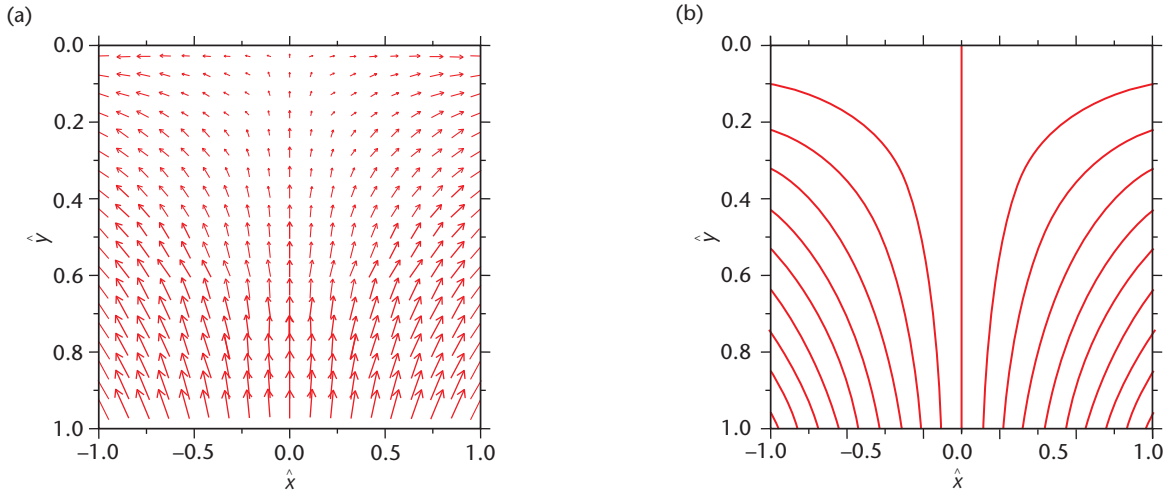

Fig. 3.28 Advection of rock in a piece of stretched continental lithosphere during finite periods of extension, showing (a) the vectors of the velocity field in dimensionless depth versus dimensionless width, and (b) the flowlines. Vertical velocity is set to zero at the surface where $y = 0$. From Wangen (2010). © Magnus Wangen 2010, reproduced with the permission of Cambridge University Press.

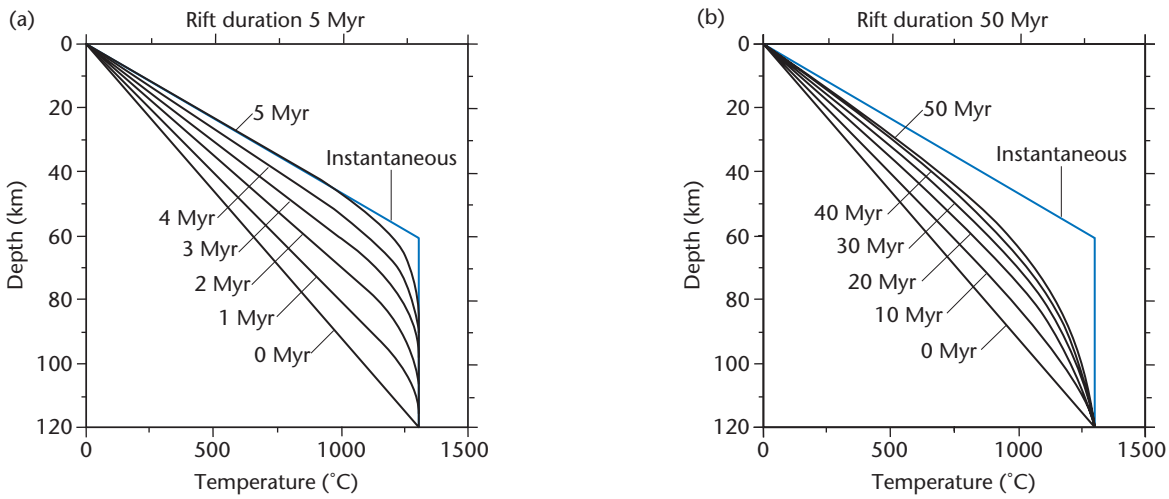

Fig. 3.29 Effect of finite rifting on the geotherm, from Wangen (2010), for rift durations of 5 Myr (a) and 50 Myr (b). Note the gradual (rather than instantaneous) increase in temperature due to the transient thermal effects, especially at long rifting times.

Critically, both sets of models make a first-order prediction – that zones of continental stretching should be characterised by elevated rift margin topography.

3.4.2.1 Discontinuous stretching with depth

Extension may not be uniform with depth because of the changing rheological properties of the lithosphere. If the lithosphere extends inhomogeneously and discontinuously, there must be a depth d at which the upper and lower parts of the lithosphere are decoupled. This zone of detachment or shear is where listric faults in the overlying brittle zone sole out (Montadert *et al.* 1979; Kusznir *et al.* 1987). Structural evidence (e.g. seismic studies of the Basin and Range province, Bay of Biscay and northwestern European continental shelf) demonstrates that some steep faults near the surface become listric into near-horizontal detachments where a transition to ductile behaviour takes place. The focal depths of earthquakes in old cratons further suggest that while the upper part of the lithosphere has relatively high strength and is seismically active, the lower part is aseismic, probably due to the operation of ductile deformation mechanisms (Sibson 1983; Scholz 1988). In some instances at least, there may therefore be decoupling of the upper and lower zones

at about mid-crustal levels, allowing the two rheological layers to extend by different amounts, giving a non-uniform discontinuous stretching.

The initial subsidence and thermal subsidence for the case of depth-dependent extension, where the zone above d extends by β_c and the zone below d extends by ductile deformation by a different amount β_{sc}, is given by Royden and Keen (1980). If the lower zone stretches by ductile deformation more than the brittle upper zone, uplift should occur if the depth to decoupling approximates the crustal thickness ($d \sim y_c$). This uplift occurs at the same time as extension, and is an attractive feature of the model in view of the updoming characteristic of many present-day rift systems such as in East Africa.

As an example of discontinuous depth-dependent stretching, in the centre of the Pattani Trough, Gulf of Thailand, the stretch factors for crust β_c and lithosphere β_L derived from subsidence plots were 2.35 and 1.90, indicating that crustal thinning was 20% greater than lithospheric thinning in the graben region (Hellinger & Sclater 1983). However, there are few examples where depth-dependent stretching can be demonstrated convincingly (Shillington *et al.* 2008).

The temporal relationship between faulting and rift flank uplift and the wavelength and amplitude of the rift flank uplift provide important constraints on the lithospheric stretching model. For example, if pre-rift sedimentary rocks are preserved in the graben but eroded from the flanks, it is a good indication that crustal uplift did not precede rifting. Footwall uplift may be due to co-seismic strain along border faults, in which case the wavelength of the uplift (c.10 km) will be smaller than the fault spacing. However, if the rift flank uplift has a much larger wavelength, it might imply that the subcrustal lithosphere was extended over a larger region than the more confined crustal extension. At first the crustal thinning, causing subsidence, outstrips the uplift from subcrustal thinning in the graben area, but the reverse is true beyond the graben edge. Later, after extensional tectonics has ceased, both flanks and graben should subside due to cooling and thermal contraction of the upwelled asthenosphere.

Regions initially at sea level that are uplifted, such as graben flanks, are subject to erosion and theoretically should subside to a position below sea level after complete cooling. But a second effect is the added crustal uplift caused by isostatic adjustment to the removed load. These two processes govern how much erosion will take place before the rift flanks subside below sea level and erosion effectively stops. In the southern Rhine Graben, the present-day surface uplift of the rift flanks is about 1 km. The erosional exhumation of footwall rocks is, however, of the order of 2.5 km (Illies & Greiner 1978). A further implication of rift flank erosion is an increase in the area of subsidence, so non-uniform extension models incorporating erosional effects predict larger subsiding basins than uniform extensional models. Regions that are not initially at sea level prior to rifting, such as the Tibet Plateau and the Basin and Range province, have a different, lower base level for erosion.

A comparison of the stratigraphies generated by the uniform (one-layer) stretching model and the two-layer (depth-dependent) stretching model from the passive margin off New Jersey, USA, is shown in Fig. 3.30. Both models show a well-developed coastal plain, hinge zone and inner shelf region underlain by a thick sequence of seaward-dipping strata. The main difference is in the stratigraphy of the coastal plain, the one-layer model over-predicting syn-rift sediment thickness. The two-layer model, however, explains the lack of syn-rift (Jurassic) stratigraphy by the lateral loss of heat to the flanks of the rift, causing uplift and subaerial emergence.

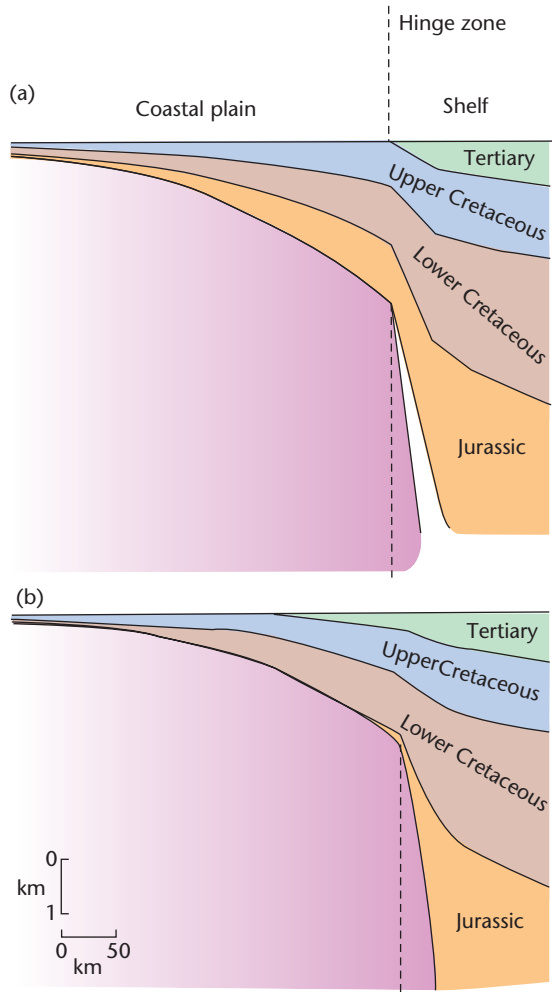

Fig. 3.30 Synthetic stratigraphy along profiles crossing the coastal plain and shelf off New Jersey, constructed using the flexural loading model of Watts & Thorne (1984). (a) One-layer uniform stretching model. (b) Two-layer model in which the lithosphere and crust are thinned by equal amounts seaward of the hinge zone, but only the mantle lithosphere is thinned landward of the hinge zone. The lithospheric thinning promotes early uplift of the zone landward of the hinge line, and helps to explain the absence of Jurassic strata from this region (after Steckler *et al.* 1988).

3.4.2.2 Continuous stretching with depth

The implication of different amounts of stretching in the crust and mantle lithosphere is that there must be a surface or zone of discontinuity separating the regions with different values of β. Although such models are successful in explaining the common rift flank uplift that accompanies extension (e.g. Nova Scotian and Labrador continental margin, East African Rift, Red Sea, Rhine Graben), they have a number of requirements:

- the existence of an intra-lithospheric discontinuity, which although evident in some settings (e.g. Biscay margin), is by no means universally 'proven';

- a mechanism by which the mantle is detached and stretched by a different amount to the overlying crust, and a means of solving the attendant space problem in the mantle.

If the stretching is non-uniform but *continuous* with depth, these objections are removed (Rowley & Sahagian 1986). It is possible that the mantle may respond to extension as a function of depth, the strain rate decreasing as the extension is diffused over a wider region. This can be modelled by considering a geometry of an upward-tapering region of stretching (Fig. 3.31). If ϕ is the angle between the vertical and the boundary of the stretched region in the mantle lithosphere, the amount of stretching depends on the depth beneath the crust and angle ϕ. The variation of β_{sc} with depth can then be integrated from the base of the crust to the base of the lithosphere to obtain estimates of initial and total subsidence in a similar fashion to the uniform stretching case. For large values of ϕ, the initial subsidence is increased but the amount of post-extension thermal subsidence is decreased. The wider zone of mantle stretching results in uplift of the rift shoulders, and the horizontal length scale of the uplift is an indication of the value of ϕ. In the Gulf of Suez region, the horizontal width over which the topographic uplift occurs is ~250 km. Since the thickness of the subcrustal lithosphere is likely to be approximately 90 km, the taper angle ϕ is given by $\phi = \tan^{-1}(250/90) = 70°$. In the Rhine Graben, ϕ is approximately $\tan^{-1}(80/90)$ ~40°.

A point in the rift shoulder region should therefore initially experience uplift, followed by a comparable amount of subsidence; if erosion has occurred, the final elevation of the point will be below its initial height. The same general pattern is observed where the crustal stretching varies from a minimum at the rift margin to a maximum at the rift centre (Fig. 3.31) (White & McKenzie 1988). The implications of stretching the mantle over a wider region than the crust (but with equal total amounts of extension) is that stratigraphic onlap should occur over previous rift shoulders during the post-rift phase, a feature commonly found in 'rift-sag' or 'steer's head' type basins.

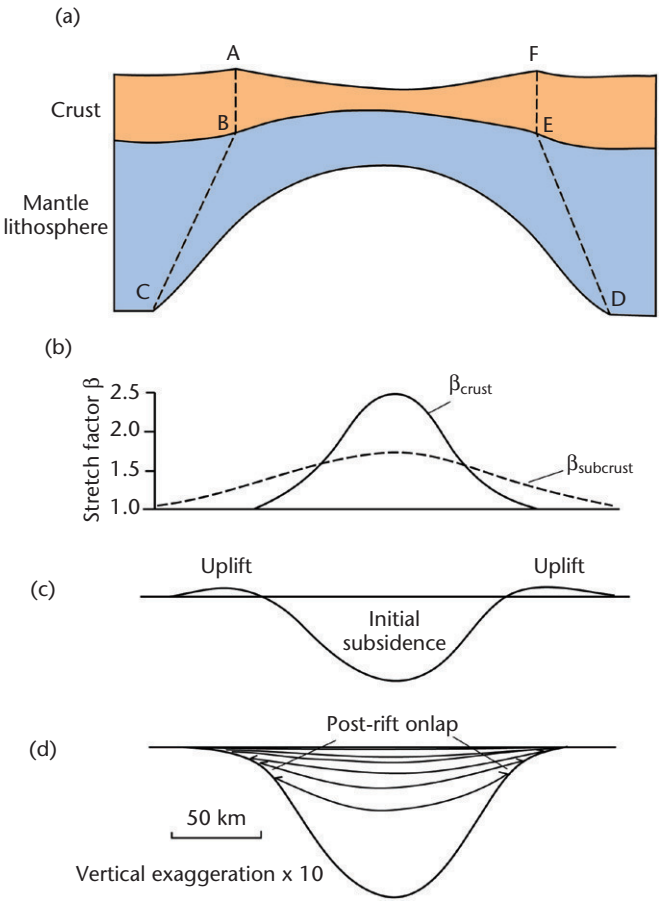

Fig. 3.31 Basin filling pattern resulting from continuous depth-dependent stretching (Rowley & Sahagian 1986; White & McKenzie 1988). (a) Geometry of a tapering region of extension in the subcrustal lithosphere. (b) Stretch factors in the crust and subcrustal lithosphere as a function of horizontal distance. (c) Initial subsidence and uplift immediately after stretching, showing prominent rift flank uplift. (d) Total subsidence 150 Myr after rifting, showing progressive onlap of the basin margin during the thermal subsidence phase, giving a steer's head geometry.

3.4.3 Pure versus simple shear

The lithosphere may extend asymmetrically where the zone of ductile subcrustal stretching is relayed laterally from the zone of brittle crustal stretching (Buck *et al.* 1988; Kusznir & Egan 1990) (Figs 3.32, 3.33). This is the situation of *simple shear*. Wernicke (1981) proposed such a model, based on studies of Basin and Range tectonics, envisaging that lithospheric extension is accomplished by displacement on a large-scale, gently dipping shear zone that traverses the entire lithosphere. Such a shear zone transfers or 'relays' extension from the upper crust in one region to the lower crust and mantle lithosphere in another region. It necessarily results in a physical separation of the zone of fault-controlled extension from the zone of upwelled asthenosphere.

Wernicke (1981, 1985) suggested that there are three main zones associated with crustal shear zones (Fig. 3.33): (i) a zone where upper crust has thinned and there are abundant faults above the detachment zone; (ii) a 'discrepant' zone where the lower crust has thinned but there is negligible thinning in the upper crust; and (iii) a zone where the shear zone extends through the subcrustal (mantle) lithosphere.

Since crustal thinning by fault-controlled extension causes subsidence, but subcrustal thinning produces uplift, we should expect subsidence in the region of thin-skinned extensional tectonics but tectonic *uplift* in the region overlying the lower crust and mantle thinning (the discrepant zone). Subsequent asthenospheric cooling may result in one of two things. Thermal subsidence of the region above the discrepant zone may simply restore the crust to its initial level. However, if subaerial erosion has taken place in the meantime, thermal subsidence will lead to the formation of a shallow basin above the discrepant zone. The basement of the basin should be unfaulted. However, beneath the zone of thin-skinned extensional tectonics there should be minimal thermal subsidence.

Stretching of the lithosphere combined with unloading along major detachment faults can result in the unroofing of mantle rocks in their footwalls. These are called *core complexes* and *gneissic domes* (Fig. 3.34). The so-called 'turtlebacks' of the Death Valley region and the Whipple Mountains of Nevada are examples (Lister and Davis 1989).

Tectonic unloading may also result in flexural uplift of adjacent footwall areas along major detachment faults (Fig. 3.35). Kusznir

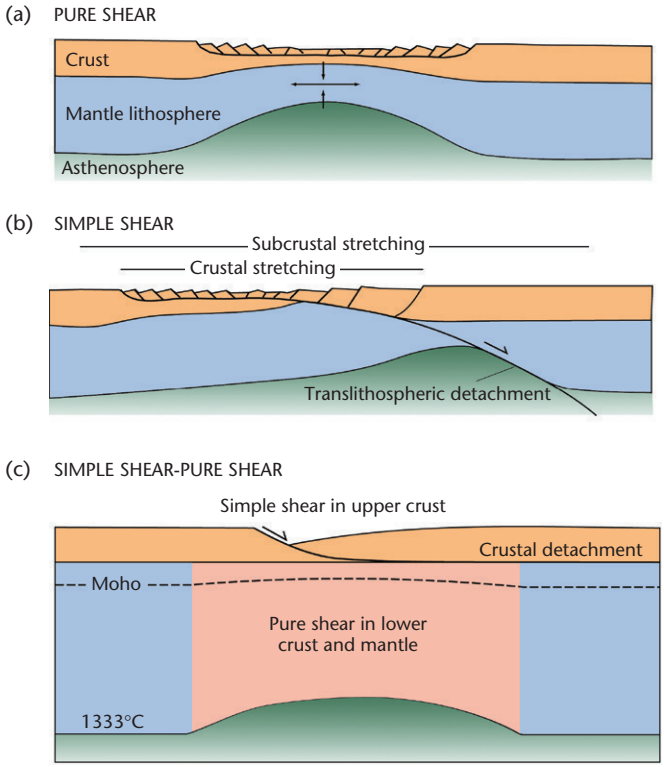

Fig. 3.32 Models of strain geometry in rifts (Coward 1986; Buck *et al*. 1988). (a) Pure shear geometry with an upper brittle layer overlying a lower ductile layer, producing a symmetrical lithospheric cross section with the initial fault-controlled subsidence spatially superimposed on the thermal subsidence. The ductile stretching may be accompanied by dilation due to the intrusion of melts (Royden *et al*. 1980). (b) Simple shear geometry with a through-going low-angle detachment dividing the lithosphere into an upper plate or hangingwall, and a lower plate or footwall. Thinning of the lower lithosphere is relayed along the detachment plane, producing a highly asymmetrical lithospheric cross-section (after Wernicke 1981, 1985). Initial fault-controlled (syn-rift) subsidence is spatially separated from the thermal subsidence. (c) Hybrid model of simple shear in the upper crust on listric (shown) or planar faults, and pure shear in the ductile lower crust and mantle lithosphere (Kusznir *et al*. 1991).

et al. (1991) refer to this as the *flexural cantilever effect*. They use a model of simple shear in the crust and pure shear in the lithospheric mantle. The scale of the flexural cantilever effect depends on the depth at which the detachment soles out. The model has been successfully used to explain footwall uplift and erosion in the Jeanne d'Arc Basin, Grand Banks of Newfoundland, and Viking Graben, North Sea (Marsden *et al*. 1990; Kusznir *et al*. 1991), and the Tanganyika Rift of East Africa (Kusznir & Morley 1990).

Models involving large-scale simple shear do not explain basins that have a thermal subsidence spatially superimposed on a fault-controlled subsidence, as in the North Sea (Klemperer 1988). Such examples are more suggestive of pure shear. However, it is possible that the upper crust may deform by simple shear and the lower crust and subcrustal mantle lithosphere by pure shear, with a mid-crustal detachment (Coward 1986) (Fig. 3.32). Symmetrical (pure shear) and asymmetrical (simple shear) geometries were both outcomes of the numerical experiments of Huismans and Beaumont (2002, 2008), dependent on the rheological structure of lithospheric layers and the strain rate of stretching (see §3.5).

3.4.4 Elevated asthenospheric temperatures

The reference uniform stretching model envisages an asthenosphere with a laterally uniform temperature (1330 °C), which rises passively to fill the region of lithospheric stretching. Some workers have suggested that continental stretching is in some cases associated with mantle plume activity (Spohn & Schubert 1983; Houseman & England 1986). Such activity may raise the local asthenospheric temperatures by as much as 200 °C (Fig. 3.36). Plume heads typically have diameters in the region of 1000 km (Griffiths & Campbell 1990) (Chapter 5). Laboratory experiments indicate that starting plumes may generate as much as 600 m of surface uplift (Hill 1991) – insufficient to solely explain the 3 km-high swells of eastern Africa. However, mantle plume activity may drive continental extension by elevating the lithosphere, including its surface, thereby giving it excess potential energy compared to its surroundings (Houseman & England 1986).

The driving stress caused by the uplift may exceed a threshold value, causing *run-away or accelerating extension*, eventually leading to ocean crust production. Alternatively, the driving stress may be considerably lower than (about half of) the threshold value, causing *negligible extension*, as in many low-strain continental rifts. If the driving stress is intermediate in value, the extension is thought to be *self-limited* by the cooling of the ductile portion of the lithosphere. This produces aborted rift provinces such as the North Sea. These ideas are further developed in §3.5.

One of the complexities of this type of model is the *time scale of the plume*. Removal of the plume head at early, intermediate or late stages has major effects on basin development. Another aspect is the *volcanicity* generated by the anomalously high asthenospheric temperatures (§3.4.5). Mantle plumes are therefore commonly associated with very high volume basaltic igneous provinces such as the Karoo, Deccan and Parana examples.

Plume activity has been invoked as a particularly effective mechanism of generating new ocean basins, such as the Atlantic. The opening of the northern Atlantic in the Paleocene has been related to the impingement of the Icelandic plume on the base of the lithosphere (White & McKenzie 1989). Mantle plume effects may have been common during supercontinental break-up of Rodinia (c.850 Ma), Gondwana (c.550 Ma) and Pangea (c.250 Ma).

3.4.5 Magmatic activity

Although melting is not predicted at low to moderate values of stretching in the reference uniform stretching model, it is well known that rift provinces are associated with minor (e.g. Western Rift, Africa; North Sea) to major (Eastern Rift, Africa; Rio Grande) volcanism. Most importantly, continental break-up at high values of stretching is commonly associated with vast outpourings of flood basalts, indicating major melting of the asthenosphere by adiabatic decompression. Melts liberated by decompression are assumed to separate from their residue and to travel upwards to either be erupted at the surface, or to be emplaced as igneous bodies in the crust. Underplating of the crust by igneous bodies can cause uplift of the surface (Brodie & White 1994) (Appendix 27). McKenzie and Bickle (1988) showed how the amount of melt generated

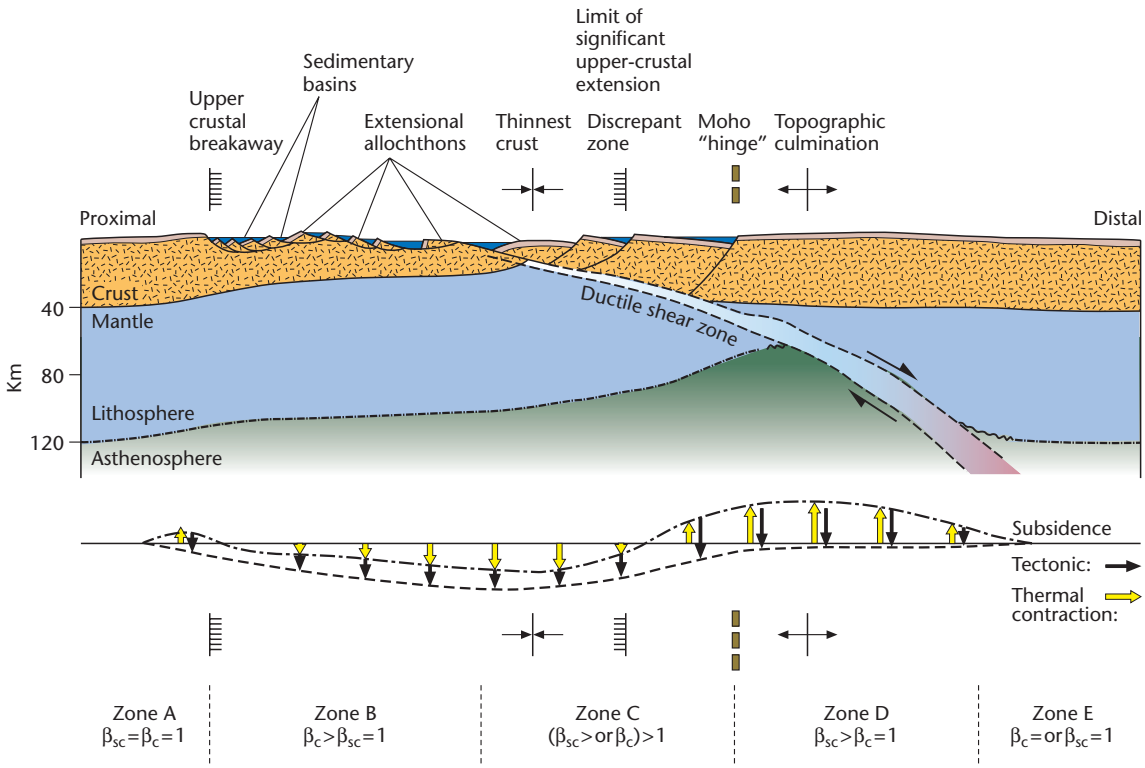

Fig. 3.33 Simple shear model of the entire lithosphere, developed from the Basin and Range province of SW USA (Wernicke 1985). This geometry takes of the order of 10–15 Myr to develop. Mid-crustal rocks in the hangingwall may initially pass through greenschist or amphibolite metamorphic conditions in the ductile shear zone, followed by uplift, cooling and deformation in the brittle field. β_c and β_{sc} refer to the stretch factors of the crust and subcrustal lithosphere respectively.

depends on the potential temperature of the asthenosphere (defined as the temperature the asthenosphere would have if brought to the surface adiabatically without melting) and the amount of stretching (Chapter 5).

Melting is greatly facilitated by the presence of volatiles and by elevated asthenospheric temperatures, as would be expected over a plume head (Chapter 5). The high plume temperatures provide long-wavelength (c.10^3 km) dynamic support for the Earth's surface. Pulsing in this dynamic support (§5.2.5) may cause periodic uplift, the formation of erosional landscapes, and the transport of sediment to the ocean, followed by subsidence, as has been interpreted for the Iceland plume at 55 Ma (White & Lovell 1997; Hartley *et al.* 2011). Pulses of hot material are thought to have travelled outward from the main conduit of the Iceland plume in a channel below the lithosphere (Rudge *et al.* 2008), producing an annulus of uplift and subsidence like a ripple travelling outwards from a stone thrown into a pond.

In summary, melting, igneous underplating and dynamic support from a hot asthenosphere affect the subsidence experienced at the Earth's surface during the period of lithospheric stretching (Fig. 3.36). Dynamic effects from the mantle are discussed further in Chapter 5.

3.4.6 Induced mantle convection

Models involving an active asthenospheric heat source should predict *uplift before rifting*. At present there is no broad consensus on the temporal relationships between uplift and extension associated with lithospheric stretching. However, Steckler (1985) suggested that in the Gulf of Suez, the rift flank uplifts were *not* formed as a precursor doming event prior to rifting, but rather formed *during* the main phase of extension. The rift appears to have initiated (by Miocene times) at near sea level, since the tilted fault blocks associated with early rifting experienced both subaerial erosion and marine deposition. The early Miocene topography of the Gulf of Suez region was subdued, and stratigraphic thicknesses are uniform over the area (Garfunkel & Bartov 1977). However, at the end of the early Miocene, 8–10 Myr after the onset of rifting, a dramatic change took place – there is a widespread unconformity, and conglomerates appear at the rift margins suggesting major uplift and unroofing at this time.

In the Gulf of Suez, the lithosphere must have extended by 2.5 times as much as the crust to explain the uplift and rift subsidence. This brings the uniform extension model seriously into doubt in terms of its ability to predict the lithospheric heating. How then does one explain the additional amount of heating that the lithosphere under the Gulf of Suez has undergone? This extra heat may have resulted from convective flow induced by the large temperature gradients set up by rifting. Numerical experiments confirm that secondary small-scale convection should take place beneath rifts (Buck 1984, 1986). Convective transport should heat the lithosphere bordering the rift, causing uplift of rift shoulders concurrent with extension within the rift itself (Fig. 3.37). If this mechanism is correct, it removes the need for additional active, sub-lithospheric heat sources.

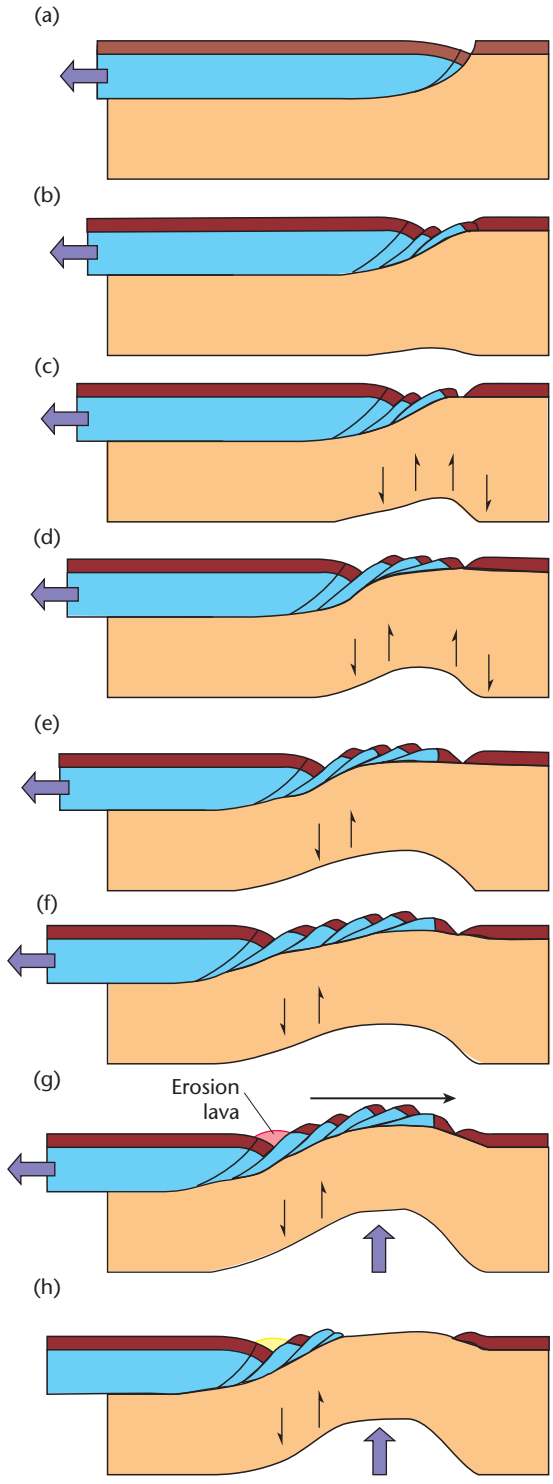

Fig. 3.34 Sequential evolution of a piece of continental lithosphere undergoing simple shear and isostatic compensation, showing the development of flat detachment faults, tilted listric fault blocks and metamorphic core complexes. Based on Wernicke & Axen (1988), from Fossen (2011, p. 339). Reproduced with the permission of Cambridge University Press.

It also removes the requirement for two-layer extension to explain high heat flows at rift margins.

Secondary small-scale convection may also affect plates adjacent to ocean–continent margins. Convective flow in the mantle may be triggered by the step in plate thickness at the ocean–continent transition (§5.2.4) as the plate migrates relative to the underlying mantle. The dynamic topography caused by these edge effects may extend c.10^3 km into the continental plate, and may also be responsible for widespread melting of the asthenosphere, producing trailing-edge magmatic provinces, such as Victoria, Australia. Further discussion of dynamic topography is found in Chapter 5.

3.4.7 Radiogenic heat production

Although the very large volume of mantle contributes 80% of the Earth's radiogenic heat, it is the crustal contribution that determines the continental geotherm and which is of importance in basin analysis. The crustal radiogenic heat production can be modelled either as a series of slabs of different internal heat production, or as an exponential that decays with depth (§2.2.3). As a rule of thumb, the radiogenic heat production may be of roughly equal importance to the basal heat flow in determining the continental geotherm.

In practice, radiogenic heat production makes little difference to the shape of the subsidence curves predicted by the reference uniform stretching model, though it potentially strongly affects paleotemperature estimations. It is therefore very important to include radiogenic contributions to the heat flow in modelling of thermal indicators in sedimentary basins, such as vitrinite reflectance (Chapter 10).

3.4.8 Flexural compensation

It is likely that at low to moderate values of stretching, the lithosphere maintains a finite strength during basin development (Ebinger *et al.* 1989), so that it responds to vertical loads by flexure (Chapter 4). The degree of compensation (between the end members of Airy isostasy for a plate with no flexural rigidity and zero compensation for an infinitely rigid plate) depends on the flexural rigidity of the plate and the wavelength of the load (§2.1.5). There are two situations where flexure is likely to be important: (i) tectonic unloading by extension along major detachments, leading to a regional cantilever-type upward flexure (Kusznir & Ziegler 1992), causing the footwall region to be mechanically uplifted; and (ii) downward flexure under the accumulating sediment loads in the syn-rift and especially post-rift phase. Flexural compensation of sediment loads should be particularly important in passive margin evolution because of the secular increase in flexural rigidity, and where sediment loads are relatively narrow, as in narrow rifts and some pull-apart basins.

3.4.9 The depth of necking

Necking is the very large-scale thinning of the lithosphere caused by its mechanical extension. Necking should take place around one of its strong layers (Braun & Beaumont 1987; Weissel & Karner 1989; Kooi *et al.* 1992). The *depth of necking* is defined as the depth in the lithosphere that remains horizontal during thinning if the effects of sediment and water loading are removed. For the reference uniform stretching model, the necking depth is implicitly 0 km. That is, all depths below the surface experience an upward advection during thinning (when sediment/water loading is removed). However, the

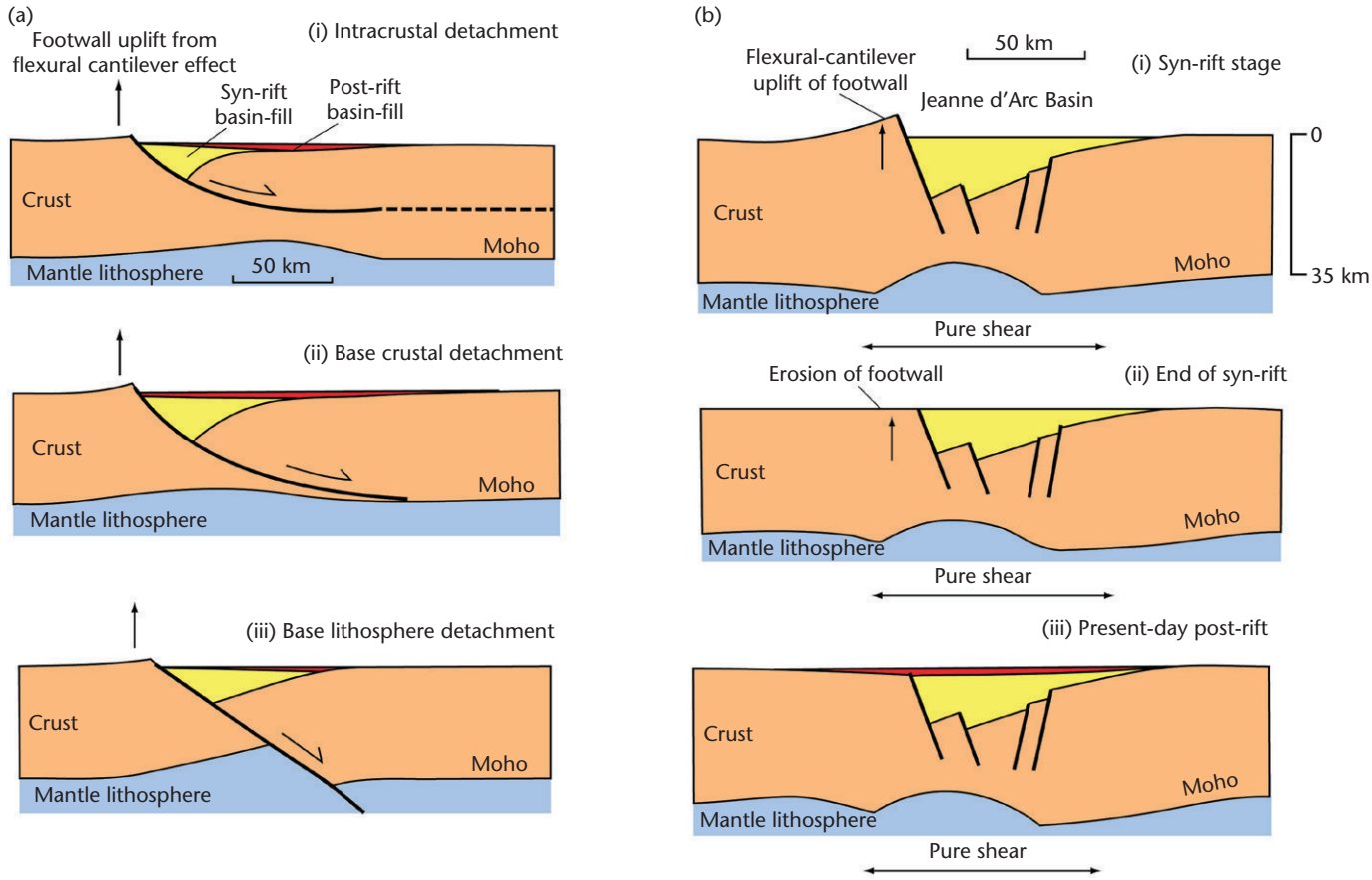

Fig. 3.35 Sedimentary basin geometry and crustal structure predicted by a simple-shear/pure-shear model including the flexural cantilever effect (Kusznir & Egan 1990; Kusznir *et al.* 1991). (a) Crustal structures after 100 Myr and 30 km extension, for an intra-crustal detachment (i), a base-crustal detachment (ii), and a base-lithosphere detachment (iii). Equivalent elastic thickness Te = 5 km. (b) Sequential development of the Hibernia-Ben Nevis profile of the Jeanne d'Arc Basin, showing flexural uplift and erosion of the unloaded footwall of the main detachment fault. The total amount of extension is 18 km, initial fault dip = 60°, initial crustal thickness is 35 km, and Te = 10 km.

necking depth may be deeper in the shallow mantle lithosphere. In this case, there is advection of material upwards from below the necking depth, but advection of material downward from above the necking depth.

If the necking depth is in the strong mantle lithosphere, there is a regional flexural uplift, causing a pronounced rift shoulder. We would expect a deep necking depth where the lithosphere is cold and strong, with a strong subcrustal mantle, such as in the Transantarctic Mountains and Red Sea region (Cloetingh *et al.* 1995). On the other hand, if the necking depth is within the upper-mid crust, there is a downward regional flexure, promoting subsidence of the rift margins. This should occur where the lithosphere is weak, or where the crust is thickened, as in the Pannonian Basin of eastern Europe. The level of necking therefore controls the amount of rift shoulder denudation, and, consequently, the sediment delivery to the basin during the syn-rift phase (van Balen *et al.* 1995; ter Voorde & Cloetingh 1996). There is theoretically an equilibrium depth of necking where there is no net flexural response. For a sediment-filled basin and initial crustal thickness of 33 km within a 100 km-thick lithosphere, this equilibrium depth is about 10 km. Odinsen *et al.* (2000) used a necking depth of 18 km for their analysis of the northern North Sea, which therefore can be viewed as a relatively deep necking depth, promoting regional flexural uplift.

3.4.10 Phase changes

Although in general the lithosphere does not melt during slow extension without the activity of an underlying plume, mineral composition may still change due to decompression (Podladchikov *et al.* 1994; Kaus *et al.* 2005). Decompression may cause mantle rocks to cross the transition from a garnet- to a plagioclase-lherzolite, which takes place at a maximum depth of approximately 50 km. It would cause a reduction in density by c.100 kg m^{-3} and therefore surface uplift. For this to occur, extension must be rapid, extending the crust to breakup (β~4) within 10 Myr.

The gabbro–eclogite phase change may cause subsidence due to the associated increase in density of around 500 kg m^{-3} (Joyner 1967; Haxby *et al.* 1976), and has been used to explain the formation of the

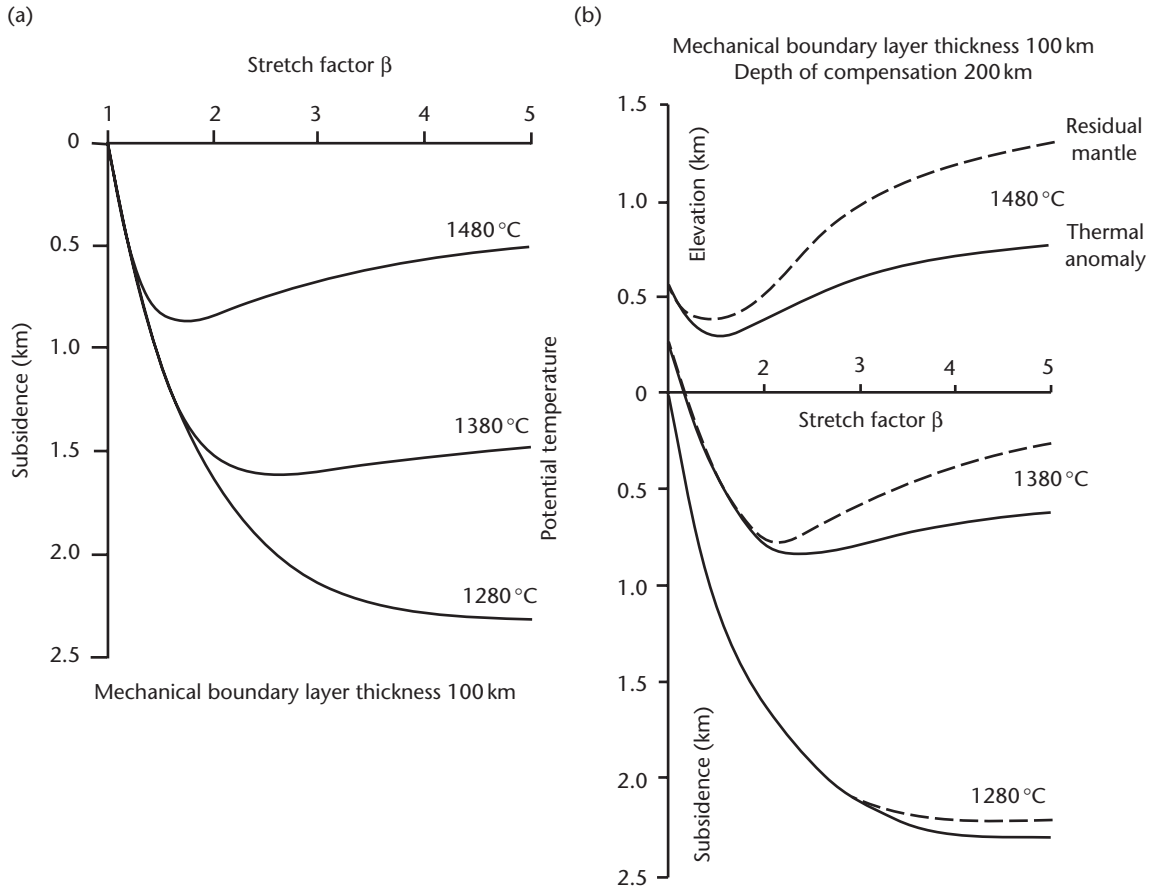

Fig. 3.36 Uplift and subsidence associated with plume activity at a spreading margin (after White & McKenzie 1989). (a) Subsidence at the time of rifting as a function of the stretch factor for potential temperatures of 1280 °C (normal), 1380 °C and 1480 °C. Each curve incorporates the effects of lithospheric thinning and crustal additions of melts caused by decompression of the mantle. (b) The effects of the reduced density of the abnormally hot asthenosphere (thermal anomaly) and the reduced density of the depleted mantle from which melt has been extracted (residual mantle) for three potential temperatures, as in (a). Plume activity causes the lithosphere to be elevated well above the level expected for an asthenosphere of normal temperature. The depth of compensation of 200 km is typical of the depth over which anomalously hot mantle is likely to extend. Reproduced with permission of the American Geophysical Union.

Williston and Michigan basins in North America (Haxby *et al.* 1976; Ahern & Dikeou 1989; Baird *et al.* 1995). Although a large proportion of the lower crust may be composed of gabbro, to generate this phase change, a large upwelling of warmer material to the base of the crust (Baird *et al.* 1995) and the presence of water (Ahrens & Schubert 1975) are required. This combination is probably rare where extension of the continental lithosphere takes place away from ocean subduction zones.

3.5 A dynamical approach to lithospheric extension

3.5.1 Generalities

Dynamic approaches to the modelling of continental extension use the constitutive laws of lithospheric materials to describe the three-dimensional deformation of the continental lithosphere under extension (§2.3). A number of *plane strain* models making a range of assumptions of lithospheric rheology (Keen 1985, 1987; Buck 1986; Braun & Beaumont 1987; Dunbar & Sawyer 1989; Lynch & Morgan 1990) show, in general, that the style of deformation is controlled by strain rate, initial geotherm and rheological structure. Consequently, any initial heterogeneities causing variability in the mechanical and thermal properties of the lithosphere are likely to be highly influential in determining the resulting deformation. These initial perturbations that cause lateral strength variations might be thickness variations, pre-existing deep faults, thermal anomalies or rheological inhomogeneities (Fernandez & Ranalli 1997).

Plane stress models approximate the lithosphere to a thin viscous sheet, in which the rheological properties of the sheet are vertically averaged (examples are England & McKenzie 1982, 1983; Houseman & England 1986; Sonder & England 1989; Newman & White 1999). A single power-law rheology is used in these models to describe lithospheric deformation.

Dynamic models require *boundary conditions* on the margins of the extending lithosphere (Appendix 18). The choice of boundary conditions has important implications for the evolution through

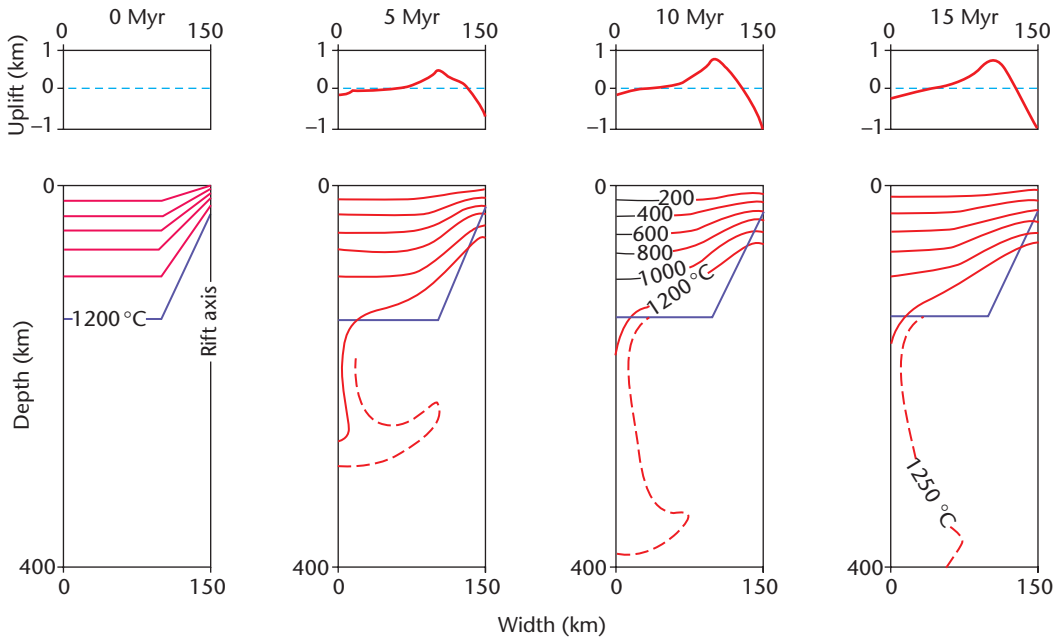

Fig. 3.37 Development of small-scale convection beneath rifts from the numerical experiments of Buck (1984). The rift is assumed to be symmetrical, with an initial half-width of 50 km. The average stretch factor is 1.6 and the internal temperature of the asthenosphere is 1300 °C. Comparison of the 1200 °C isotherm for the four time steps (0 Myr, 5 Myr, 10 Myr and 15 Myr) shows how the rift flank is progressively heated through time, causing rift shoulder uplift. Top boxes show the topography caused by combined convection and conduction. The rift flank uplift builds substantially between 5 and 10 Myr, with a maximum elevation of approximately 800 m and a width of 500–600 m. Reprinted from Buck (1984), with permission from Elsevier.

time of parameters in the model. For example, the investigator may choose a constant velocity, a constant strain rate, a constant stress, a constant heat flux or a constant basal temperature boundary condition. The latter is used in the reference uniform stretching model. Use of this boundary condition causes the heat flow from the asthenosphere to increase as stretching proceeds, since by Fourier's law, the flux is proportional to the temperature gradient, which must increase during lithospheric thinning if the basal temperature is held constant.

When regions of stretched lithosphere are plotted in terms of their bulk strain (or stretch factor) or width, and their extensional strain rate (Fig. 3.5) it is clear that there is great variability, with strain rate varying over two orders of magnitude and width varying over one order of magnitude.

Brun (1999) proposed that there are two different modes of continental extension (Fig. 3.38):

1. *Narrow rifts* with normal thickness crust (e.g. Rhine Graben; Gulf of Suez; Baikal; East Africa) are due to relatively small amounts of extension ($\beta < 2$). Narrow rifts may evolve into passive margins (e.g. Eastern Seaboard, USA; Biscay-Armorican margin) alongside oceanic spreading centres. In crust with normal thickness (30–40 km) and geothermal gradient (30 °C km^{-1}), the process of lithospheric stretching is by a very large-scale, localised thinning of the lithosphere or *necking* (Kooi *et al.* 1992). At early stages of lithospheric necking, rifts are 30–40 km wide, with the Moho elevated immediately beneath the rift. Some early rifts, such as those of East Africa, are wider (60–70 km). At late stages of necking, passive margins develop, with widths of 100–400 km and with the Moho shallowing from 30–40 km under the undisturbed lithosphere to 8–10 km at the continent–ocean boundary.
2. *Wide extended domains* where extension follows earlier crustal thickening by c.20 Myr or more, providing time for the thickened brittle crust to spread gravitationally under its own weight over a weak layer in the lower crust (Jones *et al.* 1996). The width of the extending region can be as wide as the region of previously thickened crust – as much as 1000 km in the Basin and Range, USA. As a result of spreading, crustal thicknesses return to 'normal' (c.30 km), at which point extension stops. Local zones of exhumed ductile lower crust are termed *core complexes*. Core complexes are common in the Aegean (Greece) (Lister *et al.* 1984) and the Basin and Range province (Lister & Davis 1989), and have been interpreted in orogenic belts as diverse as the Alps of Austria–Switzerland (Frisch *et al.* 2000), the Variscan of west-central Europe (Burg *et al.* 1994a) and the Pan-African of western Saudi (Blasband *et al.* 2000). Flat-lying detachments associated with core complexes have been interpreted as initially low-angle faults that traversed the entire lithosphere. More recent studies suggest that they are initially steep and progressively rotated to a very shallow dip during extension, with a flat Moho undisturbed by any trans-lithospheric faults/shear zones.

An important set of questions immediately springs to mind: what controls the duration and total stretching of a piece of continental lithosphere? Do rifts stay narrow because the driving force for extension is removed? Or is it because the mantle lithosphere gains in strength and self-limits extension (England 1983)? The first

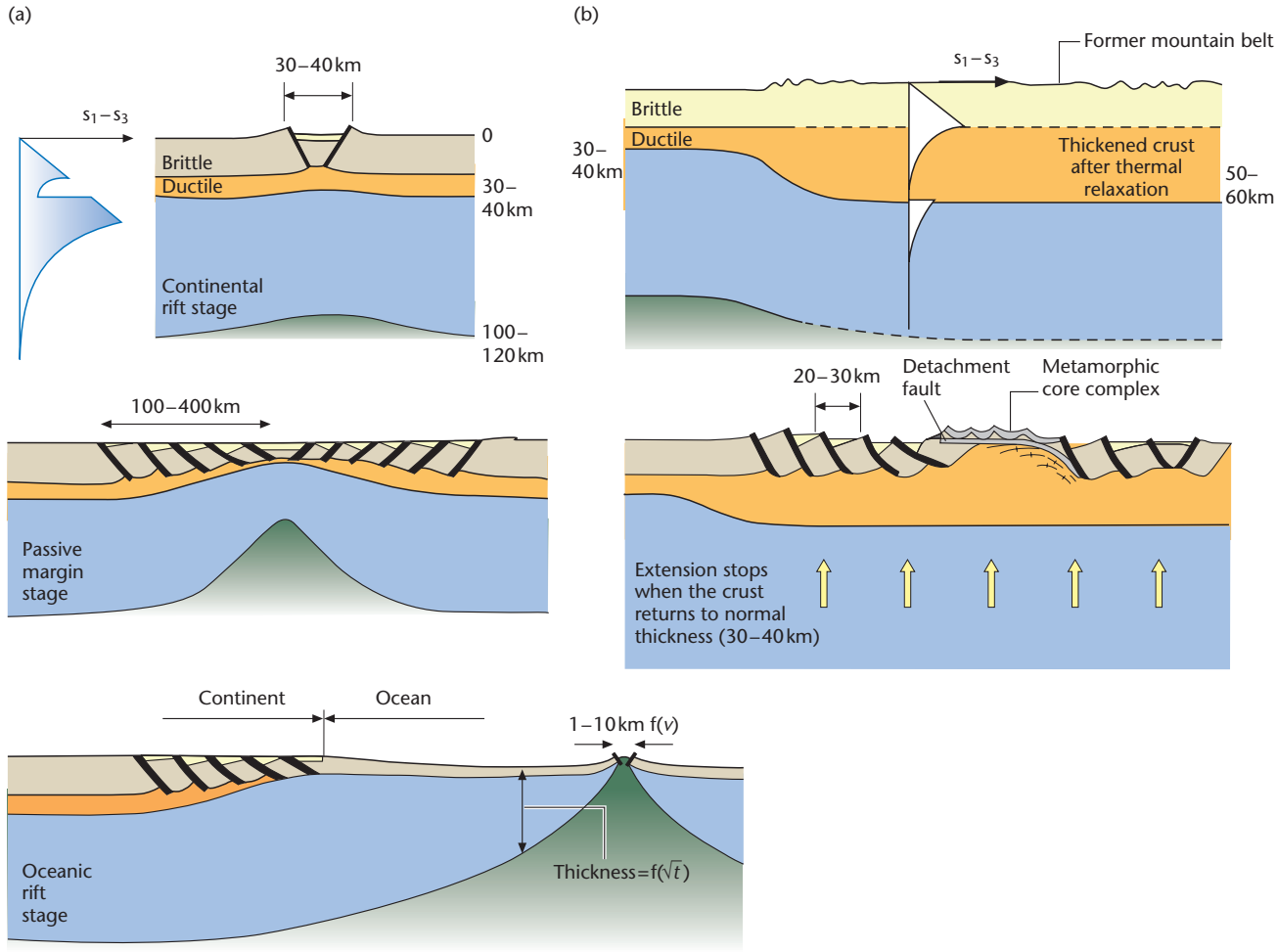

Fig. 3.38 Geological and structural differences between (a) narrow and (b) wide rifts, after Brun (1999). Wide rifts typically develop where the lithosphere has been previously thickened, with a Moho at >50 km. Extension leads to the unroofing of metamorphic core complexes. Reprinted by permission of the Royal Society.

possibility can be termed '*force-controlled extension*' and the second possibility '*viscosity-controlled extension*'.

Huismans and Beaumont (2002, 2008) also generated a complex and variable set of lithospheric geometries during extension by varying the rheological make-up of a layered lithosphere in numerical simulations. Two frictional plastic layers, representing upper and lower lithosphere, are separated by a weak ductile layer. Decoupling is possible between the upper and lower lithospheric layers across this ductile layer, with a wet quartz rheology above and a strong dry olivine rheology below. The brittle crust and upper mantle are allowed to strain-soften during deformation (that is, during deformation, the rock becomes weaker). Numerical outcomes were strongly dependent on the strength profiles, extension velocity and coupling between upper and lower lithospheric layers (Figs 3.39, 3.40):

- *AS* – asymmetric upper lithosphere rifting and symmetric lower lithospheric rifting were produced at a *low* rifting velocity where the upper and lower lithospheric layers were *decoupled*.
- *AA* – fully asymmetric rifting of both layers was produced at a *low* rifting velocity with *coupled* upper and lower lithospheric layers.
- *SS* – fully symmetric rifting of both upper and lower lithospheric layers took place at a *high* rifting velocity, for both *decoupled* and *coupled* cases.

Consequently, pure (symmetric) and simple shear (asymmetric) deformation, uniform and depth-dependent stretching, and variations in extension velocity and strain rate, are seen to be different outcomes dependent on the rheologies used, the extent of strain softening, and the coupling between different lithospheric layers.

3.5.2 Forces on the continental lithosphere

The forces responsible for stretching of the continental lithosphere in the reference uniform stretching model are not specified. Horizontal tensile stresses, however, must result from one or a combination of sources: (i) in-plane stresses transmitted from a plate boundary

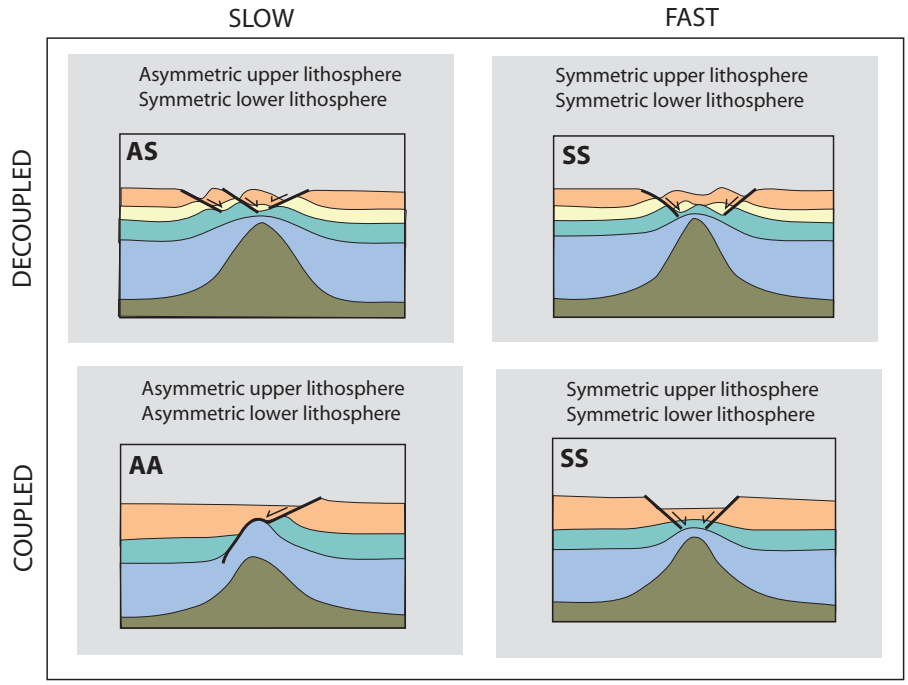

Fig. 3.39 Outline of results of numerical thermomechanical model of the extension of the continental lithosphere, redrafted and colour added, from original in Huismans & Beaumont (2002, 2008). The occurrence of symmetrical (pure shear) and asymmetrical (simple shear) of the upper and lower parts of the lithosphere is plotted in terms of the rate of extension and the coupling or decoupling of the lithospheric layers. The decoupled models include a weak, ductile lower crust with a wet quartz rheology. Note that this weak layer undergoes strong shearing. Fast extensional velocities promote pure shear.

or from basal traction; and (ii) stresses resulting from potential energy differences arising from buoyancy contrasts in the continental lithosphere. The most important cause of potential energy variations is elevation of the continental surface.

Imagine a slab of continental lithosphere acted upon by *distant extensional forces*. Changes in the distant extensional force should cause the region to experience variations in the strain rate at the same time, regardless of location. If the crust varies in thickness across our slab of lithosphere, *buoyancy forces* caused by these thickness variations should interfere with the distant extensional forces. Where the crust is thick, buoyancy forces assist the distant force to promote extension. But where the crust is thin, buoyancy forces oppose the distant extensional forces and resist extension. Could extension therefore be stopped by thinning the crust to a critical point?

It is also possible that buoyancy forces may operate in the absence of a strong distant extensional force. For example, if the crust is thick, or if the lithosphere is elevated above a mantle plume, the buoyancy forces alone may drive extension. A further source of extensional stresses is the application of shear stresses to the base of the lithosphere, for example from the convectional motion in the mantle, with extension occurring above the divergent flow of a convection cell. However, these stresses are likely to be relatively minor because the asthenosphere has a very low viscosity.

Lateral transmission of mechanical energy through the lithosphere as a result of plate collision has been proposed as a cause of continental rifting by Molnar and Tapponnier (1975). For example, the Baikal Rift of central Asia may be influenced by plate collision along the Himalayan front in the south, and a further convergent plate boundary exists in the Pacific on the east, both boundaries being roughly 3000 km distant from the rift itself. The Rhine Graben has the collision boundary of the Alps in close proximity in the south, and the opening Atlantic (1000 km distant) and subsiding North Sea (500 km distant) in the west and north. However, the frequency of collision boundaries compared to the large number of modern and ancient rifts is negligible. It therefore seems inconceivable that collision events have a *primary* role to play in providing the deviatoric in-plane forces necessary for the rifting of the continents. A numerical model of a plate of constant thickness loaded horizontally by an indenter (Neugebauer 1983), using limits of lithospheric stress under compression and extension (Brace & Kohlstedt 1980), indicates that the predicted stress regime falls considerably short of that required of a self-sustaining mechanism for rifting in the Baikal and Rhine rifts.

In addition to the forces applied at the edge of a continental plate by relative plate motion, there is an additional set of buoyancy forces set up by crustal thickness contrasts (England & McKenzie 1983; England 1983). The elevation of the continental lithosphere causes pressure differences to exist between it and neutrally elevated lithosphere. The relative importance of this driving force compared to that caused by applied forces at the plate boundaries can be gauged by an *Argand number* ***Ar*** (see also §4.5.6). If the Argand number is small, that is, the effective viscosity is large for the ambient rate of strain, the deformation of the continental lithosphere will be entirely due to boundary forces. If ***Ar*** is large, however, the effective viscosity

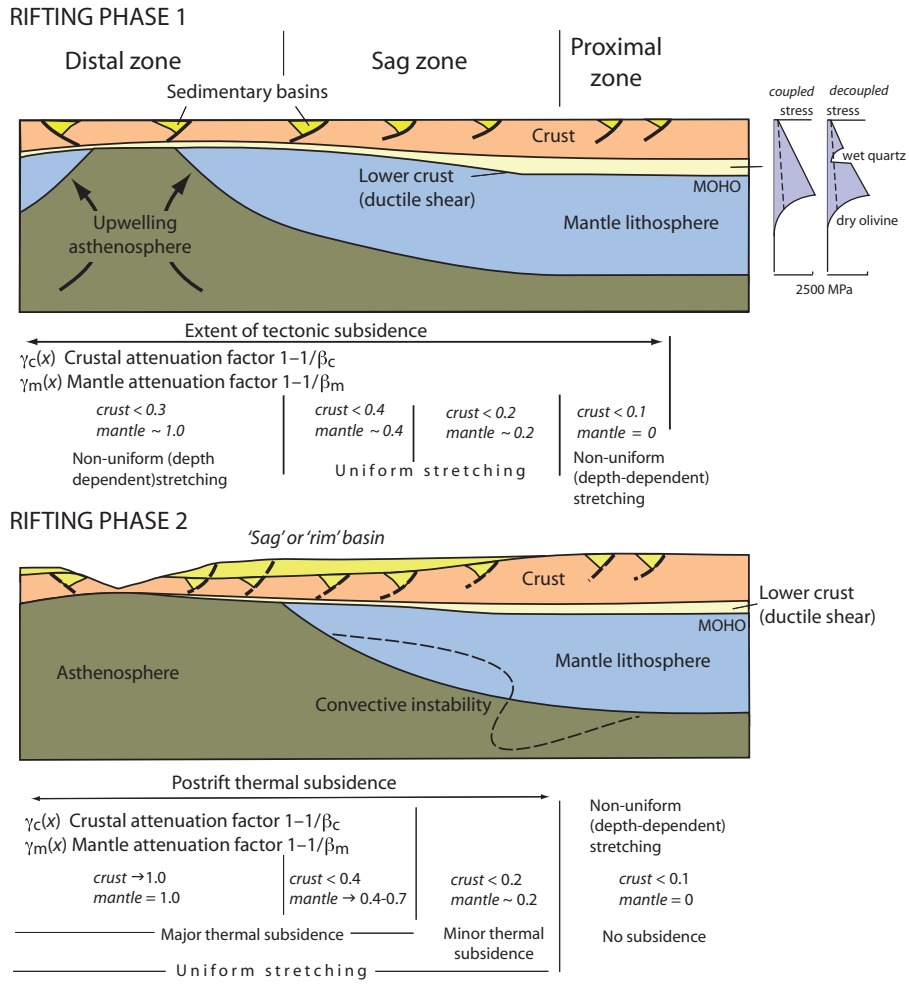

Fig. 3.40 Summary of depth-dependent (non-uniform) stretching resulting from extension of continental lithosphere in the numerical thermomechanical model of Huismans & Beaumont (2002, 2008). Three zones can be differentiated: a distal continental margin, a sag zone, and a proximal zone. During phase 1, mantle thinning is concentrated in the distal zone and decreases progressively towards the proximal zone. However, crustal thinning is concentrated in the sag zone due to shearing of the lower crust and brittle deformation of the upper crust. With further extension (rifting phase 2), a post-rift sag or continental rim basin forms due to thermal subsidence, whereas brittle deformation of the crust continues in more distal positions. Convective instabilities may form at the base of the mantle lithosphere.

will appear to be small and the medium will not be strong enough to support the elevation contrasts, so the forces due to crustal thickness changes will dominate deformation. Numerical modelling using this approach explained the tectonic styles of major crustal shortening in the Himalayas and extension in Tibet (England & Houseman 1988, 1989).

3.5.3 Rheology of the continental lithosphere

The link between the forces on the lithosphere and its deformation is the rheology of lithospheric materials (§2.3). The rheology of the lithosphere controls its deformation under any set of initial and boundary conditions. Consequently, rheology underpins all dynamical models of basin development. Key to the correct treatment of rheology is the concept of the strength envelope (Goetze & Evans 1979; Ranalli 1995; Fernandez & Ranalli 1997) (§2.3.4). The continental lithosphere is widely regarded as rheologically layered, so that at its simplest, it is a four-layer model. The high-strength regions of stabilised or 'standard' continental lithosphere (with a Moho temperature of about 600 °C) occur in the mid-crust and mantle lithosphere immediately beneath the Moho. Two low-strength regions also occur – in the lower crust, and at greater depths in the mantle lithosphere.

Information on rock rheology necessary for basin modelling essentially comes from laboratory experiments of rock deformation. Ignoring, for the moment, brittle failure, the constitutive laws derived from these experiments express strain rate as a function of temperature, pressure and deviatoric stress. Although laboratory experiments may not be fully representative of conditions in the lithosphere, the strain rate of rocks in the lithosphere is thought to obey a *power-law creep* relationship, as follows:

$$\dot{\varepsilon} = A\tau^{n}\exp(-E_a/RT) \qquad [3.4]$$

where τ is the deviatoric stress, T is the absolute temperature, R is the universal gas constant (8.3144 J mol^{-1} K^{-1}), and A, Q and n are constants dependent on the type of material undergoing deformation (Fernandez & Ranalli 1997). The activation energy E_a ranges from about 500 kJ mol^{-1} for dry olivine to about 160 kJ mol^{-1} for quartz. The power exponent n is in the range 3 to 5. Eqn. [3.4] is in fact the common form of many temperature-activated processes, for example the maturation of organic matter to form petroleum.

It is a simple matter to calculate the difference in strain rate for dry olivine in the uppermost mantle lithosphere for a 20 °C temperature change from 600 °C to 580 °C (873 K to 853 K). We assume that the driving deviatoric stress τ, exponent n and material coefficient A are constant. A temperature change of just 20 °C (from 600 °C to 580 °C) causes over an order of magnitude change in the strain rate. This is because *viscosity* is highly dependent on temperature.

Although it is possible to measure strain rates of the surface of the Earth using techniques such as global positioning system geodesy (e.g. Clarke *et al.* 1998; Bennett *et al.* 1997; Kreemer *et al.* 2003), it is not known how representative this is of longer time scales and of the lithosphere as a whole. Whereas deformation of the upper crust is by brittle faulting, it is not known whether this fault-related upper crustal extension follows the same strain rate pattern as the ductile lower crust and lithospheric mantle. In some parts of the world (such as the Basin and Range province of SW USA, and the Aegean region of Greece and Turkey) upper crustal extension is diffuse and widespread, being distributed on very many individual faults. This suggests that extension of the ductile layers of the lithosphere may control the brittle extension of the upper crust. The strain rate of ductile deformation is determined by viscosity. It is open to question whether the amount of extension varies as a function of depth, but in the general case it can be assumed that strain and strain rate are independent of depth, representing the case of *pure shear*. The entire lithosphere is then assumed to extend at a rate determined by the depth-integrated viscosity.

3.5.4 Numerical and analogue experiments on strain rate during continental extension

Using a relatively simple rheological model of a low-viscosity crust (not temperature-dependent) and a power-law creep lithospheric mantle, Newman and White (1999) showed the strain rate history of a piece of extending continental lithosphere assuming pure shear. A number of scenarios are possible, depending on the initial strain rate/magnitude of the distant driving force (Fig. 3.41).

- At *high initial strain rate*, complete rifting of the lithosphere takes place before any significant heat loss. The strain rate increases through time because the same distant driving force acts on progressively thinner lithosphere.
- At *lower initial strain rate*, strain rate rises at first because of the same lithospheric thinning effect, but mantle cooling becomes important and reduces the strain rate. The time taken for the strain rate to become negligible (less than about 10^{-17} s^{-1}) depends on the initial strain rate – it is short for high initial strain rates and long for smaller initial strain rates. In other words, extension continues longer where the initial strain rate is slower.

How likely is it that the mantle lithosphere will cool sufficiently to significantly increase viscosity and stop extension? Let us take eqn. [3.4] and derive an expression for the temperature change at the

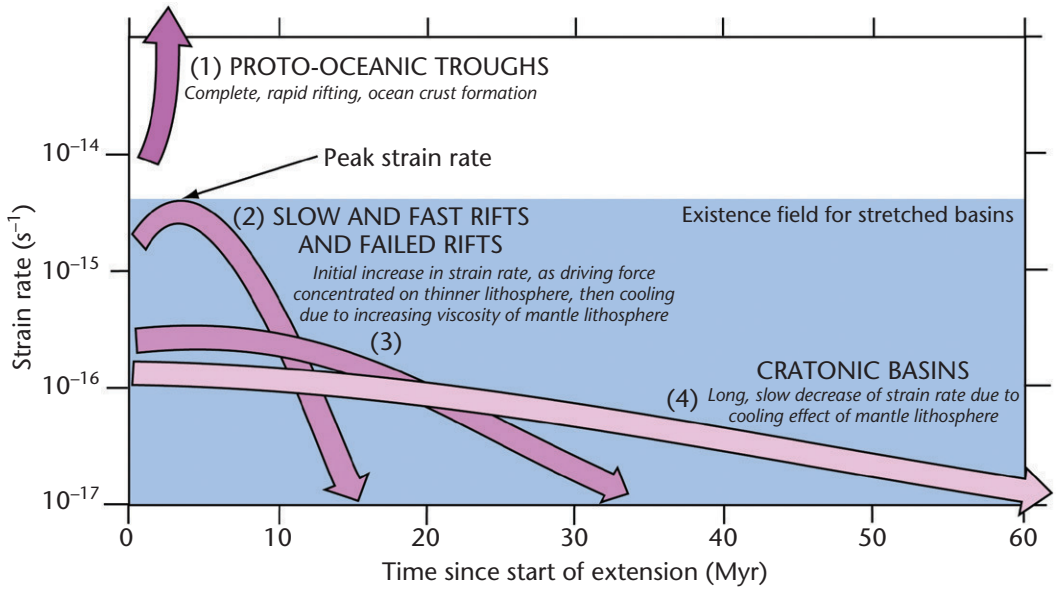

Fig. 3.41 Variation of the strain rate with time based on a set of 1D numerical experiments by Newman & White (1999), adapted by Allen & Armitage (2012) and reproduced with permission of John Wiley & Sons, Ltd. Each experiment uses the same rheology, but the driving force varies, resulting in different initial strain rates. At very high initial strain rates (1), complete, rapid rifting of the lithosphere occurs. In (2) and (3) the strain rate rises at first because the same driving force acts on a progressively thinner lithosphere. Strain rate then falls because of the effect of cooling on viscosity in the mantle lithosphere. In (4) initial strain rates are low, so the mantle cooling effect dominates. Apart from passive margins, peak strain rates in extensional sedimentary basins rarely exceed 2×10^{-15} s^{-1}.

Moho of a piece of continental lithosphere extending with a stretch factor β required to cause a fall in the strain rate from an initial value $\dot{\varepsilon}_0$ to a new value $\dot{\varepsilon}_1$

$$\log_e \dot{\varepsilon}_0 - \log_e \dot{\varepsilon}_1 = \frac{E_a \Delta T}{R T_{MOHO}^2} - n \log_e \beta \qquad [3.5]$$

where T_{MOHO} is the temperature at the Moho, and the other parameters are defined above. The temperature change, ΔT, required to lower the strain rate by an order of magnitude is then

$$\Delta T = \{2.3 + n \log_e \beta\} \frac{R T_{MOHO}^2}{E_a} \qquad [3.6]$$

If the lithospheric stretch factor β is 1.2, $E_a = 500\,\text{kJ mol}^{-1}$, $T_{MOHO} = 580\,°\text{C}$ (853 K), $n = 3$, $R = 8.314\ \text{J mol}^{-1}\ \text{K}^{-1}$, and the temperature change required to lower the strain rate by an order of magnitude is 34 °C. If the stretch factor β is 2.5, the answer is 61 °C. This is because, with the higher stretch factor, the driving force is concentrated on a thinner slab of lithosphere, which causes the deviatoric stress to increase by a factor β as the lithosphere thins. This effect offsets the increase in viscosity caused by cooling.

How long should it take to accomplish the temperature reduction causing an order-of-magnitude fall in the strain rate? To answer this question requires us to know something about the geothermal gradient in the lithospheric mantle G_m, the thermal conductivity of crust K_c and mantle lithosphere K_m, the radiogenic heat production of the crust A_c, the thermal time constant of the lithosphere τ, the initial thickness of the crust y_{c0}, and initial Moho temperature T_o. The expression for the time period required, t, simplifies to

$$t = K(\dot{\varepsilon}_0)^{-1/2} \qquad [3.7]$$

where the coefficient K is equal to 4×10^{-7} for the following parameter values: initial geotherm $G_m = 25\,°\text{C km}^{-1}$, lithospheric time constant $\tau = 60$ Myr, initial Moho temperature $T_o = 580\,°\text{C}$, thermal conductivity of crust $K_c = 2.5\,\text{W m}^{-2}\ \text{K}^{-1}$, thermal conductivity of mantle $K_m = 3.0\,\text{W m}^{-2}\ \text{K}^{-1}$, crustal radiogenic heat production $A_c = 1.1\,\mu\text{m W m}^{-3}$, initial crustal thickness $y_{c0} = 33$ km, and initial lithospheric thickness $y_{L0} = 120$ km.

The striking result is that the time taken to reduce the strain rate by an order of magnitude depends on the inverse square root of the initial strain rate. That is, if the initial strain rate is high, the time taken to reduce it by an order of magnitude is short. If the initial strain rate is low, the time taken to reduce the strain rate by an order of magnitude is long. If the initial strain rate is $3 \times 10^{-15}\,\text{s}^{-1}$, the strain rate reduces to an order of magnitude smaller than this initial value in 7 Myr. When the initial strain rate is $3 \times 10^{-16}\,\text{s}^{-1}$, this time scale becomes 23 Myr. This compares favourably with the observed time scale of rifting known from the geological record.

If the initial strain rate is less than c.$10^{-16}\,\text{s}^{-1}$, it may take as much as 60 Myr for the extension to stop. It is likely that during this long period of time the driving force may be removed, for example, by changes in relative plate motion, or by changes in the convectional motion in the mantle (see also Chapter 5).

The subsidence history of sedimentary basins allows the stretch factor and peak strain rate of the underlying continental lithosphere to be estimated. White (1994) and Newman and White (1999) developed this technique and applied it to literally thousands of borehole subsidence records. They discovered that there was a strong relationship between the peak strain rate and the final stretch factor in all of the sedimentary basins studied (Fig. 3.42).

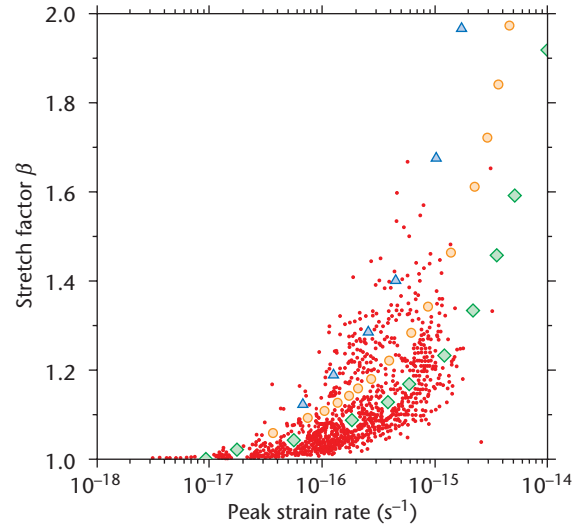

Fig. 3.42 Relation between peak strain rate and stretch factor for 2195 separate rifting episodes (small dots). Model results are for activation energies E_a of 300 kJ mol^{-1} (triangles), 500 kJ mol^{-1} (circles) and 1200 kJ mol^{-1} (diamonds). After White (1994) and Newman & White (1999).

If continental extension is controlled by a distant driving force, we would expect large variations in this relationship between peak strain rate and stretch factor, since continental lithosphere is heterogeneous. However, if viscosity controls extension, we should expect just the relationship observed. Differences caused by variations in the magnitude of the distant driving forces are much smaller than the effects of viscosity (or values of the activation energy E_a, which may vary significantly).

If the viscosity-controlled extension model is correct, previously stretched lithosphere should be *stronger* than 'normal' lithosphere. That is, for a given peak strain rate, we should expect a smaller stretch factor in the case of the previously stretched lithosphere. This appears to be supported by the data of Newman and White (1999). However, there is still an unanswered question: do previously rifted pieces of lithosphere tend to rift again? The geological record suggests 'yes'. The numerical model suggests perhaps 'no'.

Considerable insights have also been gained from analogue experiments. Analogue models are experiments conducted with materials of carefully chosen viscosities, strengths and densities, scaled in such a way to represent the deformation of a layered lithosphere at the appropriate strain rates. These models are informative about lithospheric stretching under a variety of conditions. Different results are obtained dependent on the strength profile of the lithospheric model and the scaled strain rate of the analogue experiment. The analogue experiments replicate many of the different styles of continental extension, particularly narrow, localised rifts versus extensive tilted fault block terranes (Brun 1999) (Fig. 3.38).

- For a simple two-layer model (brittle upper layer over a ductile lower layer), at low strain rates (and therefore low ductile

strengths), deformation remains localised in an asymmetric graben; at high strain rate, the faulted zone is much wider, with highly tilted fault blocks.
- For a simple two-layer model with constant strain rate, small brittle layer thicknesses (therefore low brittle strength) produced extensively faulted models, whereas high brittle strength resulted in localised rifts.
- Where the two-layer analogue model is able to extend under its own weight, faulting invades the whole model, producing a wide rift with highly tilted fault blocks rather than horsts and graben.

These results therefore suggest that ductile and brittle strengths and spreading under gravity play major roles in style of deformation. Horsts and graben appear to typify regions of slow strain rate, whereas multiple tilted fault blocks are typical of high strain rate regions.

In four-layer models (two high-strength zones, corresponding to the upper crust and upper mantle lithosphere), low strain rates produce a narrow rift whose delimiting faults sole out into the brittle–ductile interface. Whereas a single zone of necking develops at low strain rates, at higher strain rates multiple necking (that is, *boudinage*) causes a widening of the extending zone, as in the passive margin stage. A local, low-viscosity heterogeneity beneath the brittle–ductile interface (such as caused by the thermal effects of a large pluton, or by partial melting) causes an increase in stretching and allows the ductile layer to exhume to form core complexes. Initially steep normal faults are rotated into flat-lying detachments. In wide rifts, therefore, local anomalies are prone to amplification to produce strong variations in extension and exhumation.

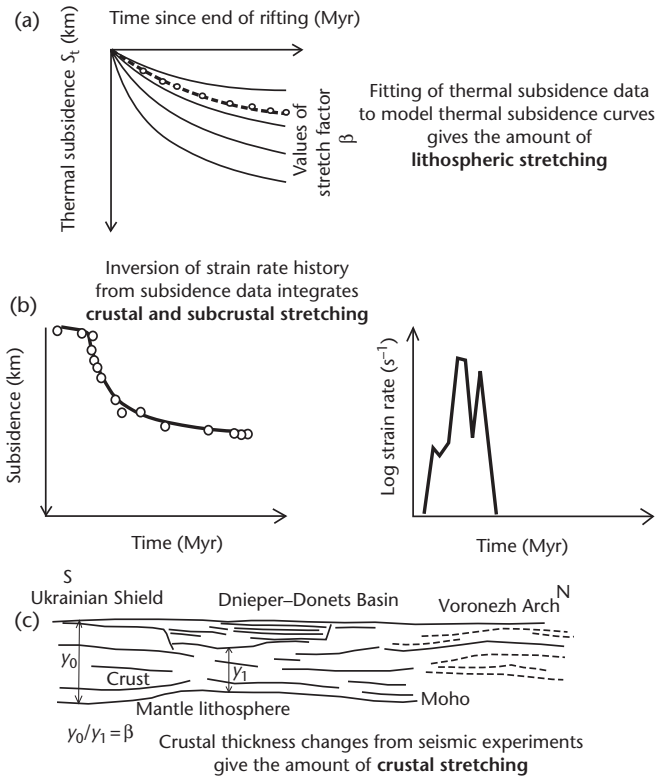

Fig. 3.43 Methods for calculation of the amount of stretching. (a) Calculation of the lithospheric stretch factor from thermal subsidence curves. (b) Inversion of strain rate history of the lithosphere from subsidence curves. (c) Calculation of the crustal stretching from mapping of the Moho.

3.6 Estimation of the stretch factor and strain rate history

An estimate of the amount of extension that has taken place can be obtained from a number of methods (Fig. 3.43). Knowledge of the strain rate history or total stretch factor is important as a basis for predicting the geothermal gradient and heat flow history of basin sediments, as well as in showing the role of rift structures in accommodating basin sediments.

3.6.1 Estimation of the stretch factor from thermal subsidence history

It has previously been shown (§3.3) that the 'reference' uniform stretching model predicts initial uplift or subsidence depending on the ratio of crustal to lithospheric thickness y_c/y_L and the stretch factor β. If y_c/y_L is known for a particular basin, the fault-controlled initial subsidence could in theory be used to estimate the amount of stretching (see equations in Appendix 21). However, the extreme variations in syn-rift thicknesses make this a very unreliable technique.

The rate of thermal subsidence in a basin generated by uniform stretching is dependent on the stretch factor. The post-rift thermal subsidence phase of sedimentary basins also lacks the extreme thickness variations characteristic of syn-rift deposits. The standard technique is the construction of a set of subsidence curves for different values of the stretch factor β (Appendix 19). Curves can be constructed for a water-loaded basin, where the density of the infill is $\rho_w = 1000\,\mathrm{kg\,m^{-3}}$. In this case the post-rift sediment thicknesses need to be decompacted and backstripped to reveal the water-loaded tectonic subsidence history (Appendices 56, 57 and §9.4). The observed backstripped post-rift subsidence can then be compared with the model curves to reveal the best-fitting stretch factor (Appendix 19). Alternatively, model curves can be constructed that show the thermal subsidence for different values of the stretch factor β for a sediment-loaded basin. Construction of such curves requires estimation of the bulk density of the sediment column as a function of time. The model sediment-loaded curves can then be compared with the decompacted total subsidence curve derived from borehole data or outcrop sections.

Thermal subsidence data can also be inverted to obtain the stretch factor, as shown in Appendix 20. A workflow showing the steps taken from decompacting a stratigraphic succession, through inversion of the stretch factor, to estimating paleotemperatures of selected horizons, is given in Appendix 58.

3.6.2 Estimation of the stretch factor from crustal thickness changes

In some circumstances the attenuation of the crust can be estimated from deep seismic (refraction and wide-angle reflection) results. For example, the Moho rises by 5 km in the southern part of the Rhine Graben, and 3 km of sediment has accumulated. The crust has therefore thinned by 8 km (Emter 1971; Mueller *et al.* 1973). Similarly, the nearby Limagne Graben (France) contains 2 km of sediments, and

the Moho rises to within 24 km of the surface (Hirn & Perrier 1974). Since the crust is about 30 km thick in the Massif Central, which separates the Rhine–Bresse rift system from the Limagne Graben, the amount of crustal attenuation in these two cases can be estimated to be between 1.2 and 1.3.

The North Sea is a failed rift that underwent rifting in the Jurassic–Early Cretaceous. Regional deep seismic reflection profiles and gravity profiles in the Viking Graben–Shetland Platform area have been used to estimate the depth to the Moho (Barton 1986; Klemperer 1988). More recently, the deep structure of the Viking Graben and adjacent areas of the northern North Sea (60–62°N) has been investigated based on an integrated study of deep seismic reflection and refraction data, gravity and magnetic data (Christiansson *et al.* 2000) (Fig. 3.10). Where unaffected by Caledonian crustal roots and by Mesozoic stretching, the Moho lies at a depth of 30–32 km. It shallows to about 20–22 km beneath the Viking Graben. Since the graben is filled with approximately 10 km of Triassic to Cenozoic sedimentary rocks, the thickness of crystalline and Paleozoic crustal rocks in the Viking Graben is only about 10 km. This represents a stretch factor of over 3. In contrast, the East Shetland and Horda platforms have stretch factors of less than 1.5. These values reflect the cumulative effects of several post-Caledonian stretching events.

The estimates of crustal stretching derived from mapping of the Moho have been compared with estimates from subsidence analysis (Giltner 1987; Badley *et al.* 1988; Christiansson *et al.* 2000) and forward tectonostratigraphic modelling (Odinsen *et al.* 2000). The former are somewhat higher than the stretch factors derived from the other two methods, which emphasises the care that needs to be taken in the interpretation of β estimates. A similar exercise in the Rockall, mid-Norway and SW Barents Sea areas also showed large discrepancies between the crustal stretching estimated from deep seismic imagery and subsidence analysis (Skogseid *et al.* 2000).

3.6.3 Estimation of the stretch factor from forward tectonostratigraphic modelling

Stretch factors have been estimated along transects of the northern North Sea where the crustal profile, stratigraphic thicknesses and faults are very well constrained (Odinsen *et al.* 2000). Forward tectonostratigraphic models simulate crustal structure and basin development through time using a rheological model of the lithosphere, with a finite flexural strength based on Braun and Beaumont (1987) and Kooi *et al.* (1992). The forward model has the advantage of discriminating the stretching from each rifting event. Odinsen *et al.* (2000) compared the stretching in the Permo-Triassic (maximum of $\beta = 1.41$ in the Viking Graben) versus Jurassic (maximum of $\beta = 1.53$ in the Viking Graben) rifting events in the northern North Sea. The calculated distribution of stretch factors along two well-constrained crustal transects (Fig. 3.10) matches well earlier estimates based on 1D subsidence analysis (Giltner 1987; Badley *et al.* 1988).

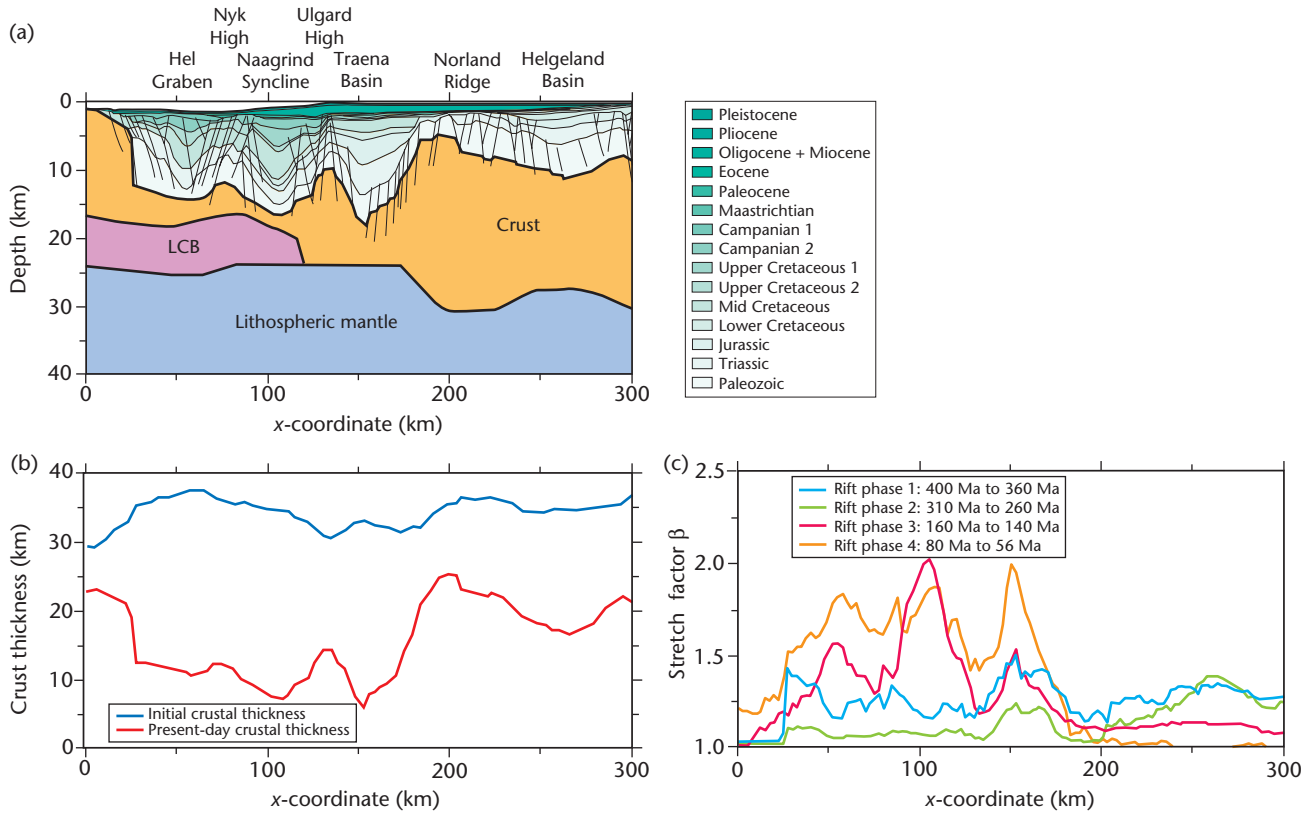

Fig. 3.44 Multiple phases of rifting, Voring margin, mid-Norway. (a) Sedimentary basin, crust and lower crustal body (LCB) across a 300 km-wide transect. (b) Thickness of present-day crust and estimate of its initial thickness. (c) Calculated stretch factors along the profile for four rifting episodes. From Wangen (2010, p. 247). © Magnus Wangen 2010, reproduced with the permission of Cambridge University Press.

3.6.4 Inversion of strain rate history from subsidence data

White (1993, 1994) has taken the novel approach of calculating the strain rate history from the subsidence history of sedimentary basins using inverse methods. The stretch factor β can be viewed as representative of the total strain integrated over the time scale of extension. The stretch factor is therefore related to the vertical strain rate $\dot{\varepsilon}_v(t)$ by

$$\beta = \exp\left(\int_0^{\Delta t} \dot{\varepsilon}_v(t)dt\right) \quad [3.8]$$

where Δt is the duration of stretching. If the strain rate is constant, $\beta = \exp(\dot{\varepsilon}_v \Delta t)$. In the inverse method, the subsidence as a function of time is solved iteratively to give the strain rate as a function of time $\dot{\varepsilon}_v(t)$. Multiple stretching episodes can be resolved by this technique.

3.6.5 Multiple phases of rifting

Many extended provinces have experienced a number of distinct rifting episodes. The Voring margin, offshore mid-Norway, for example, extended in the Devonian (400–360 Ma), Permian (310–260 Ma), Late Jurassic (160–140 Ma) and finally in the Late Cretaceous and Paleocene (80–56 Ma), which led to break-up and the formation of the North Atlantic Ocean (Lundin & Doré 1997; Wangen *et al.* 2007). The strain rate history therefore shows multiple peaks. The crustal stretch factors for each of these stretching phases can be plotted across a basin transect (Fig. 3.44). If the crustal thickness before the first rifting phase can be constrained, it allows the stretch factors for each phase and the total crustal stretch to be calculated. The initial thickness of the crust can be determined if Airy isostasy is assumed and the water depth, sediment thickness, sediment bulk density and crustal thickness are known from the present-day profile (see Chapter 9).

The total (cumulative) crustal stretch is

$$\beta_{max} = \beta_1\beta_2\beta_3\beta_4 \quad [3.9]$$

where 1 to 4 are the rift phases. The cumulative stretch factor at any point in the geohistory t can also be found by a comparison of the crustal thickness initially and at the time of interest:

$$\beta_{max}(t) = \frac{y_{c,0}}{y_c(t)} = \frac{y_{c,0}}{y_{c,0} - f_w W_d(t) - f_s(t) y_s(t)} \quad [3.10]$$

where $y_{c,0}$ is the initial crustal thickness, y_c(t) is the crustal thickness at time t, f_w is a density factor for water equal to $(\rho_m - \rho_w)/(\rho_m - \rho_c)$, f_s is a density factor for bulk sediment $(\rho_m - \rho_w)/(\rho_m - \rho_b(t))$, and $\rho_b(t)$ is the average bulk density of the sediment columns as a function of time.

Table 3.2 Results of estimates of crustal stretch factor for multiple stretching phases of the Voring margin, mid-Norway (from Wangen 2010, p. 251) © Magnus Wangen 2010, reproduced with the permission of Cambridge University Press

Phase i	y_i	$\rho_{b,i}$	Wd_i	$y_{c,i}$	$f_{s,i}$	$\beta_{max,i}$	β_i
1	1	2200	0	35028	2.2	1.00	1.18
2	1800	2200	300	29690	2.2	1.18	1.07
3	2300	2250	550	27670	2.1	1.27	1.77
4	10000	2550	950	15660	1.5	2.24	1.96
5	15000	2560	1050	8000	1.5	4.38	–

Input data and calculated stretch factors for the four rift phases recognised in the Voring margin are given below. Note that the cumulative stretch factor increases over time and reaches $\beta_{max} > 4$ by the time of ocean crust formation in the Paleocene.